

ISU  
1981  
B325  
c.3

Hydrogel coated silicone rubber  
for catheter applications

304

by

Michael David Baudino

A Thesis Submitted to the  
Graduate Faculty in Partial Fulfillment of the  
Requirements for the Degree of  
MASTER OF SCIENCE

Major: Biomedical Engineering

Approved:

---

Signatures have been redacted for privacy

Iowa State University  
Ames, Iowa

1981

1328245

## TABLE OF CONTENTS

	<u>Page</u>
LIST OF SYMBOLS	xvi
INTRODUCTION	1
LITERATURE REVIEW	2
Catheters	2
Hydrogels	2
Thrombosis	9
Surface Energy	11
MATERIALS AND METHODS	14
Techniques	14
Fabrication	14
Blood Data	15
Surgery	16
Scanning Electron Microscopy	20
Contact Angle Determination	21
SEM Micrograph Ratings	22
RESULTS	23
Materials	23
Implantation	35
Method 1	35
Method 2	41
Method 3	118
DISCUSSION	124
SEM Analysis	124
Contact Angle	125
Thrombogenicity Index	125
CONCLUSION	127
RECOMMENDATIONS FOR FUTURE RESEARCH	129
LITERATURE CITED	130
ACKNOWLEDGEMENTS	134

## LIST OF FIGURES

	<u>Page</u>
Figure 1. Schematic illustration of the unsatisfied bonding capacity at a free surface. (Andrade, 1973).	12
Figure 2. The asymmetric nature of the forces exerted on surface atoms resulting in an attraction towards the bulk. The atom depleted surface is then in tension. (Andrade, 1973)	12
Figure 3. The contact angle measurement. (Andrade, 1973).	12
Figure 4. Schematic diagrams of glass capillary support tubing inserted in the Silastic <sup>®</sup> tubing.	14
Figure 5. Schematic diagram of the catheter introduction unit placement in the external jugular vein, method 1.	17
Figure 6. Schematic diagram of the catheter placement in the external jugular vein, method 2.	18
Figure 7. Schematic diagram of the catheter placement in the vessel, method 3.	19
Figure 8. Sectioning of the catheter for SEM analysis.	20
Figure 9. Measurement of contact angle of H <sub>2</sub> O on silicone rubber.	21
Figure 10a. Scanning electron micrograph of Silastic <sup>®</sup> (scale bar = 100 $\mu$ m). 15 keV.	24
Figure 10b. Higher magnification of Figure 10b (scale bar = 10 $\mu$ m). 15 keV.	24
Figure 10c. Radiation grafted 20% HEMA/0% NVP in silicone rubber (scale bar = 100 $\mu$ m) 15 keV.	24
Figure 10d. Higher magnification of Figure 10c (scale bar = 10 $\mu$ m). 15 keV.	24
Figure 10e. Radiation grafted 15% HEMA/5% NVP on silicone rubber (scale bar = 100 $\mu$ m). 15 keV.	26

Figure 10f.	Higher magnification of Figure 10e (scale bar = 10 $\mu\text{m}$ ). 15 keV.	26
Figure 10g.	Radiation grafted 10% HEMA/10% NVP on silicone rubber (scale bar = 100 $\mu\text{m}$ ). 15 keV.	26
Figure 10h.	Higher magnification of Figure 10g (scale bar = 10 $\mu\text{m}$ ). 15 keV.	26
Figure 10i.	Radiation grafted 5% HEMA/15% NVP in silicone rubber (scale bar = 100 $\mu\text{m}$ ). 15 keV.	28
Figure 10j.	Higher magnification of Figure 10i (scale bar = 10 $\mu\text{m}$ ). 15 keV.	28
Figure 10k.	Radiation grafted 0% HEMA/20% NVP on silicone rubber (scale bar = 100 $\mu\text{m}$ ). 15 keV.	28
Figure 10l.	Higher magnification of Figure 10k (scale bar = 10 $\mu\text{m}$ ). 15 keV.	28
Figure 11.	Crosssectional view of radiation grafted 15% HEMA/5% NVP on silicone rubber. (S) designates silicone rubber, (H) designates hydrogel coating. Hydrogel coating thickness is 0.05 mm.(scale bar = 100 $\mu\text{m}$ ).	30
Figure 12.	Zisman plot for determining the critical surface tension of each formulation. ( $\bullet$ ) is silicone rubber, ( $\circ$ ) is 15% HEMA/5% NVP, ( $\Delta$ ) is 10% HEMA/10% NVP, ( $\blacktriangle$ ) is 0% HEMA/20% NVP. Linear regression was utilized for line placement. $p \leq 0.06$ for all correlation coefficients.	33
Figure 13.	Sample platelet counting area (scale bar = 10 $\mu\text{m}$ ). The counting area equals 2500 $\mu\text{m}^2$ .	37
Figure 14a.	Graphs of platelet densities for dog 2148. Catheter coating was 10% HEMA/10% NVP.	38
Figure 14b.	Graphs of platelet densities for dog 2148. Catheter coating was 5% HEMA/15% NVP.	39
Figure 14c.	Graphs of platelet densities for dog 2148. Catheter coating was 0% HEMA/20% NVP.	40
Figure 15a.	Scanning electron micrograph of Silastic <sup>®</sup> catheter, section 1, at 15 minutes (scale bar = 100 $\mu\text{m}$ ). 15 keV. dog 2146.	43

- Figure 15b. Higher magnification of Figure 15a (scale bar = 10  $\mu\text{m}$ ). dog 2146. 15 keV. 43
- Figure 15c. Silastic<sup>®</sup> catheter, section 2, at 15 minutes (scale bar = 10  $\mu\text{m}$ ). 15 keV. 20° tilt. dog 2146. 43
- Figure 15d. Silastic<sup>®</sup> catheter, section 6, at 15 minutes (scale bar = 33.3  $\mu\text{m}$ ). 15 keV. 20° tilt. dog 2146. 43
- Figure 16a. Scanning electron micrograph of Silastic<sup>®</sup> catheter, section 2, at 30 minutes (scale bar = 100  $\mu\text{m}$ ). 15 keV. dog 2146. 44
- Figure 16b. Higher magnification of Figure 16a (scale bar = 10  $\mu\text{m}$ ). 15 keV. dog 2146. 45
- Figure 16c. Silastic<sup>®</sup> catheter, section 4, at 30 minutes (scale bar = 33.3  $\mu\text{m}$ ). 15 keV. 30° tilt. dog 2146. 45
- Figure 16d. Silastic<sup>®</sup> catheter, section 8, at 30 minutes (scale bar = 33.3  $\mu\text{m}$ ). 15 keV. 30° tilt. dog 2146. 45
- Figure 17a. Scanning electron micrograph of Silastic<sup>®</sup> catheter, section 1, at 60 minutes (scale bar = 100  $\mu\text{m}$ ). 15 keV. dog 2146. 47
- Figure 17b. Silastic<sup>®</sup> catheter, section 4 at 60 minutes (scale bar = 20  $\mu\text{m}$ ). 15 keV. 20° tilt. dog 2146. 47
- Figure 17c. Silastic<sup>®</sup> catheter, section 5 at 60 minutes (scale bar = 10  $\mu\text{m}$ ). 15 keV. dog 2146. 47
- Figure 17d. Silastic<sup>®</sup> catheter, section 7, at 60 minutes (scale bar = 2  $\mu\text{m}$ ). 15 keV. dog 2146. 49
- Figure 17e. Silastic<sup>®</sup> catheter, section 8, at 60 minutes (scale bar = 33.3  $\mu\text{m}$ ). 15 keV. 30° tilt. dog 2146. 49
- Figure 17f. Higher magnification of Figure 17e (scale bar = 100  $\mu\text{m}$ ). 15 keV. 30° tilt. dog 2146. 49

Figure 18a.	Scanning electron micrograph of Silastic <sup>®</sup> catheter, section 1, at 15 minutes (scale bar = 100 $\mu\text{m}$ ). 15 keV. dog 2130.	52
Figure 18b.	Higher magnification of Figure 18a (scale bar = 10 $\mu\text{m}$ ). 15 keV. dog 2130.	52
Figure 18c.	Silastic <sup>®</sup> catheter, section 7, at 15 minutes (scale bar = 10 $\mu\text{m}$ ). 15 keV. dog 2130.	52
Figure 19a.	Scanning electron micrographs of Silastic <sup>®</sup> catheter, section 1, at 30 minutes (scale bar = 100 $\mu\text{m}$ ). 15 keV. dog 2130.	54
Figure 19b.	Scanning electron micrograph of Silastic <sup>®</sup> catheter, section 1, at 60 minutes (scale bar = 100 $\mu\text{m}$ ). 15 keV. dog 2130.	54
Figure 19c.	Photograph of the recovered thrombi stripped during withdrawal (scale bar = 1 inch).	54
Figure 20a.	Scanning electron micrograph of the 20% HEMA/0% NVP grafted catheter, section 1, at 15 minutes (scale bar = 100 $\mu\text{m}$ ). 15 keV. dog 2146.	52
Figure 20b.	Higher magnification of Figure 20a (scale bar = 10 $\mu\text{m}$ ). 15 keV. dog 2146.	56
Figure 20c.	20% HEMA/0% NVP, Section 2 at 15 minutes (scale bar = 20 $\mu\text{m}$ ). 15 keV. dog 2146.	56
Figure 20d.	20% HEMA/0% NVP, Section 4, at 15 minutes (scale bar = 33.3 $\mu\text{m}$ ). 15 keV. dog 2146.	56
Figure 21a.	Scanning electron micrograph of the 20% HEMA/0% NVP grafted catheter, section 1, at 30 minutes (scale bar = 100 $\mu\text{m}$ ). 15 keV. dog 2146.	58
Figure 21b.	Higher magnification of Figure 21a (scale bar = 10 $\mu\text{m}$ ). 15 keV. dog 2146.	58
Figure 21c.	20% HEMA/0% NVP grafted catheter, section 2, at 30 minutes (scale bar = 33.3 $\mu\text{m}$ ). 15 keV. dog 2146.	60
Figure 21d.	20% HEMA/0% NVP grafted catheter, section 4, at 30 minutes (scale bar = 33.3 $\mu\text{m}$ ). 15 keV. dog 2146.	60

- Figure 21e. 20% HEMA/0% NVP grafted catheter, section 7, at 30 minutes (scale bar = 10  $\mu\text{m}$ ). 15 keV. dog 2146. 60
- Figure 22a. Scanning electron micrograph of the 20% HEMA/0% NVP grafted catheter, section 1, at 60 minutes (scale bar = 100  $\mu\text{m}$ ). 15 keV. dog 2146. 62
- Figure 22b. Higher magnification of Figure 22a (scale bar = 10  $\mu\text{m}$ ). 15 keV. dog 2146. 62
- Figure 22c. 20% HEMA/0% NVP grafted catheter, section 2, at 60 minutes (scale bar = 0.4 mm). 15 keV. dog 2146. 62
- Figure 23a. Scanning electron micrograph of the 20% HEMA/0% NVP grafted catheter, section 1, at 60 minutes (scale bar = 100  $\mu\text{m}$ ). 15 keV. dog 2130. 65
- Figure 23b. Higher magnification of Figure 23a (scale bar = 10  $\mu\text{m}$ ). 15 keV. dog 2130. 65
- Figure 23c. 20% HEMA/0% NVP grafted catheter, section 1, at 60 minutes (scale bar = 10  $\mu\text{m}$ ). Thrombus partially stripped. 15 keV. dog 2130. 65
- Figure 24a. Scanning electron micrograph of the 15% HEMA/5% NVP grafted catheter, section 1, at 15 minutes (scale bar = 100  $\mu\text{m}$ ). 15 keV. dog 2146. 67
- Figure 24b. Higher magnification of Figure 24a (scale bar = 10  $\mu\text{m}$ ). 15 keV. dog 2146. 67
- Figure 24c. 15% HEMA/5% NVP, grafted catheter, section 2, at 15 minutes (scale bar = 10  $\mu\text{m}$ ). 15 keV. 10 tilt. dog 2146. 67
- Figure 24d. 15% HEMA/5% NVP, grafted catheter, section 3, at 15 minutes (scale bar = 10  $\mu\text{m}$ ). 15 keV. dog 2146. 67

- Figure 24e. The 15 % HEMA/5% NVP grafted catheter, section 4, at 15 minutes (scale bar = 10  $\mu\text{m}$ ). 15 keV, 10° tilt. dog 2146. 67
- Figure 24f. Lower magnification of Figure 24e (scale bar = 33.3  $\mu\text{m}$ ). 15 keV. dog 2146. 69
- Figure 24g. 15% HEMA/5% NVP grafted catheter, section 6, at 15 minutes (scale bar = 33.3  $\mu\text{m}$ ). 15 keV. dog 2146. 69
- Figure 24h. 15% HEMA/5% NVP grafted catheter, section 8, at 15 minutes (scale bar = 33.3  $\mu\text{m}$ ). 15 keV. 10° tilt. dog 2146. 69
- Figure 25a. Scanning electron micrograph of the 15% HEMA/5% NVP grafted catheter, section 1, at 30 minutes (scale bar = 100  $\mu\text{m}$ ). 15 keV. dog 2146. 71
- Figure 25b. Higher magnification of Figure 25a (scale bar = 10  $\mu\text{m}$ ). 15 keV. dog 2146. 71
- Figure 25c. The 15% HEMA/5% NVP grafted catheter, section 3, at 30 minutes (scale bar = 100  $\mu\text{m}$ ). 15 keV. dog 2146. 73
- Figure 25d. Higher magnification of Figure 25c. (scale bar = 10  $\mu\text{m}$ ). 15 keV. dog 2146. 73
- Figure 25e. 15% HEMA/5% NVP grafted catheter, section 2, at 30 minutes (scale bar = 0.25 mm). 15 keV. dog 2146. 73
- Figure 25f. 15% HEMA/5% NVP grafted catheter, section 4, at 30 minutes (scale bar = 0.25 mm). 15 keV. dog 2146. 73
- Figure 25g. The 15% HEMA/5% NVP grafted catheter, section 6, at 30 minutes (scale bar = 0.25 mm). 15 keV. dog 2146. 75
- Figure 25h. 15% HEMA/5% NVP grafted catheter, section 7, at 30 minutes (scale bar = 10  $\mu\text{m}$ ). 15 keV. dog 2146. 75
- Figure 25i. 15% HEMA/5% NVP grafted catheter, section 8 at 30 minutes (scale bar = 100  $\mu\text{m}$ ). 15 keV. dog 2146. 75

Figure 25j.	Higher magnification of Figure 25i (scale bar = 10 $\mu\text{m}$ ). 15 keV. dog 2146.	75
Figure 26a.	Scanning electron micrograph of the 15% HEMA/5% NVP grafted catheter, section 1, at 60 minutes (scale bar = 50 $\mu\text{m}$ ). 15 keV. dog 2146.	78
Figure 26b.	Higher magnification of Figure 26a (scale bar = 3.33 $\mu\text{m}$ ). 15 keV. dog 2146.	78
Figure 26c.	15% HEMA/5% NVP grafted catheter, section 2 at 60 minutes (scale bar = 10 $\mu\text{m}$ ). 15 keV. dog 2146.	78
Figure 26d.	15% HEMA/5% NVP grafted catheter, section 4, at 60 minutes (scale bar = 10 $\mu\text{m}$ ). 15 keV. 10° tilt. dog 2146.	78
Figure 26e.	The 15% HEMA/5% NVP grafted catheter, section 6, at 60 minutes (scale bar = 10 $\mu\text{m}$ ). 15 keV. dog 2146.	80
Figure 26f.	15% HEMA/5% NVP grafted catheter, section 7, at 60 minutes (scale bar = 10 $\mu\text{m}$ ). 15 keV. dog 2146.	80
Figure 26g.	15% HEMA/5% NVP grafted catheter, section 8, at 60 minutes (scale bar = 10 $\mu\text{m}$ ). 15 keV. dog 2146.	80
Figure 27a.	Scanning electron micrograph of the 15% HEMA/5% NVP grafted catheter, section 1, at 15 minutes (scale bar = 100 $\mu\text{m}$ ). 15 keV. dog 2130.	82
Figure 27b.	Higher magnification of Figure 27a (scale bar = 10 $\mu\text{m}$ ). 15 keV. dog 2130.	82
Figure 27c.	15% HEMA/5% NVP, grafted catheter, section 1, at 15 minutes (scale bar = 10 $\mu\text{m}$ ). 15 keV. dog 2130.	82
Figure 27d.	15% HEMA/5% NVP grafted catheter, section 7, at 15 minutes (scale bar = 10 $\mu\text{m}$ ). 15 keV. dog 2130.	82

- Figure 28a. Scanning electron micrograph of the 10% HEMA/  
10% NVP grafted catheter, section 1, at 15  
minutes (scale bar = 100  $\mu\text{m}$ ). 15 keV.  
dog 2146. 84
- Figure 28b. Higher magnification of Figure 28a (scale bar =  
10  $\mu\text{m}$ ). 15 keV. dog 2146. 84
- Figure 28c. 10% HEMA/10% NVP grafted catheter, section 2,  
at 15 minutes (scale bar = 10  $\mu\text{m}$ ). 15 keV.  
dog 2146. 84
- Figure 28d. 10% HEMA/10% NVP grafted catheter, section 6,  
at 15 minutes (scale bar = 33.3  $\mu\text{m}$ ). 15 keV.  
30° tilt. dog 2146. 84
- Figure 29a. Scanning electron micrograph of the 10% HEMA/  
10% NVP grafted catheter, section 1 at 30  
minutes (scale bar = 100  $\mu\text{m}$ ). 15 keV. dog  
2146. 86
- Figure 29b. Higher magnification of Figure 29a (scale bar =  
10  $\mu\text{m}$ ). 15 keV. dog 2146. 86
- Figure 29c. 10% HEMA/10% NVP grafted catheter, section 2,  
at 30 minutes (scale bar = 10  $\mu\text{m}$ ). 15 keV.  
20° tilt. dog 2146. 88
- Figure 29d. 10 % HEMA/10% NVP grafted catheter, section 3,  
at 30 minutes (scale bar = 10  $\mu\text{m}$ ). 15 keV.  
dog 2146. 88
- Figure 29e. 10% HEMA/10% NVP grafted catheter, section 6,  
at 30 minutes (scale bar = 10  $\mu\text{m}$ ). 15 keV.  
30° tilt. dog 2146. 88
- Figure 30a. Scanning electron micrograph of the 10% HEMA/  
10% NVP grafted catheter, section 1, at 60  
minutes (scale bar = 100  $\mu\text{m}$ ). 15 keV. dog  
2146. 90
- Figure 30b. Higher magnification of Figure 30a (scale bar =  
10  $\mu\text{m}$ ). 15 keV. dog 2146. 90
- Figure 30c. 10% HEMA/10% NVP grafted catheter, section 5,  
at 60 minutes (scale bar = 10  $\mu\text{m}$ ). 15 keV.  
dog 2146. 90

- Figure 30d. 10% HEMA/10% NVP grafted catheter, section 6, at 60 minutes (scale bar = 30  $\mu\text{m}$ ). 15 keV. 20° tilt. dog 2146. 90
- Figure 31a. Scanning electron micrograph of the 5% HEMA/15% NVP grafted catheter, section 1, at 15 minutes (scale bar = 100  $\mu\text{m}$ ). 15 keV. dog 2146. 93
- Figure 31b. Higher magnification of Figure 31a (scale bar = 10  $\mu\text{m}$ ). 15 keV. dog 2146. 93
- Figure 31c. 5% HEMA/15% NVP grafted catheter, section 2, at 15 minutes (scale bar = 33.3  $\mu\text{m}$ ). 15 keV. 20° tilt. dog 2146. 93
- Figure 31d. 5% HEMA/15% NVP grafted catheter, section 3, at 15 minutes (scale bar = 10  $\mu\text{m}$ ). 15 keV. dog 2146. 93
- Figure 31e. 5% HEMA/15% NVP grafted catheter, section 5, at 15 minutes (scale bar = 10  $\mu\text{m}$ ). 15 keV. dog 2146. 95
- Figure 31f. 5% HEMA/15% NVP grafted catheter, section 6, at 15 minutes (scale bar = 20  $\mu\text{m}$ ). 15 keV. 20° tilt. dog 2146. 95
- Figure 31g. 5% HMEA/15% NVP grafted catheter, section 7, at 15 minutes (scale bar = 10  $\mu\text{m}$ ). 15 keV. dog 2146. 95
- Figure 32a. Scanning electron micrograph of the 5% HEMA/15% NVP grafted catheter, section 1, at 30 minutes (scale bar = 100  $\mu\text{m}$ ). 15 keV. dog 2146. 97
- Figure 32b. Higher magnification of Figure 32a (scale bar = 10  $\mu\text{m}$ ). 15 keV. dog 2146. 97
- Figure 32c. 5% HEMA/15% NVP grafted catheter, section 2, at 30 minutes (scale bar = 33.3  $\mu\text{m}$ ). 15 keV. 20° tilt. dog 2146. 97
- Figure 32d. 5% HEMA/15% NVP grafted catheter, section 3, at 30 minutes (scale bar = 10  $\mu\text{m}$ ). 15 keV. dog 2146. 97

- Figure 32e. 5% HEMA/15% NVP grafted catheter, section 4, at 30 minutes (scale bar = 33.3  $\mu\text{m}$ ). 15 keV. dog 2146. 99
- Figure 32f. Figure 32e at 30° tilt (scale bar = 33.3  $\mu\text{m}$ ). 15 keV. dog 2146. 99
- Figure 33a. Scanning electron micrograph of the 5% HEMA/15% NVP grafted catheter, section 1, at 60 minutes (scale bar = 100  $\mu\text{m}$ ). 15 keV. dog 2146. 101
- Figure 33b. Higher magnification of Figure 33a (scale bar = 33.3  $\mu\text{m}$ ). 15 keV. dog 2146. 101
- Figure 33c. 5% HEMA/15% NVP grafted catheter, section 2, at 60 minutes (scale bar = 33.3  $\mu\text{m}$ ). 15 keV. 20° tilt. dog 2146. 101
- Figure 33d. 5% HEMA/15% NVP grafted catheter, section 6, at 60 minutes (scale bar = 33.3  $\mu\text{m}$ ). 15 keV. 20° tilt. dog 2146. 101
- Figure 34a. Scanning electron micrograph of the 0% HEMA/20% NVP grafted catheter, section 1, at 15 minutes (scale bar = 100  $\mu\text{m}$ ). 15 keV. dog 2146. 104
- Figure 34b. 0% HEMA/10% NVP grafted catheter, section 2, at 15 minutes (scale bar = 10  $\mu\text{m}$ ). 15 keV. 5° tilt. dog 2146. 104
- Figure 34c. 0% HEMA/20% NVP grafted catheter, section 5, at 15 minutes (scale bar = 10  $\mu\text{m}$ ). 15 keV. dog 2146. 104
- Figure 34d. 0% HEMA/20% NVP grafted catheter, section 6, at 15 minutes (scale bar = 10  $\mu\text{m}$ ). 15 keV. 30° tilt. dog 2146. 104
- Figure 35a. Scanning electron micrograph of the 0% HEMA/20% NVP grafted catheter, section 1, at 30 minutes (scale bar = 100  $\mu\text{m}$ ). 15 keV. dog 2146. 106
- Figure 35b. Higher magnification of Figure 35a (scale bar = 10  $\mu\text{m}$ ). 15 keV. dog 2146. 106

Figure 35c.	0% HEMA/20% NVP grafted catheter, section 2, at 30 minutes (scale bar = 33.3 $\mu\text{m}$ ). 15 keV. 20° tilt. dog 2146.	106
Figure 35d.	0% HEMA/20% NVP grafted catheter, section 6, at 30 minutes (scale bar = 33.3 $\mu\text{m}$ ). 15 keV. 20° tilt. dog 2146.	108
Figure 35e.	0% HEMA/20% NVP grafted catheter, section 7, at 30 minutes (scale bar = 10 $\mu\text{m}$ ). 15 keV. dog 2146.	108
Figure 35f.	0% HEMA/20% NVP grafted catheter, section 7, at 30 minutes (scale bar = 10 $\mu\text{m}$ ). 15 keV. dog 2146.	108
Figure 36a.	Scanning electron micrograph of the 0% HEMA/20% NVP grafted catheter, section 1, at 60 minutes (scale bar = 100 $\mu\text{m}$ ). 15 keV. dog 2146.	110
Figure 36b.	Higher magnification of Figure 36a (scale bar = 10 $\mu\text{m}$ ). 15 keV. dog 2146.	110
Figure 36c.	0% HEMA/20% NVP grafted catheter, section 2, at 60 minutes (scale bar = 33.3 $\mu\text{m}$ ). 15 keV. 20° tilt. dog 2146.	110
Figure 36d.	0% HEMA/20% NVP grafted catheter, section 5, at 60 minutes (scale bar = 3.33 $\mu\text{m}$ ). 15 keV. dog 2146.	112
Figure 36e.	0% HEMA/20% NVP grafted catheter, section 7, at 60 minutes (scale bar = 10 $\mu\text{m}$ ). 15 keV. dog 2146.	112
Figure 36f.	0% HEMA/20% NVP grafted catheter, section 8, at 60 minutes (scale bar = 33.3 $\mu\text{m}$ ). 15 keV. 20° tilt. dog 2146.	112
Figure 37a.	Scanning electron micrograph of the 0% HEMA/20% NVP grafted catheter, section 1, at 15 minutes (scale bar = 100 $\mu\text{m}$ ). 15 keV. dog 2130.	115
Figure 37b.	Higher magnification of Figure 37a (scale bar = 10 $\mu\text{m}$ ). 15 keV. dog 2130.	115

- Figure 38a. Scanning electron micrograph of the 0% HEMA/  
20% NVP grafted catheter, sections 1-2, at 30  
minutes (scale bar = 100  $\mu\text{m}$ ). 15 keV. dog  
2130. 115
- Figure 38b. Higher magnification of Figure 38a (scale bar =  
10  $\mu\text{m}$ ). 15 keV. dog 2130. 115
- Figure 39. Thrombogenicity index vs. critical surface  
tension for experimental animals 2442, 2504,  
and 2297. (●) is silicone rubber, (○) is  
15% HEMA/5% NVP, (△) is 10% HEMA/10% NVP,  
(▲) is 0% HEMA/20% NVP. 122
- Figure 40. Thrombogenicity index vs. contact angle for  
experimental animals 2442, 2504, and 2297.  
(●) is silicone rubber, (○) is 15% HEMA/  
5% NVP, (△) is 10% HEMA/10% NVP, (▲) is  
0% HEMA/20% NVP. 123

## LIST OF TABLES

	<u>Page</u>
Table 1. Review of Catheter Literature	3
Table 2. Chemical formulae for HEMA and NVP	7
Table 3. Blood compatibility testing of hydrogel coated devices	10
Table 4. Hydrogel deposition thickness	23
Table 5. Surface energies of the liquids used in the contact angle measurements	31
Table 6. Results of the contact angle determinations	32
Table 7. Comparison of contact angle measurements	34
Table 8. Experimental data for dog 2148	36
Table 9. Experimental data for dogs 2346 and 2130	41
Table 10. Analysis of cellular deposition thickness on catheter surfaces for dog number 2146	117
Table 11. Formulations compared to the Silastic <sup>®</sup> control, method 2	118
Table 12. Experimental data for dogs 2442, 2504, 2232, and 2297, Method 3	119
Table 13. Results of the 5 minute implantation of catheters, Method 3	120

## LIST OF SYMBOLS

pHEMA	poly (hydroxyethyl methacrylate)
pNVP	poly (n-vinyl pyrrolidone)
EMA	ethyl methacrylate
SiR	silicone rubber
PE	polyethylene
PVC	polyvinyl chloride
PVC(1)	polyvinyl chloride supplied by Dural Plastics, Ltd., Dural, NSW, Australia
PVC(2)	polyvinyl chloride supplied by Portex, Ltd., Hythe, Kent, England
H-RSD	heparinized hydrophilic polymer
SEM	scanning electron microscopy
TEM	transmission electron microscopy
ESCA	surface analysis with X-ray photoelectron spectroscopy
IPN	interpenetrating network
F	French gauge
$\mu\text{m}$	micrometer
I.V.	intravenous
RBC	red blood cell
WBC	white blood cell
USCI	A division of C.R. Bard, Inc.
B-D	Becton-Dickinson
Mrad	megarad

$\gamma_C$	critical surface tension
$\gamma_L$	surface tension of a liquid
$\gamma_S$	surface tension of a solid
$\gamma_{SL}$	solid-liquid interfacial surface tension
EDTA	edetic acid
wt.	weight

## INTRODUCTION

Venous catheters are commonly employed for long-term intravascular access. Hecker (1979) states that there is ample evidence that thrombiform on vascular catheters, but that few studies have addressed this problem. Thrombus formation on the catheter surface can lead to catheter occlusion or vessel occlusion, both of which require treatment to correct the problem and placement of a new catheter at a different site. Also with thrombus formation, emboli formation and migration may lead to death. Since the vascular catheter is probably the most frequently used implant in man, development of a hemocompatible material which may diminish the risks associated with long term catheterization is desirable.

A series of polyhydroxyethyl methacrylate (HEMA) and/or N-vinyl-2-pyrrolidone (NVP) copolymers were radiation grafted onto a silicone rubber substrate by Vale and Greer (Vale, 1980, pp. 71-139) to produce materials of varied wettability, but similar texture. These materials were found to produce acceptable results when tested in an ex-vivo arterial shunt system and consequently were chosen as candidates for testing as catheter coatings.

In this study, the series of copolymers of HEMA and/or NVP were radiation grafted onto silicone rubber tubing to determine whether changing the hydrophobic character of the silicone rubber could increase its thromboresistance. The coated silicone rubber catheters were tested by implantation in the venous system of the dog.

## LITERATURE REVIEW

### Catheters

Catheters are used for a number of diagnostic monitoring purposes; these include: pressure measurements within the arterial and venous systems, continuous blood sampling, and angiography. Therapeutically, they are used for long-term venous infusions.

A tabulated review of selected catheter literature follows. The table emphasizes current experimental data and clinical evaluations. This offers an overview of some of the recent investigations of catheter testing and the results of these trials.

As can be seen in Table 1 there are some discrepancies in findings. Durst et al. (1974a), Hoar et al. (1978), and Hecker (1979) all report thrombus formation on the catheters tested, while Bottino et al. (1979) reports that 91% of the catheters were unassociated with any clinical complications. Durst et al. (1974b) reported no difference between siliconized and control surfaces, while Welch et al. (1974), Boros et al. (1975), and Hecker (1979) reported that silicone rubber catheters produced a favorable response. Lisback and Kollmeyer (1979) found no positive correlation between catheter roughness and resulting thrombus formation, while Bourassa et al. (1976) and Hecker and Edwards (1981) associated surface irregularities with thrombus formation.

### Hydrogels

Hydrogels are a family of synthetic polymers which are capable of imbibing large amounts of water. They were first introduced as useful

Table 1. Review of Catheter Literature

Author, Date	Subjects	Material
Durst, et al. 1974(a)	dogs	Cook Teflon Cordis Polyurethane Cook PE USCI Dacron Red Kifa PE B-D PE Rothene Elecath PE
Durst, et al. 1974(b)	3 dogs	5 uncoated 5 silicone coated, & 5 heparin coated PE catheters
Welch, et al. 1974	21 dogs	PE and Silastic <sup>R</sup> catheters
Anderson, et al. 1974	-----	Teflon, PE, and Polyurethane. (15 of each)
Boros, et al. 1975	20 newborn infants	10 Silastic <sup>R</sup> 10 PVC
Kaganov, et al. 1979	human	HEMA Coated PE
Bourassa, et al. 1976	human	Polyurethane and Polyethylene Catheters
Clawson and Boros, 1978	-----	Silastic <sup>R</sup> PVC
Hoar, et al. 1978	10 cardiac surgery patients	Swan-Ganz Catheters

Location, Duration	Analysis
Right Femoral Artery, 30 cm of catheter Exposed to Free Flowing Blood; 1 Hour	All Catheters Proved to be Thrombogenic
Abdominal Aorta; 30 Minutes	No difference between control and siliconized surfaces, Heparinized showed no fibrin buildup.
External Jugular Veins; (8) on Alternative even days (10) at 10 days (3) at 10 days, excised in situ.	Silastic-small amount of reaction, vein remained patent. P.E. - Consistently thrombosed, little observable flow.
SEM Study	Although the presence of surface irregularities are of interest, clinical significance requires further investigation.
Umbilical Artery; Silastic 24-164 hrs. PVC 35-232 hrs.	Silastic - 9 normal, 1 thrombosed PVC - 1 normal, 9 thrombosed.
Femoral, Subclavian and Jugular Veins; Duration 2-7 days.	No formation of thrombi was observed nor did the catheters cause phlebitis
Coronary Arteriography via femoral approach; 10-12 minutes	Surface irregularities play an important role in the initiation of thrombosis.
SEM Study	Although Silastic is smoother, differences are minimal.
Pulmonary Artery via the external Jugular; 104 ± 6 minutes.	Thrombus found on all catheter surfaces

Table 1. (continued)

---

Author, Date	Subjects	Material
Wilner, et al. 1978	Adult Dogs	PE, Teflon, Wired PE, Polyurethane, Woven Dacron
Yonaha, 1978	Human	Heparinized - Hydrophilic polymer (H-RSD), PVC, PE, Teflon, Silicone Rubber
Bottino, et al. 1979	81 Patients with malign- ant diseases	Silicone Elastomer
Hecker, 1979	48 ewes sheep	PE, PVC(1), PVC(2), Silicone Rubber
Lisback and Kollmeyer, 1979	8 Adult Dogs	Argyle Umbilical Catheters (PVC).
Mortensen & Schaap; 1980	Adult Dogs	Commercial and Proprietary catheters
Hecker and Edwards; 1981	40 ewes sheep	Polyvinylchloride Tubing of Varying Surface Roughness

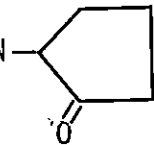
---

Location, Duration	Analysis
Femoral Artery; 30 Minutes	Platelet and Fibrin Deposition.
Central vein; 3 to 85 days	Thrombus formation and a large number of platelets seen in PVC, PE, Teflon, 70% of SiR and 14% of H-RSD.
Basilic or Cephalic vein; 5 to 171 days, 45 days mean time	91% of the catheters were un-associated with clinical complications.
Right Saphenous Vein Right Femoral Artery; 9 days	Significantly more thrombosis on venous than arterial catheters. PE most thrombosed, SiR least thrombosed PVC(1) produced most renal infarction.
Superior Vena Cava, Descend- ing thoracic aorta, Abdominal aorta, Inferior Vena Cava; 200 ± 30 minutes.	Found no positive correlation between catheter roughness and catheter thrombus formation.
Carotid, Brachial and femoral arteries; 30 minutes	Thrombogenicity index, mg/mm <sup>2</sup>
Saphenous vein and Aorta; 9 days	More thrombus on rougher tubing, but smoother tubing was associated with considerably greater areas of renal infarction

biomaterials by Wichterle and Lim in 1960. Their usefulness as biomaterials is handicapped because they are generally weak when unsupported. Because of their lack of mechanical strength, techniques to incorporate or graft the hydrogel onto a substrate material, e.g. silicone rubber, were initiated by Predecki (1974) and Ratner and Hoffman (1974).

The monomers used to prepare hydrogels are 2-hydroxyethyl methacrylate (HEMA) and N-vinyl-2-pyrrolidone (NVP). Their chemical formulae are given in Table 2.

Table 2. Chemical formulae for HEMA and NVP

Monomer	Chemical Formula
HEMA	$\begin{array}{c} \text{CH}_2 = \text{C} - \text{COOCH}_2\text{CH}_2\text{OH} \\   \\ \text{CH}_3 \end{array}$
NVP	$\text{CH}_2 = \text{CH} - \text{N} - \begin{array}{c} \diagup \\ \text{---} \\ \diagdown \\ \text{O} \end{array}$ 

The HEMA monomer can be polymerized by cobalt-60 irradiation to form a chemically stable three-dimensional gel. The gel is hydrophilic due to the presence of large numbers of hydroxyl groups within its structure.

The NVP monomer is unique because in its uncrosslinked form it is extremely soluble in water and many other polar and nonpolar solvents. Because of this strong interaction with water, the NVP monomer can be used for preparing gels that will exhibit high water contents. (Hoffman

et al., 1977).

A number of hypotheses have been offered to explain why the hydrogel family may be successful biomaterials. One hypothesis is that if a surface were similar to a plane through an aqueous saline solution, there could be no driving force for either protein adsorption or platelet adhesion, and thus no clotting (Kronick and Rembaum, 1977). Hydrogels with a high water content might resemble such a structure.

Another hypothesis suggests that a proper distribution of hydrophilic (both neutral and charged) and hydrophobic regions on a biomaterial interface could yield the optimum synthetic biocompatible material (Nakashima et al., 1977). By polymerizing monomers of hydrophilic and hydrophobic character, this distribution could be achieved.

Jhon and Andrade (1973) state that the organization of water molecules at the interface strongly influences the interfacial free energy, which affects the thrombus formation process. The water structure in living tissues has been studied, and it is believed that some amount of water is associated with the macromolecules in the tissue. In the hydrogels, it has been shown that there is also some water bound to the polymer. This suggests that binding of water to the polar groups in the hydrophilic material might play an important role in the inhibition of blood coagulation (Nakashima et al., 1977).

Baier (1972) argues that compatibility of biomaterials is based upon the critical surface energy. A material with a critical surface tension of 20-30 dynes/cm is the most compatible. This region offers an optimum surface for plasma protein adsorption in that the proteins

will not denature. Denaturation may initiate the coagulation process. The flexibility in the choice of monomers and solvents allows for control of the surface characteristics as shown by Vale (1980). With the proper combination, the possibility of achieving a low surface energy may exist.

Andrade (1973) argues that zero interfacial free energy is the parameter which should be considered instead of critical surface tension or surface free energy. By having zero interfacial free energy, the blood-solid interface would essentially be eliminated. The ability of the hydrogel system to imbibe up to 90% its own weight in water may reduce the interfacial energy to a minimal value.

Successful applications of hydrogel coated devices have been reported by a number of investigators. Selected examples are tabulated in Table 3.

### Thrombosis

The primary event following contact between a foreign surface and blood is the deposition of a stable film of plasma proteins (albumins, globulins, fibrinogens, etc.). This occurs almost instantly (Beugeling, 1979; Barber et al., 1978; Kronick and Rembaum, 1977; Fromageot et al., 1976; Baier and Dutton, 1969). This is followed by a series of reactions involving platelet activation and release of additional clotting factors, platelet aggregation, fibrin strand formation and the formation of an interaggregate mesh of fibrin strands that trap cells (Dutton et al., 1969; Baier and Akers, 1978). Since the earliest common event is

Table 3. Blood compatibility testing of hydrogel coated devices

Investigator	Hydrogel	Application
Singh & Melrose 1971	HEMA on suture material	sutures in dog atrium
Hoffman & Harris 1972	HEMA, NVP on silicone rubber	enhanced blood compatibility
Kaganov et al. 1976	HEMA on polyethylene	catheters
Abrahams and Ronel 1976	HEMA coated catheter	arterial, venous and tissue O <sub>2</sub> monitoring
Greer & Knoll 1980	HEMA on Dacron velour	arterial prosthesis
Vale & Greer (Vale, 1980 pp. 71-139)	HEMA/NVP on silicone rubber	ex-vivo A-V shunts

proteinaceous film deposition, any adsorption of an activatable factor of blood constituents must involve displacement of, or interaction with, this initially formed macromolecular monolayer (Beugling, 1979; Fromgeot et al., 1976). Thus, the chemical constitution of this adsorbed film will determine the ultimate compatibility of the surface.

There is evidence that fibrinogen is quantitatively the most important component of the adsorbed layer on both the hydrophilic and hydrophobic surfaces (Barber, et al., 1978). Albumin has been shown to passivate the rate of thrombus formation while fibrinogen accelerates the deposition rate (Barber et al., 1979; 1978). Therefore, the most suitable material may be one which adsorbs minimal amounts of

fibrinogen during the initial time period of blood contact (Barber et al., 1979; 1978).

The adsorption of the clotting factors to various catheter surfaces may be influenced by a variety of parameters such as flow conditions, surface properties, catheter size, morphology, duration of infusion and interactions with the plasma proteins and platelets. A possible explanation for surface influence is direct activation of the clotting mechanism due to the severe conformational alterations of the deposited proteins adsorbed to high and very low energy surfaces, and lesser modification of proteins adsorbed onto materials of mid range critical surface tensions (Wilner et al., 1978).

### Surface Energy

A surface can be represented by a surface energy, a measure of the unsatisfied bonding capacity of the surface (Figure 1). The surface energy may be a result of unsatisfied primary or secondary bonds. Surface tension is often used in describing a surface. The surface atoms in any condensed phase are attracted towards the bulk. The atom-depleted surface is then in tension Figure 2. Solids may have minimal or zero surface tension. The surface tension is also referred to as the surface free energy. Surface free energy can be measured using the concept of contact angle. When a drop of liquid (e.g. water) is placed on the surface, it will come to an equilibrium state characteristic of the surface and the surface free energy. The angle,  $\theta$ , which is the angle of a tangent at the bubble/surface interface Figure 3 is

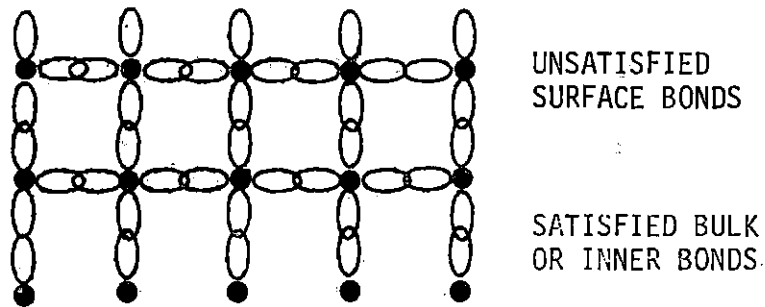


Figure 1. Schematic illustration of the unsatisfied bonding capacity at a free surface. (Andrade, 1973).

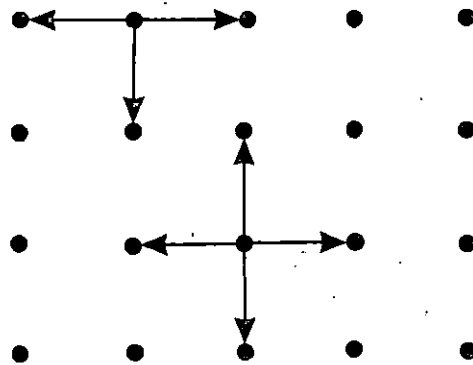


Figure 2. The asymmetric nature of the forces exerted on surface atoms resulting in an attraction towards the bulk. The atom depleted surface is then in tension. (Andrade, 1973)

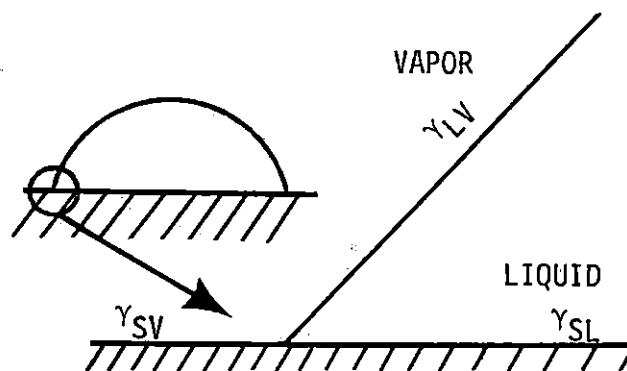


Figure 3. The contact angle measurement. (Andrade, 1973).

then described as the contact angle, and is a measure of the surface energy. This is the angle used in the Young-Dupree Equation for surface energy,  $\gamma_{SV} = \gamma_{SL} + \gamma_{LV}(\cos \theta)$ . If  $\theta = 0$ , the liquid spreads completely and the surface is said to be completely wettable. The critical surface tension ( $\gamma_c$ ) is defined as  $\cos \theta = 1$  and is sometimes used in predicting the compatibility of the substrate (Andrade, 1973). This value is obtained by extrapolating to  $\cos \theta = 1$  the Zisman plot of  $\cos \theta$  vs.  $\gamma_L$ . These types of measurements are used to determine the hydrophilicity ( $\theta$  approaches 0) or hydrophobicity ( $\theta$  greater than 0) of the substrate.

Hoffman et al. (1977) state that the biological data on radiation grafted hydrogel polymer materials in general support a picture of a hydrophilic, low energy interface where proteins and cells adhere less strongly. Also, studies on surface induced coagulation indicated that the low energy hydrophobic polymer surfaces (e.g. silicone rubber) are less platelet adherent than high energy surfaces (Lymen, 1972).

## MATERIALS AND METHODS

## Techniques

Fabrication

Radiation grafting according to methods developed by Ratner and Hoffman (1974, 1975) was used to coat silicone rubber tubing (Dow Corning, Silastic<sup>®</sup> Medical Grade Tubing, Lot H030081, 0.030 in I.D. x 0.065 in . O.D.). The Silastic<sup>®</sup> tubing, cut to 100 mm lengths, was ultrasonically washed with a nonoily soap (Ivory<sup>R</sup> Flakes) for 15 minutes, rinsed three times in deionized water, and stored in distilled water. A clean glass capillary tube (0.7-1 mm O.D.) was inserted into the Silastic<sup>®</sup> tubing to act as a support to ensure that the Silastic<sup>®</sup> would maintain a straight profile while suspended in the monomer solutions, see Figure 4.

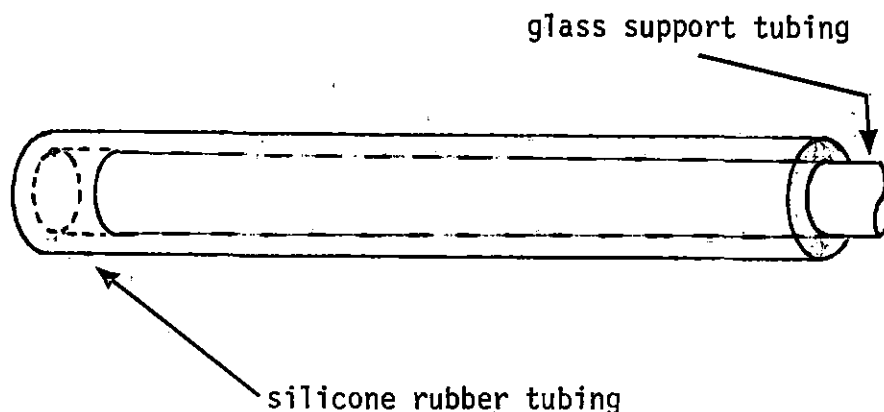


Figure 4. Schematic diagram of glass capillary support tubing inserted in the Silastic<sup>®</sup> tubing.

The Silastic<sup>®</sup> tubing was suspended in pint jars which were filled with monomer solutions in a solvent of 15% methanol, 65% water. The five monomer solutions used were 20% HEMA<sup>1</sup>/0% NVP<sup>2</sup>, 15% HEMA/5% NVP, 10% HEMA/10% NVP, 5% HEMA/15% NVP and 0% HEMA/20% NVP. The solutions were de-oxygenated by bubbling nitrogen gas through the solution for 30 minutes. Then, a 0.25 Mrad dose from a cobalt-60 source was used for polymerization.

After grafting, the Silastic<sup>®</sup>/Hydrogel tubes were removed from the bulk polymer. Adhering bulk polymer was removed by vigorous rubbing with a gauze pad soaked in an ethanol/water mixture, (50:50 v/v). The tubes were then soaked in this mixture for 30 minutes to leach out any unreacted monomer. After soaking, the tubes were stored in distilled water.

#### Blood Data

Healthy, mongrel dogs weighing 16-22 kilograms were used for the experiments. Data recorded for each dog included the following: weight, sex, and activated coagulation time. For some dogs hematocrit and platelet count were also recorded. Hematocrit was determined from venous blood collected in a vacuum tube containing 5 mg EDTA (vacutainer #6453)<sup>3</sup>. Capillary tubes were filled with the venous blood and then

---

<sup>1</sup>HEMA Purchased from Alcolac, Lot No. B889F9.

<sup>2</sup>NVP Purchased from Monomer-Polymer & Dajak Labs, Inc., Lot No. 236-12.

<sup>3</sup>Becton-Dickinson of Beckton, Dickinson and Co., Rutherford, NJ.

centrifuged. The percent hematocrit was read using a Spiracrit Microhematocrit Tube Reader.

Activated Coagulation Time (ACT) was determined by allowing 2 milliliters of venous blood to fill a vacuum tube containing 12 mg of silicious earth (Vacutainer #6522)<sup>1</sup>, incubating the tube at 37°C, and recording the time required for the first clot to appear.

Platelet counts were made using the Platelet Unopette<sup>®</sup><sup>2</sup> method. Venous blood, diluted in an ammonium oxalate solution, was used to charge a hemacytometer. Platelets in the center square were then counted and the result multiplied by 1000 to determine the count.

### Surgery

Method 1 The dogs were fasted overnight and anesthetized with sodium pentobarbital. Presurgery blood values were determined. Cut-downs were performed to expose both jugular veins. The fasciae covering the vessels were removed. Side branches near where the catheters were to be introduced were ligated. A slit was made in the vessel wall to introduce a plastic sheath which was then held in place by a purse string suture pattern, (see Figure 5), similar to the technique described by Anderson et al. (1974). This allowed repeated access to the venous system. After catheter placement using the plastic sheath, a lactated Ringers solution drip insured that the lumen of the catheter remained patent.

---

<sup>1</sup>Becton-Dickinson of Beckton, Dickinson and Co., Rutherford, NJ.

<sup>2</sup>Becton-Dickinson of Beckton, Dickinson and Co., Rutherford, NJ.

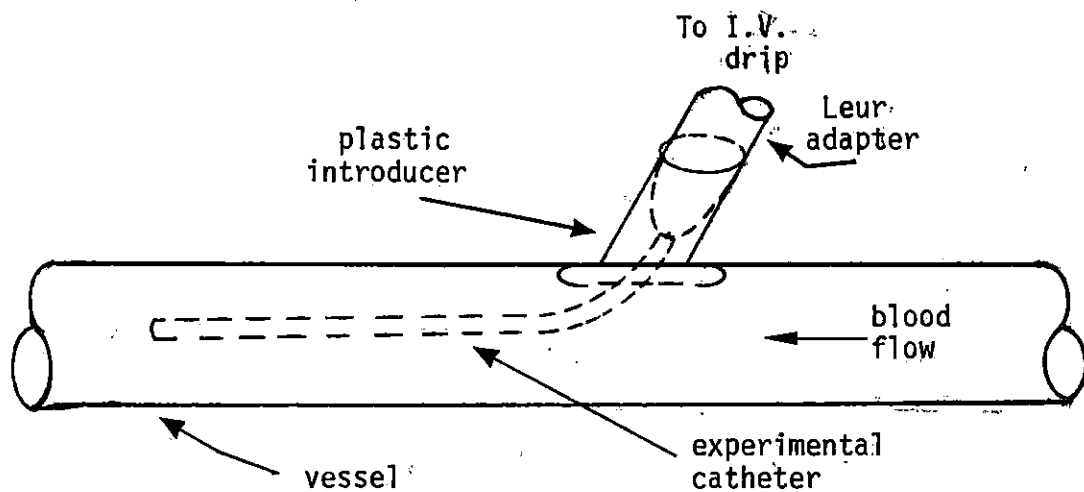


Figure 5. Schematic diagram of the catheter introduction unit placement in the external jugular vein, method 1.

Sampling times were at 15, 30, and 60 minutes. At the end of each period, the catheter was slowly withdrawn through the slit and suspended in a 2% glutaraldehyde/Sorenson's buffer solution (Hayat, 1970). A new catheter of the same formulation was then inserted for the next time period, e.g. 30 minutes. After the 60 minute period, a new series using a different formulation was begun. This continued until all 5 formulations and the Silastic<sup>®</sup> control were exposed.

Method 2 The Method 1 protocol was modified in the following manner. A 7 mm longitudinal slit was made in the vessel to permit introduction of the catheter. After catheter insertion, the slit was held closed around the catheter with a mosquito hemostat as shown in Figure 6.

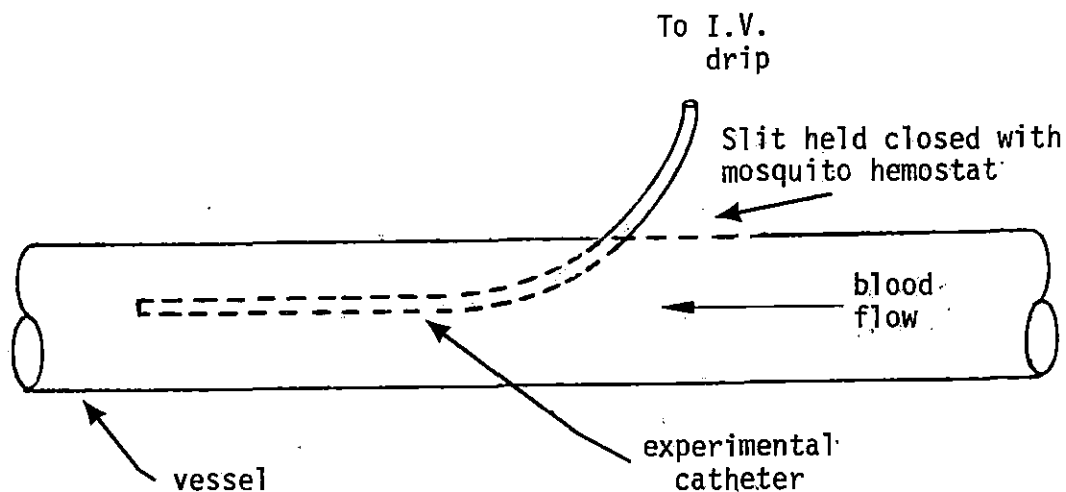


Figure 6. Schematic diagram of the catheter placement in the external jugular vein, method 2.

Method 3 The dogs were fasted overnight and anesthetized with sodium pentobarbital. Cutdowns were performed to expose both jugular veins and both femoral veins. The fasciae covering the vessels were removed. The side branches near where the catheters were to be introduced were ligated. Blood flow was interrupted by clamps proximal and distal to the introduction site. The catheter was filled with saline and clamped distally with a hemostat; this prevented blood from entering the lumen. A puncture was made in the vessel wall with an 18 gauge needle and the catheter was inserted in a retrograde fashion at the puncture site, see Figure 7. The clamps were removed from the vessel and the catheter exposed to blood for 5 minutes. The clamps

were again placed on the vessel, and the vessel wall was slit longitudinally to allow removal of the catheter. The catheter was fixed in a 2% glutaraldehyde/Sorenson's buffer solution.

Both presurgery and post surgery catheter weights were recorded to allow determination of thrombus weight. The thrombus weight was divided by the surface area exposed to the blood to determine a thrombogenicity index for the implants:

$$\text{Thrombogenicity index} = \frac{(\text{post surgery catheter wt}) - (\text{presurgery catheter wt})}{\text{surface area exposed}}$$

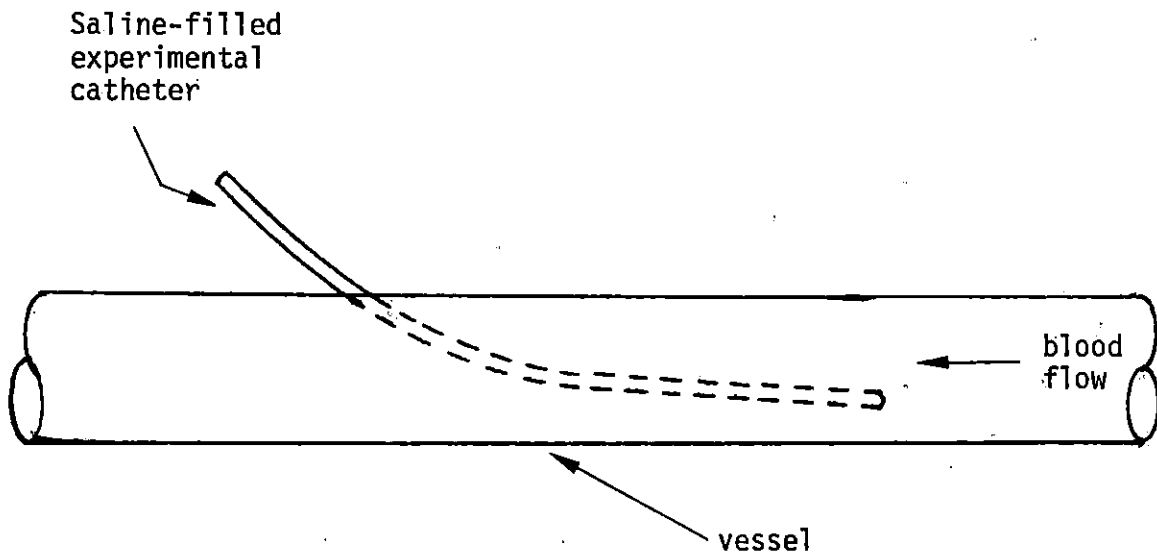


Figure 7. Schematic diagram of the catheter placement in the vessel, method 3.

### Scanning Electron Microscopy

After glutaraldehyde fixation, the samples were dehydrated in a series of acetone rinses (30, 60, 75, 90, 100, 100%, 30 minutes each), sectioned in 8,  $\frac{1}{4}$ " sections, (See Figure 8), and critical point dried with  $\text{CO}_2$ . After drying, the sections were then hemisected. Sections 1, 3, 5, and 7 were mounted, using colloidal graphite, on aluminum stubs to permit observation of the outer, blood contacting surfaces. Sections 2, 4, 6, and 8 were used to obtain cross-sectional thrombus layer information. The samples were sputter coated with 200 Å of gold and examined in a JOEL-U3 scanning electron microscope at 5-15 KeV. Micrographs made at 25x to 5000x were used to examine the homogeneity of cellular deposition, platelet numbers, and cellular condition.

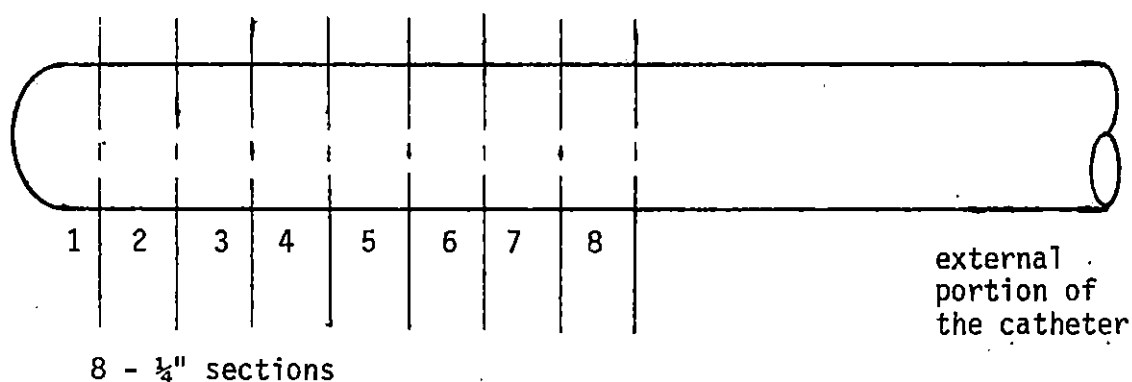


Figure 8. Sectioning of the catheter for SEM analysis.

### Contact Angle Determination

The contact angles for the Silastic<sup>®</sup>, (Medical Grade Silastic<sup>®</sup> Non-Reinforced Sheeting, Lot No. H118110), 0% HEMA/20% NVP, 10% HEMA/10% NVP, and 5% HEMA/15% NVP were determined using the following liquids: (1) water, (2) glycerol, (3) pyridine, (4) benzene, (5) formamide, (6) chlorobenzene, and (7) O-dibromobenzene. A drop of each liquid was placed on the water imbibed, blotted surface and photographed with a 35 mm camera with appropriate close up capabilities. The contact angles were measured directly from the photographs as shown in Figure 9.

The critical surface tension,  $\gamma_c$  was then found by plotting the cosine of the contact angle versus the  $\gamma_L$  of the contacting liquid. The intersection of the extrapolated line with  $\cos \theta = 1$  yielded the value for  $\gamma_c$  of the material.

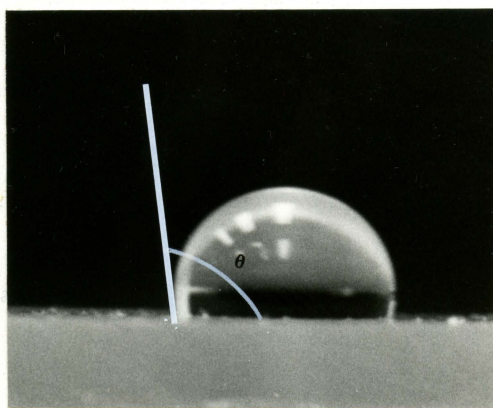


Figure 9. Measurement of contact angle of  $H_2O$  on silicone rubber.

### SEM Micrograph Ratings

When method 2 was used, the SEM micrographs of the hydrogel surfaces were compared to those of the control surface, silicone rubber. If the response was more reactive, a plus (+) is indicated; less reactive, a minus (-) is indicated; and for a similar response a (0) is indicated.

## RESULTS

## Materials

The materials which resulted from the radiation grafting of HEMA and/or NVP onto the substrate silicone rubber can be seen in Figures 10a through 10f. The microstructure in all cases is similar, with a thin coating of polymer on the samples containing 5% - 20% HEMA. Upon polymerization, the HEMA, in a poor solvent such as water, will precipitate. The precipitated polymer is covalently bonded to the substrate surface. In the case of the 0% HEMA/20% NVP copolymers, little deposition occurs since both H<sub>2</sub>O and methanol are good solvents for the NVP. Figure 11 shows a cross sectional view of the 15% HEMA/5% NVP formulation; the hydrogel coating thickness is 0.05 mm. The hydrogel deposition thicknesses for the five formulations are shown in Table 4.

Table 4. Hydrogel deposition thickness

Formulation	Thickness (mm)
20% HEMA/0% NVP	0.09
15% HEMA/5 % NVP	0.05
10% HEMA/10% NVP	0.05
5% HEMA/15% NVP	0.05
0% HEMA/ 20% NVP	—

- Figure 10a. Scanning electron micrograph of Silastic<sup>®</sup> (scale bar = 100  $\mu\text{m}$ ). 15 keV.
- Figure 10b. Higher magnification of Figure 10a (scale bar = 10  $\mu\text{m}$ ). 15 keV.
- Figure 10c. Radiation grafted 20% HEMA/0% NVP in silicone rubber (scale bar = 100  $\mu\text{m}$ ). 15 keV.
- Figure 10d. Higher magnification of Figure 10c (scale bar = 10  $\mu\text{m}$ ). 15 keV.

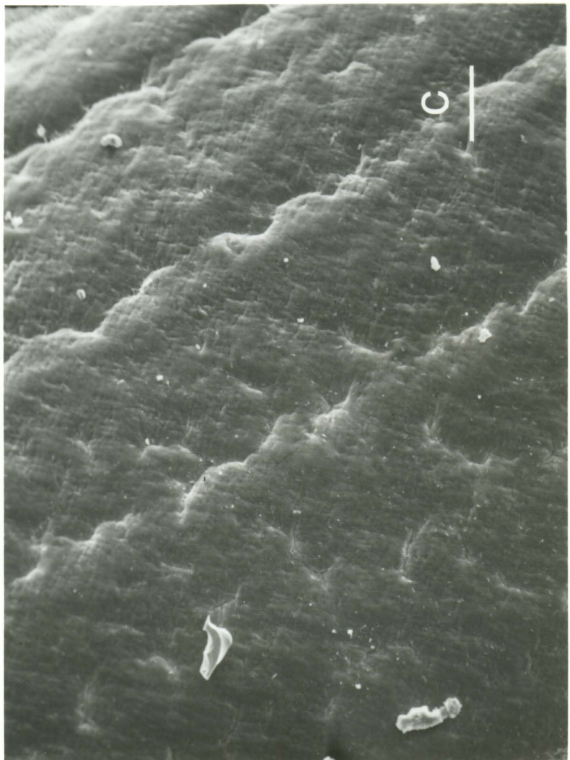
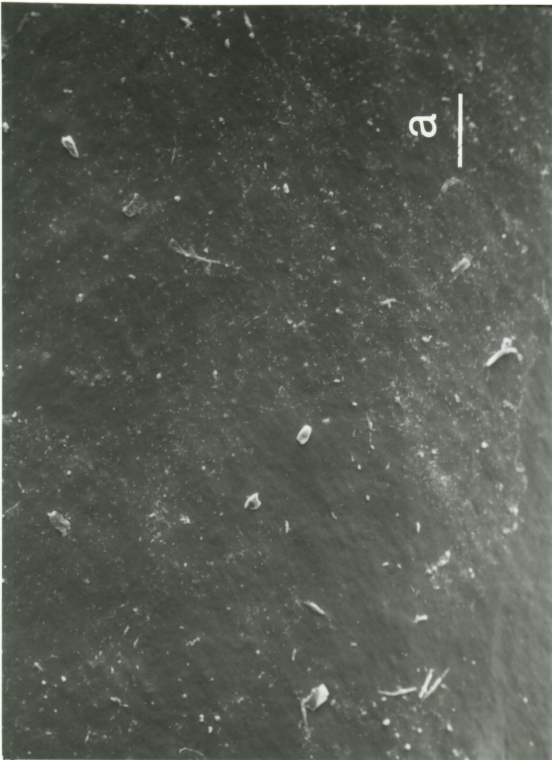
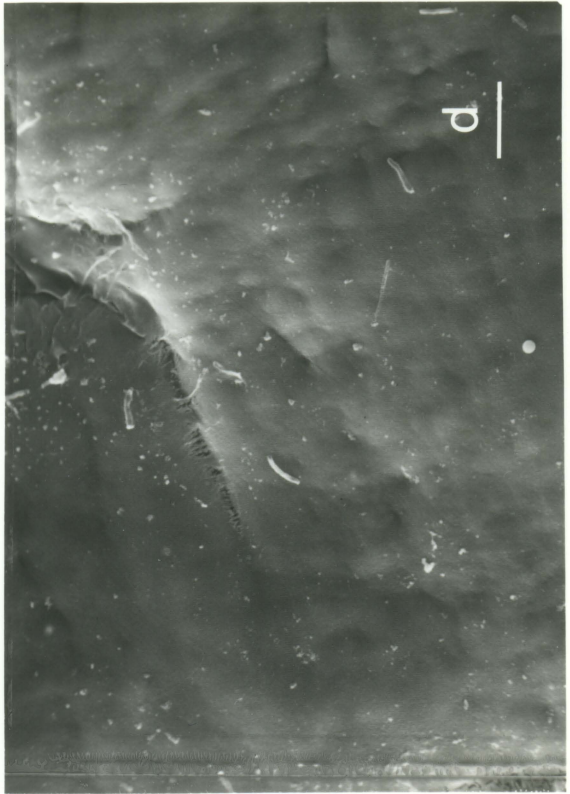
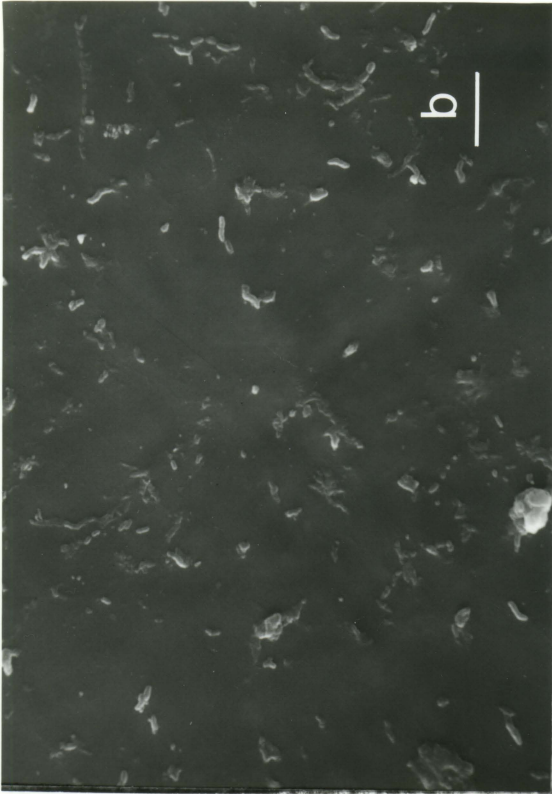


Figure 10e. Radiation grafted 15% HEMA/5% NVP on silicone rubber (scale bar = 100  $\mu\text{m}$ ). 15 keV.

Figure 10f. Higher magnification of Figure 10e (scale bar = 10  $\mu\text{m}$ ). 15 keV.

Figure 10g. Radiation grafted 10% HEMA/10% NVP on silicone rubber (scale bar = 100  $\mu\text{m}$ ). 15 keV.

Figure 10h. Higher magnification of Figure 10g (scale bar = 10  $\mu\text{m}$ ). 15 keV.

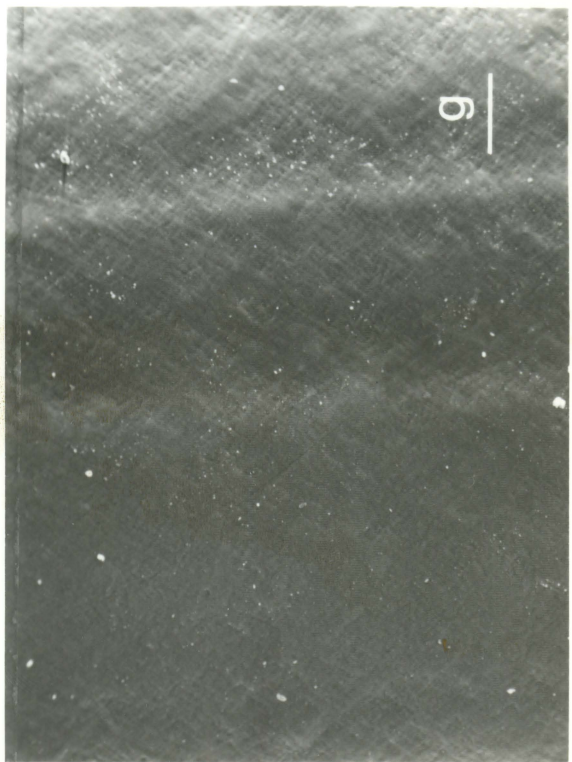
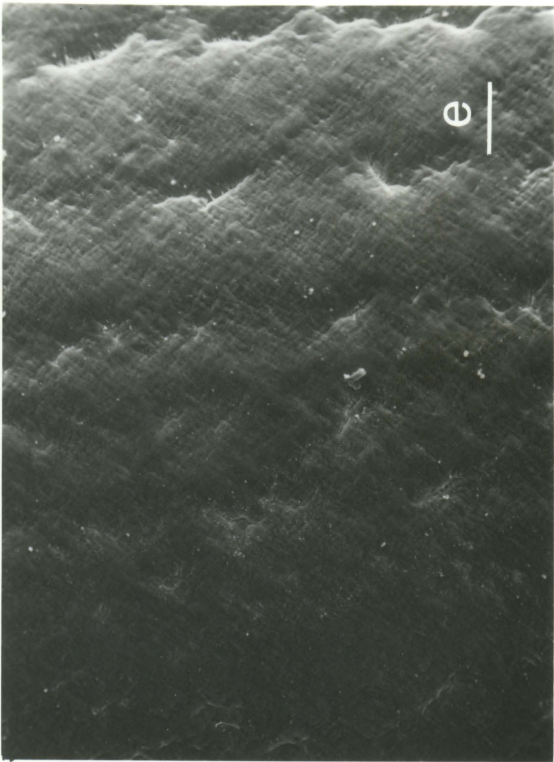
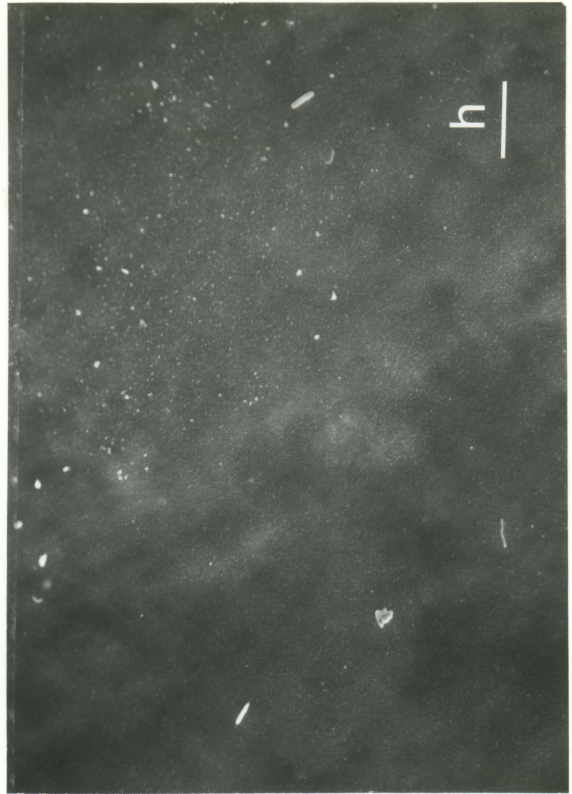
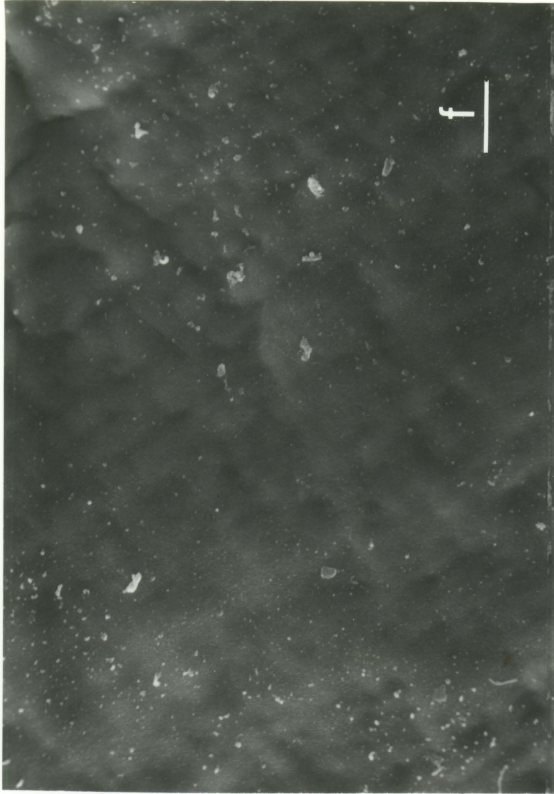
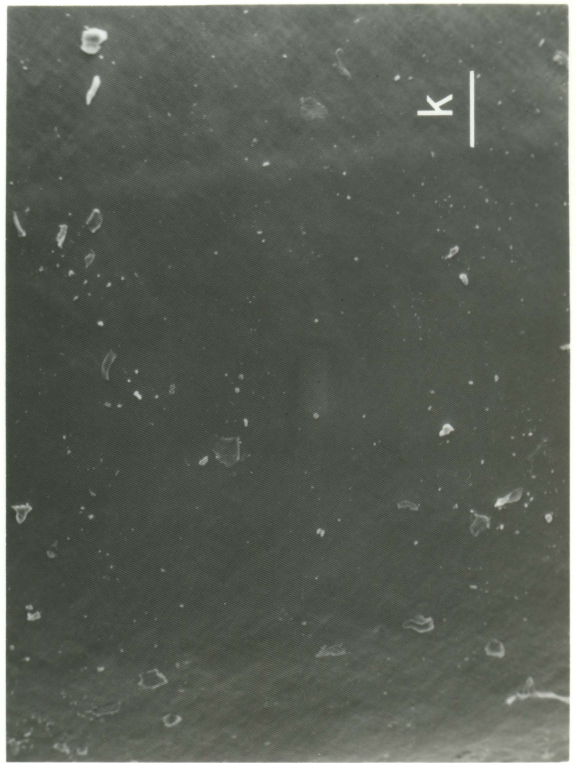
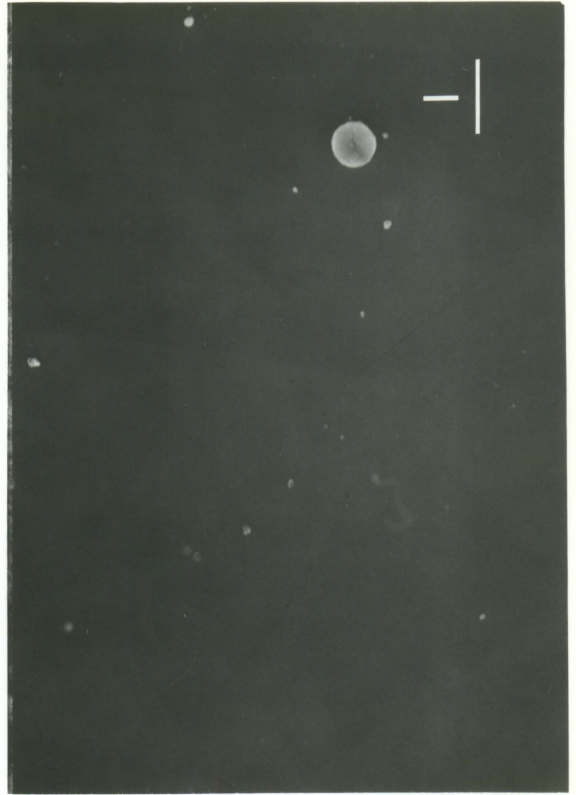
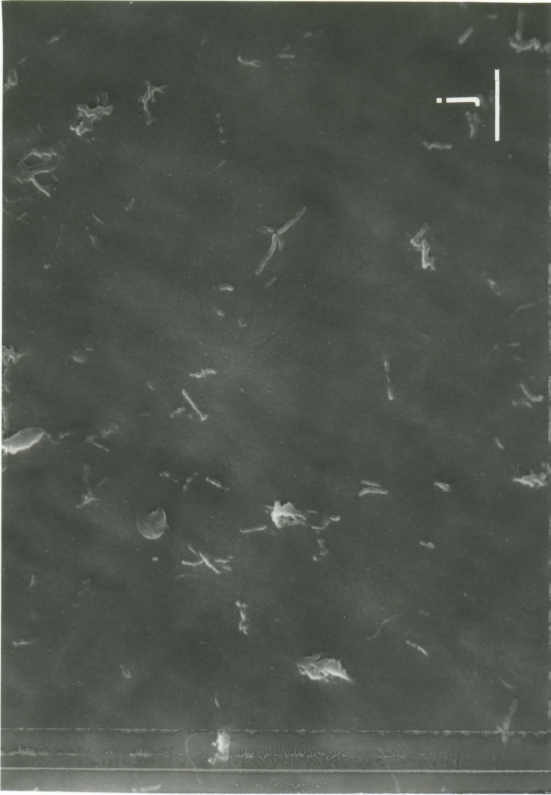


Figure 10i. Radiation grafted 5% HEMA/15% NVP in silicone rubber (scale bar = 100  $\mu\text{m}$ ). 15 keV.

Figure 10j. Higher magnification of Figure 10i (scale bar = 10  $\mu\text{m}$ ). 15 keV.

Figure 10k. Radiation grafted 0% HEMA/20% NVP on silicone rubber (scale bar = 100  $\mu\text{m}$ ). 15 keV.

Figure 10l. Higher magnification of Figure 10k (scale bar = 10  $\mu\text{m}$ ). 15 keV.



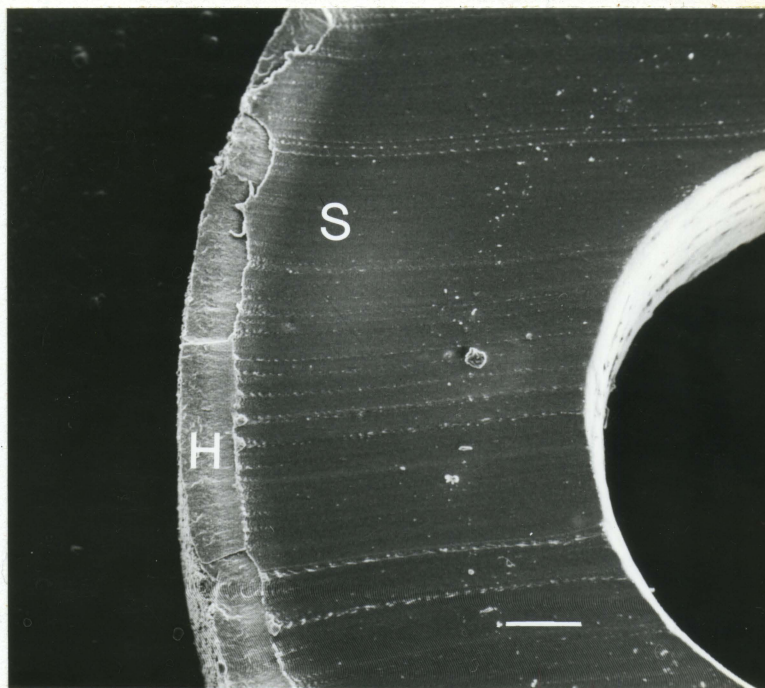


Figure 11. Crosssectional view of radiation grafted 15% HEMA/5% NVP on silicone rubber. (S) designates silicone rubber, (H) designates hydrogel coating. Hydrogel coating thickness is 0.05 mm. (scale bar = 100  $\mu$ m).

Table 5 lists the surface energies of the various liquids used in the contact angle determinations. Table 6 shows the results of the contact angle determinations. Figure 12 shows the Zisman plot for determining the critical surface tension from surface energy and contact angle.

Table 5. Surface energies of the liquids used in the contact angle measurements

Liquid	$\gamma_L$ (ergs/cm <sup>2</sup> )
H <sub>2</sub> O	72.8
Glycerol	63.4
Pyridine	38.0
Benzene	28.8
Formamide	58.2
Chlorobenzene	37.0
O-dibromobenzene	42.0

The contact angle measurements differ from the values reported by Vale (1980). Table 7 shows a comparison of the values. The differing values may be caused by variations in the compositions of different lot numbers for the components used. The HEMA used by Vale may have had more ethyleneglycol dimethacrylate, a crosslinking agent, which

Table 6. Results of the contact angle determinations

Formulation	H <sub>2</sub> O	Glycerol	Pyridine	Benzene	Formamide	Chloro- benzene	O-dibromo benzene
Silastic	100.3	89	32.7	22.3	91	32	52.5
15% HEMA 5% NVP	58	46	C.S. <sup>a</sup>	C.S.	41	C.S.	C.S.
10% HEMA 10% NVP	70	49.8	C.S.	C.S.	33.8	C.S.	C.S.
0% HEMA 20% NVP	90.5	88.5	C.S.	C.S.	89.5	25.5	55.3

<sup>a</sup>. C.S. designates that the liquid completely spreads on the substrate.

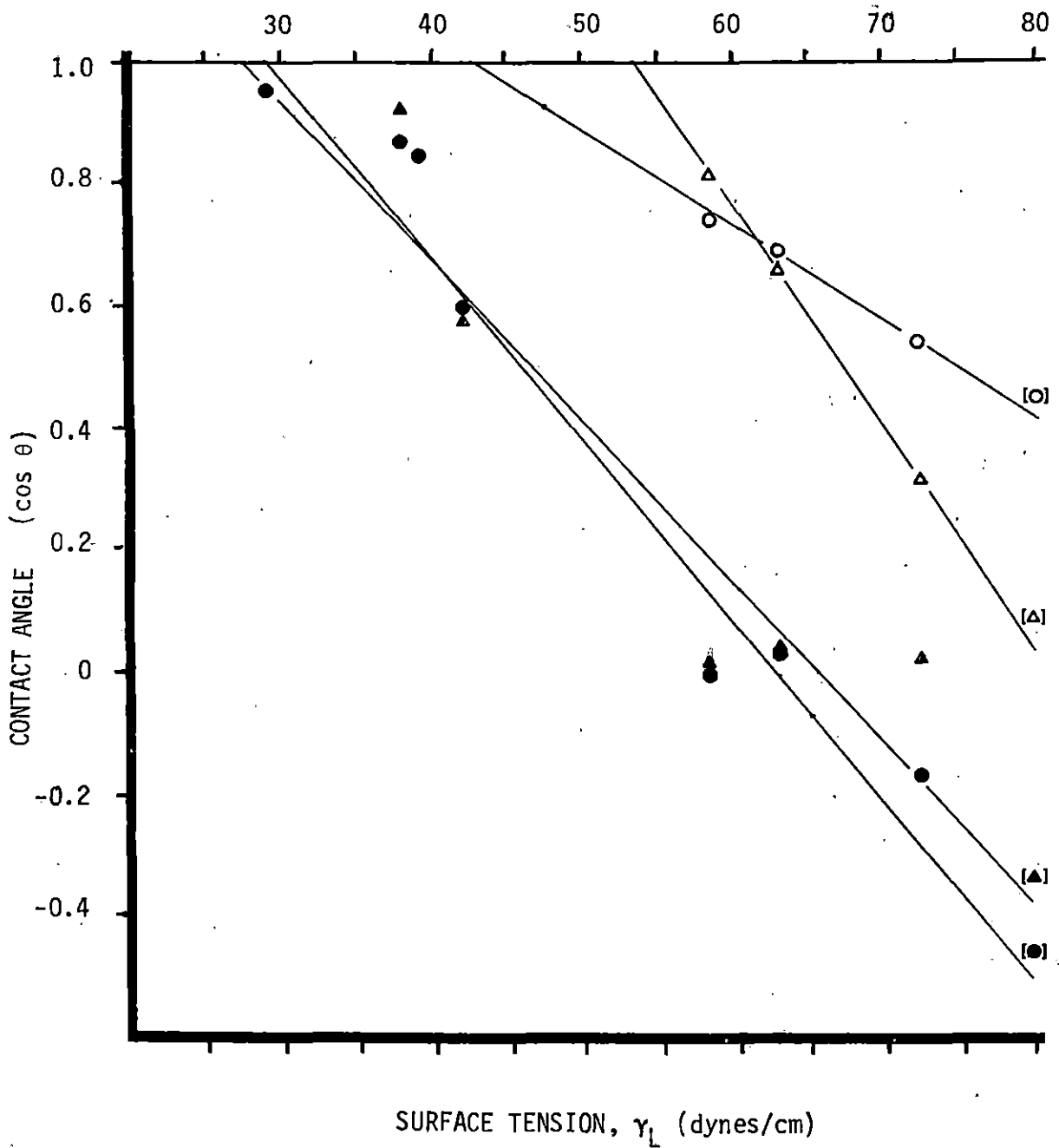


Figure 12. Zisman plot for determining the critical surface tension of each formulation. (●) is silicone rubber, (○) is 15% HEMA/5% NVP, (△) is 10% HEMA/10% NVP, (▲) is 0% HEMA/20% NVP. Linear regression was utilized for line placement.  $p \leq 0.06$  for all correlation coefficients.

Table 7. Comparison of contact angle measurements

	<u>Chemicals used in Methods 1 and 2</u>			<u>Chemicals used in Method 3</u>		
Silastic	Lot No.	HH0699	Dow Corning	Lot No.	H118110	Dow Corning
HEMA	Lot No.	unspecified	Alcolac	Lot No.	B889F9	Alcolac
NVP	Lot No.	unspecified	Alcolac	Lot No.	236-12	Alcolac
Silastic	80 <sup>a</sup>		--	100 <sup>b</sup>		
15% HEMA 5% NVP	69 <sup>a</sup>		84 <sup>b</sup>	58 <sup>b</sup>		
10% HEMA 10% NVP	57 <sup>a</sup>		40 <sup>b</sup>	70 <sup>b</sup>		
0% HEMA 20% NVP	87 <sup>a</sup>		88 <sup>b</sup>	91 <sup>b</sup>		

<sup>a</sup> Values reported by Vale (1980).

<sup>b</sup> Values measured in the experiments reported in this thesis.

would alter the polymerization process. A thicker layer of HEMA may mask the effect of the silicone rubber.

The results of the Zisman Plot for the various hydrogel coatings indicate that examination of the surface can indicate the effect of the hydrogel coating on the silicone rubber surface. Note that while the HEMA/NVP copolymer grafts have decreased the hydrophobicity of the silicone rubber substrate, the copolymers have raised the critical surface tension. The critical surface tension is an approximation of the surface free energy of the material.

### Implantation

A series of HEMA/NVP copolymers were radiation grafted onto silicone rubber tubing and implanted into the venous system of the dog. Three methods of implantation and the two methods of analysis were utilized in testing the response of blood to these materials. The results of each are as follows. A total of 7 dogs were used and are designated by their Laboratory Animal Resource identification number.

#### Method 1

The experimental data for dog 2148 are given in Table 8. In method 1, a plastic introducer was used to gain access to the venous system. Although this allowed repeated access for catheterization, this technique was inadequate due to formation of blood clots within the introducer. This clotting interfered with the catheter retrieval. Also, in some cases, the plastic introducer stripped adherent thrombus from the

catheter.

Table 8. Experimental data for dog 2148

Experimental Data

Method 1

Dog Number	2148
Hematocrit	36
Platelet Count (per mm <sup>3</sup> )	140,000
Activated Clotting Time (sec)	112
Formulations	Comp <sup>a</sup>
Implantation Site	Right and Left Jugular Veins
Time (minutes)	15, 30, and 60

<sup>a</sup> Comprehensive set - (1) Silastic, (2) 20% HEMA/0% NVP, (2) 15% HEMA/5% NVP, (3) 10% HEMA/10% NVP, (4) 5% HEMA/15% NVP, (6) 0% HEMA/20% NVP.

The dog was subsequently systemically heparinized (3 mg/kg) to counter this thrombus formation. Remaining formulations were evaluated as to density of platelets adherent to the surface. Figure 13 shows a platelet density counting area. The results of platelet counting can be seen in Figure 14a through 14c. As depicted in these graphs, the 0% HEMA/20% NVP copolymers had the lowest platelet density while the 10% HEMA/10% NVP and the 5% HEMA/10% NVP copolymers had higher platelet

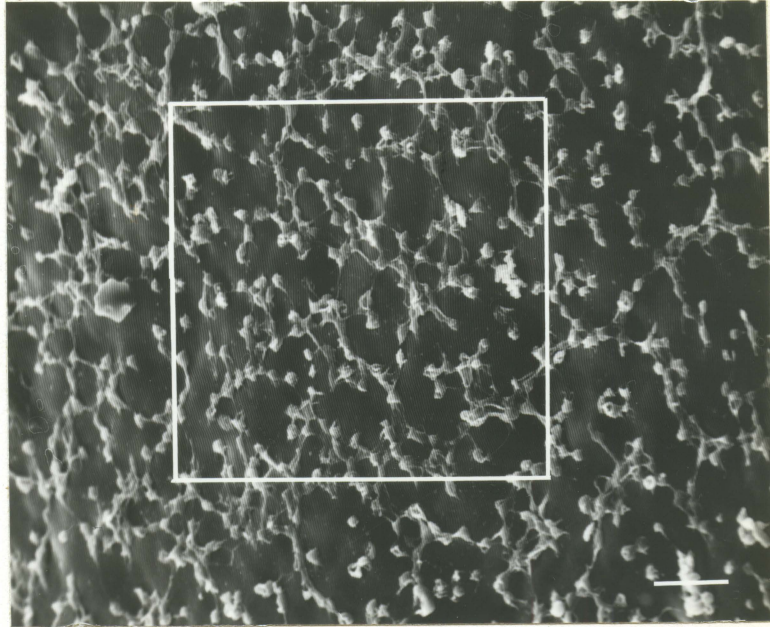


Figure 13. Sample platelet counting area (scale bar = 10  $\mu\text{m}$ ).  
The counting area equals 2500  $\mu\text{m}^2$ .

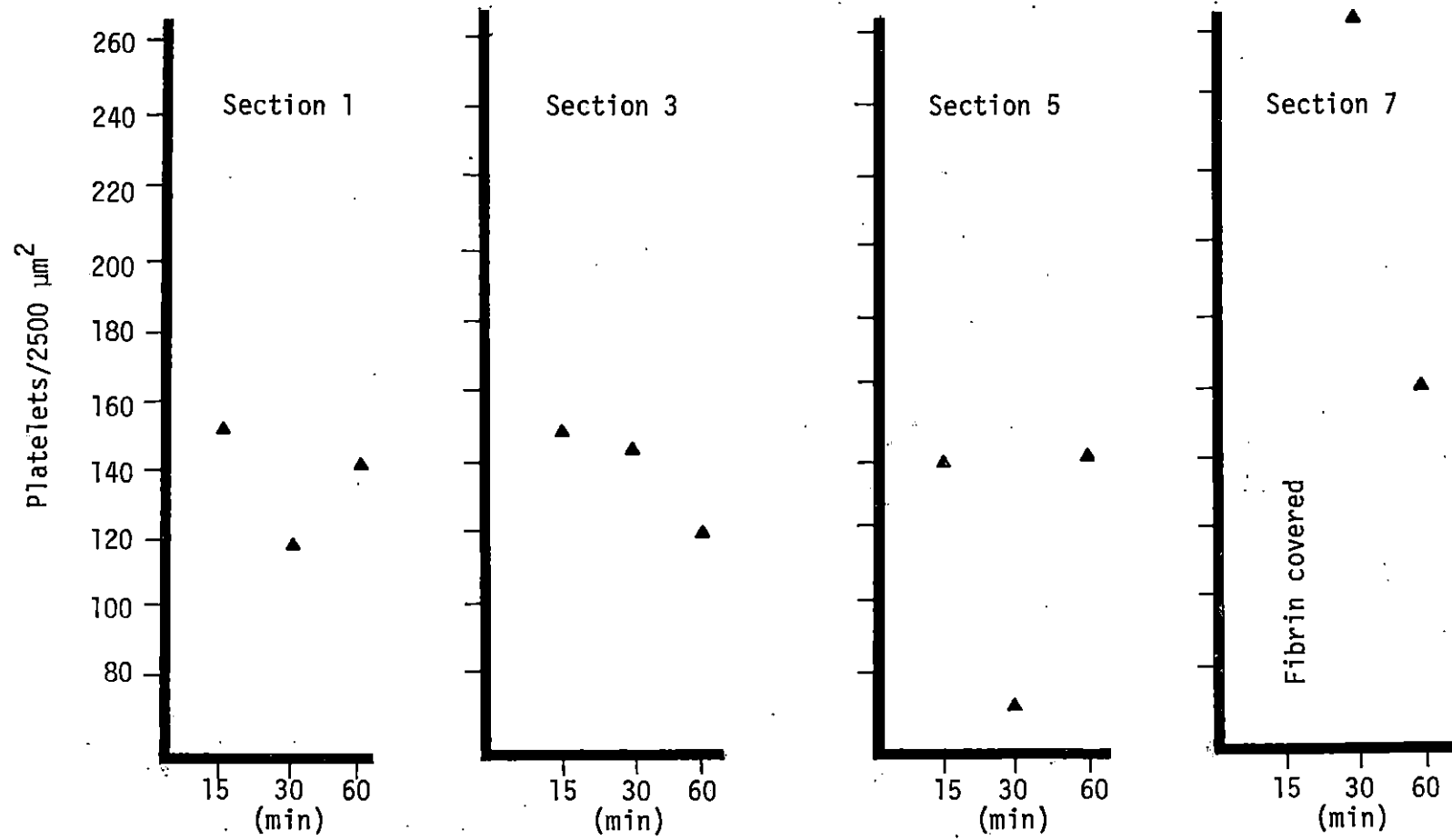


Figure 14a. Graphs of platelet densities for dog 2148. Catheter coating was 10% HEMA/10% NVP.

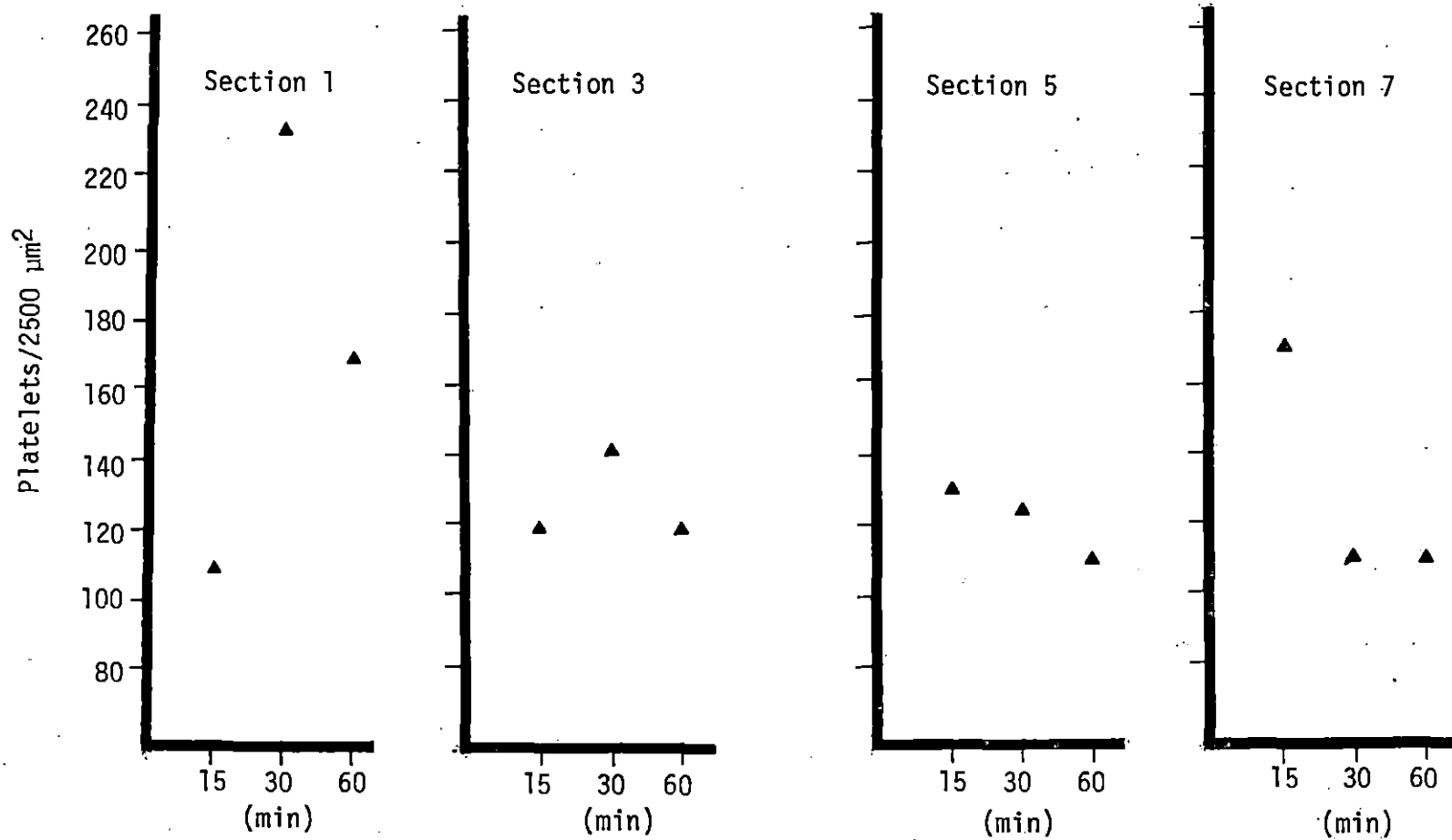


Figure 14b. Graphs of platelet densities for dog 2148. Catheter coating was 5% HEMA/15% NVP.

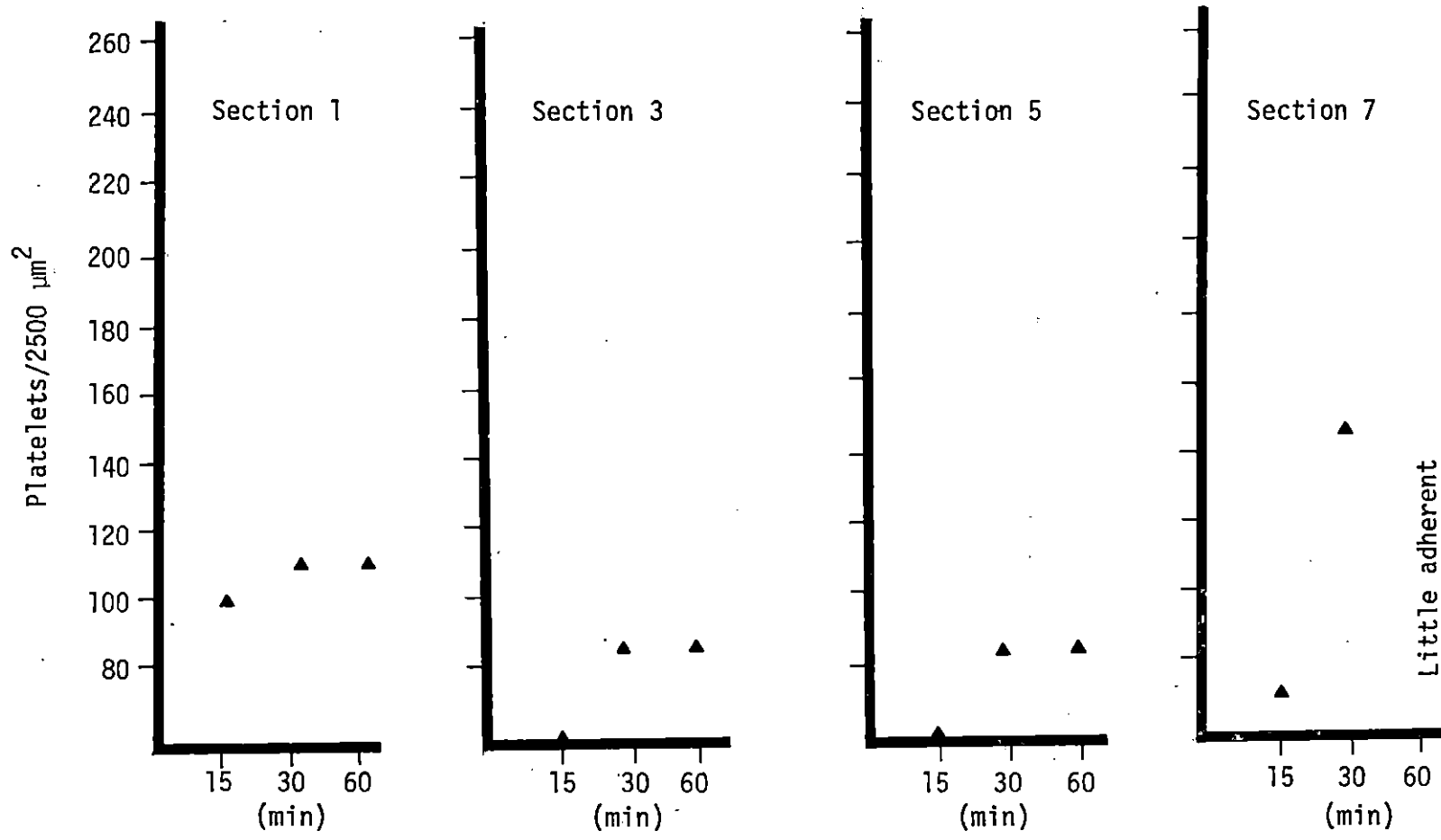


Figure 14c. Graphs of platelet densities for dog 2148. Catheter coating was 0% HEMA/20% NVP.

densities. The reaction of the 0% HEMA/20% NVP polymers also remained stable through the course of 60 minutes; platelet densities remaining constant indicates a steady-state condition. The 5% HEMA/15% NVP and 10% HEMA/10% NVP samples have increasing and decreasing platelet densities indicating a sloughing of the populations and adherence of new platelet populations.

### Method 2

The experimental data for dogs 2146 and 2130 are given in Table 9.

Table 9. Experimental data for dogs 2146 and 2130

#### Experimental Data

##### Method 2

Dog Number	2146	2130
Hematocrit	36	35
Platelet count (per mm <sup>3</sup> )	230,000	98,000
Activated Clotting Time (sec)	81	95
Formulations	Comp <sup>a</sup>	Comp <sup>a</sup>
Implantation Site	Right and Left Jugular veins	Right and Left Jugular veins
Time (minutes)	15, 30, & 60	15, 30, and 60

<sup>a</sup> Comprehensive set - (1) Silastic, (2) 20% HEMA/0% NVP, (2) 15% HEMA/5% NVP, (3) 10% HEMA/10% NVP, (4) 5% HEMA/15% NVP, (6) 0% HEMA/20% NVP.

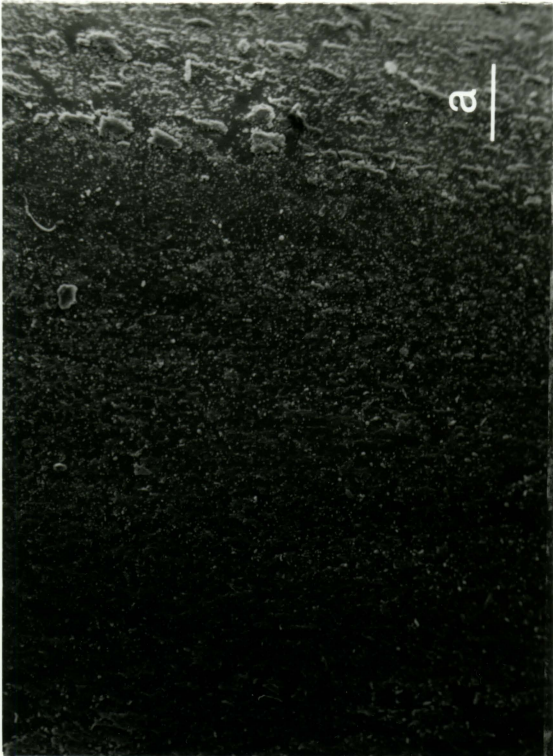
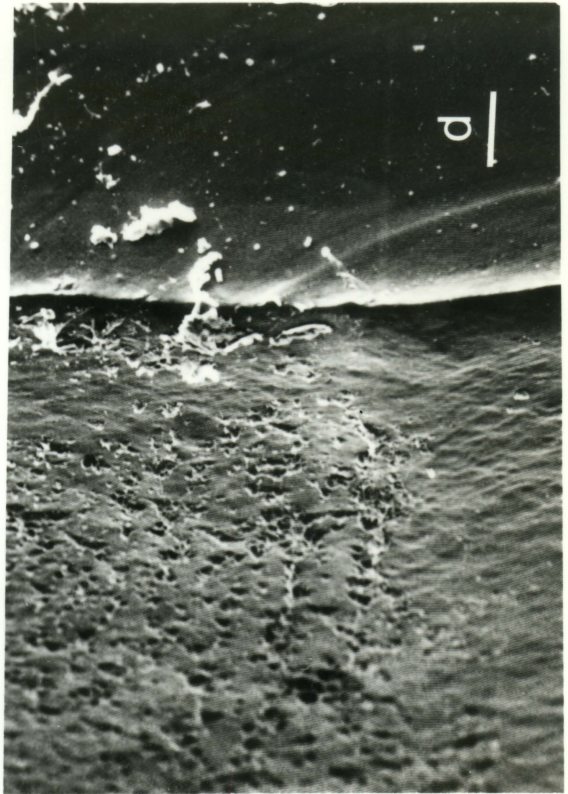
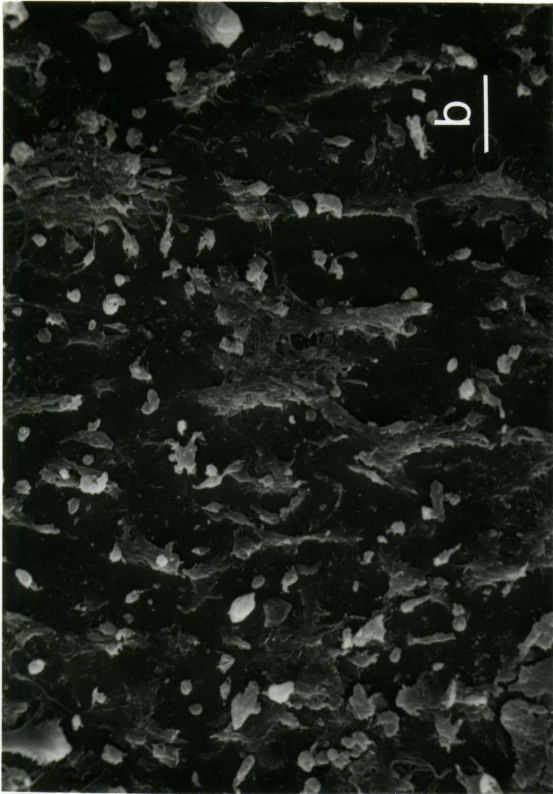
In method 2, the plastic introducers were deleted. This technique was successful for gaining access for multiple insertions, but also had drawbacks upon implant retrieval. A few cases were noted in which the thrombi were stripped from the catheters upon withdrawal. The samples retrieved were prepared for SEM analysis and are seen in the micrographs in Figures 15 through 38. Selected micrographs for dog 2130 are presented when the results were not comparable to those of dog 2146. Thrombus formation was observed on the surfaces of all catheters. The types of cells deposited and amount adherent to the surface varied.

Silastic<sup>®</sup>

Silastic<sup>®</sup>, dog 2146 SEM micrographs of the Silastic<sup>®</sup>

catheters used in dog 2146 are shown in Figures 15 through 17. The analysis of the 15 minute interval (Figures 15a through 15d) shows a light reaction with platelet activity the main cellular event. At 30 minutes, the cellular activity in section 2 (Figures 16a and 16b) is leukocytes adherent to the surface and incorporated in a fibrin deposit. As seen in Figures 16c and 16d, the cellular activity has become areas of reaction versus a homogeneous distribution. In the 60 minutes implantation (Figures 17a through 17f), the surface cellular deposition ranges from a light reaction in section 1 to a heavy sheath in section 8. Section 8 is nearest the entry site in the vessel and first in contact with the flowing blood. The fibrin network is highly developed and RBCs have been incorporated, see Figures 17d through 17f.

- Figure 15a. Scanning electron micrograph of Silastic<sup>®</sup> catheter, section 1, at 15 minutes (scale bar = 100  $\mu\text{m}$ ). 15 keV. dog 2146.
- Figure 15b. Higher magnification of Figure 15a (scale bar = 10  $\mu\text{m}$ ). dog 2146. 15 keV.
- Figure 15c. Silastic<sup>®</sup> catheter, section 2, at 15 minutes (scale bar = 10  $\mu\text{m}$ ). 15 keV. 20° tilt. dog 2146.
- Figure 15d. Silastic<sup>®</sup> catheter, section 6, at 15 minutes (scale bar = 33.3  $\mu\text{m}$ ). 15 keV. 20° tilt. dog 2146.



- Figure 16a. Scanning electron micrograph of Silastic<sup>®</sup> catheter, section 2, at 30 minutes (scale bar = 100  $\mu\text{m}$ ). 15 keV. dog 2146.
- Figure 16b. Higher magnification of Figure 16a (scale bar = 10  $\mu\text{m}$ ). 15 keV. dog 2146.
- Figure 16c. Silastic<sup>®</sup> catheter, section 4, at 30 minutes (scale bar = 33.3  $\mu\text{m}$ ). 15 keV. 30° tilt. dog 2146.
- Figure 16d. Silastic<sup>®</sup> catheter, section 8, at 30 minutes (scale bar = 33.3  $\mu\text{m}$ ). 15 keV. 30° tilt. dog 2146.

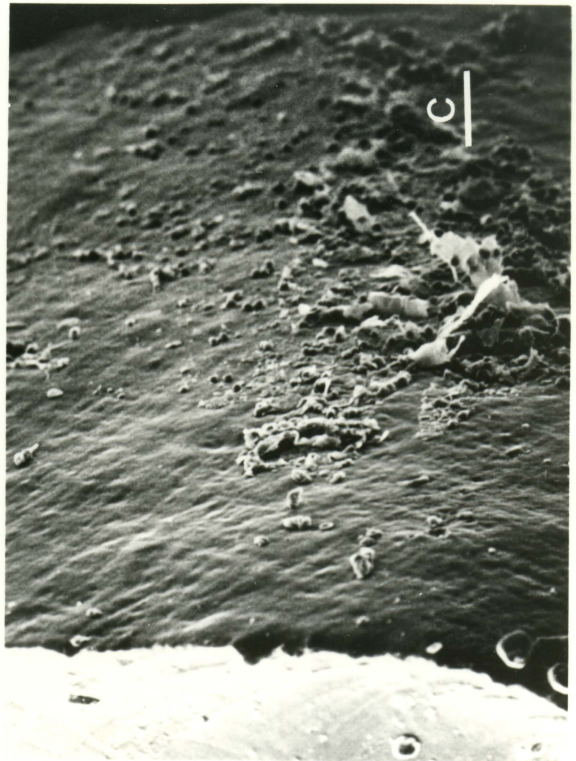
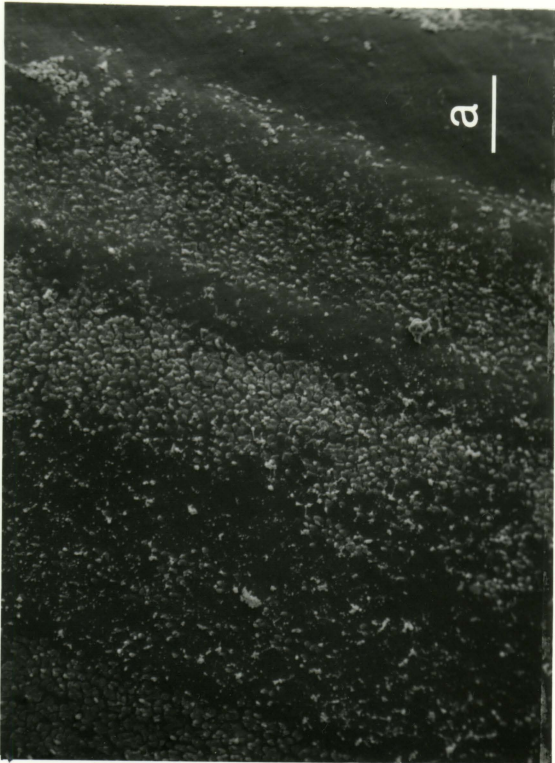
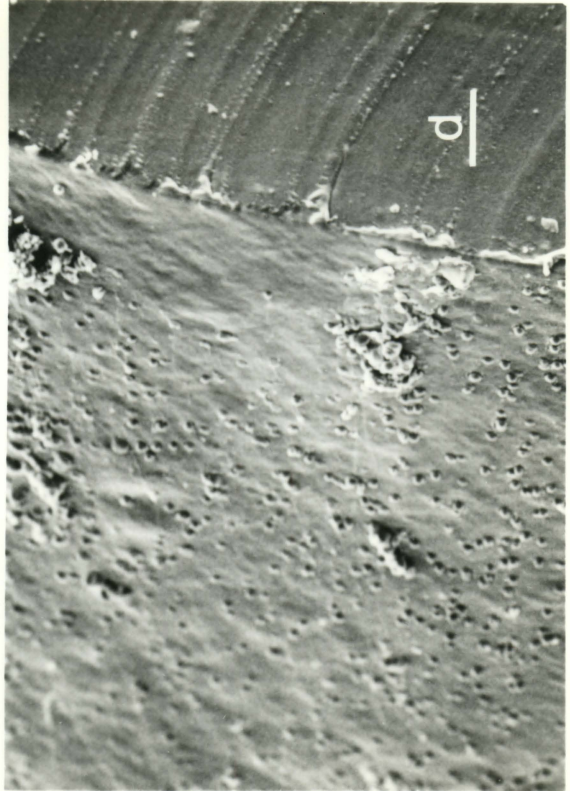
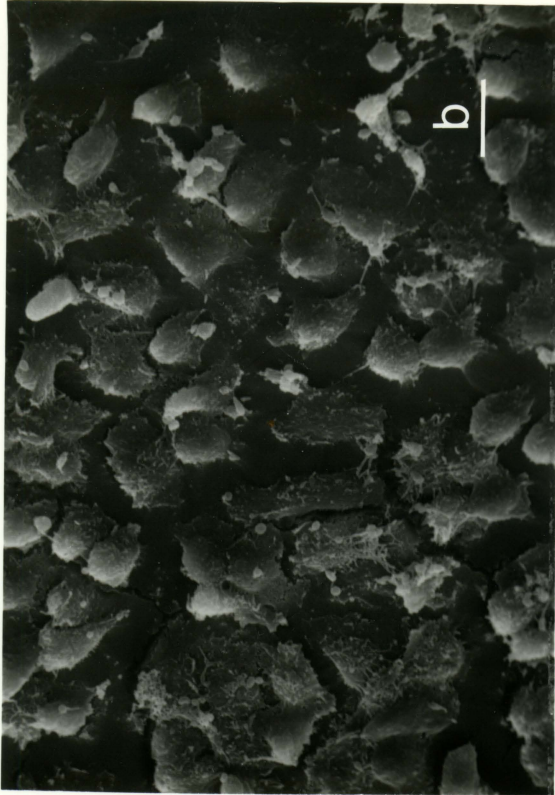


Figure 17a. Scanning electron micrograph of Silastic<sup>®</sup> catheter, section 1, at 60 minutes (scale bar = 100  $\mu\text{m}$ ). 15 keV. dog 2146.

Figure 17b. Silastic<sup>®</sup> catheter, section 4 at 60 minutes (scale bar = 20  $\mu\text{m}$ ). 15 keV. 20° tilt. dog 2146.

Figure 17c. Silastic<sup>®</sup> catheter, section 5 at 60 minutes (scale bar = 10  $\mu\text{m}$ ). 15 keV. dog 2146.

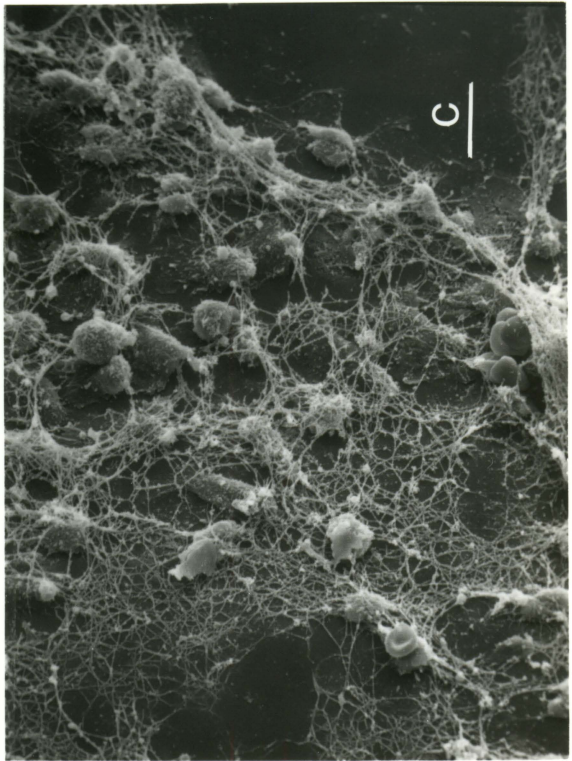
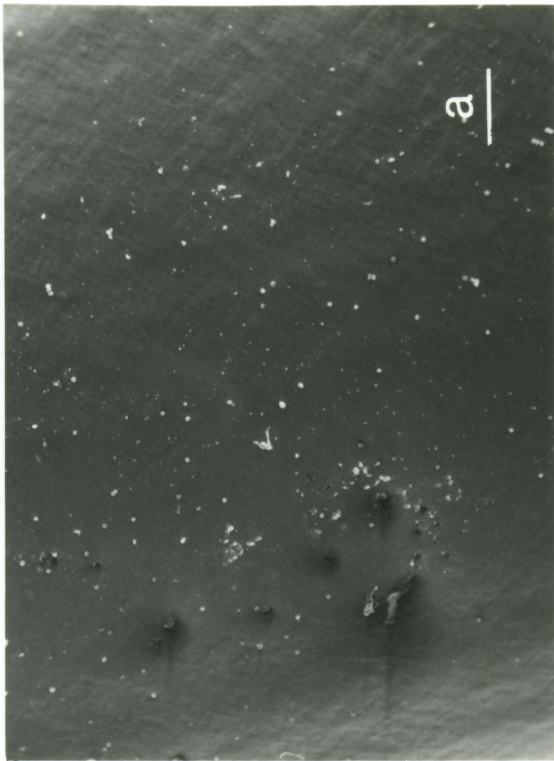
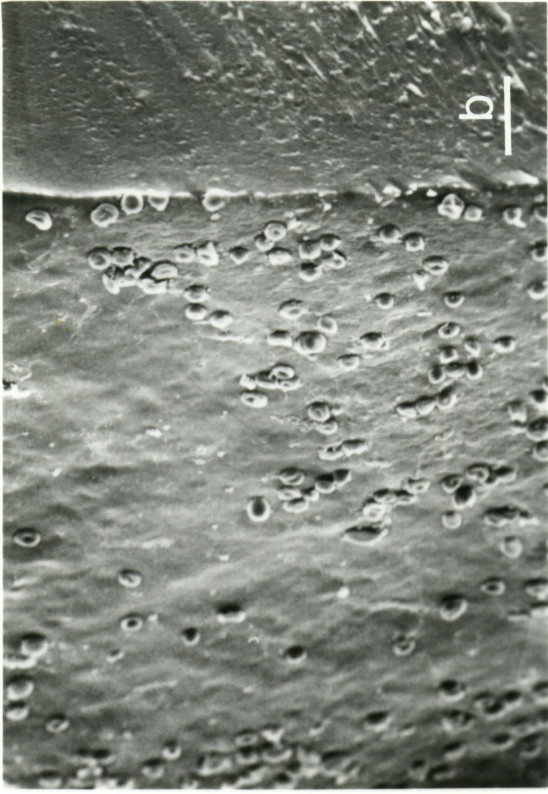
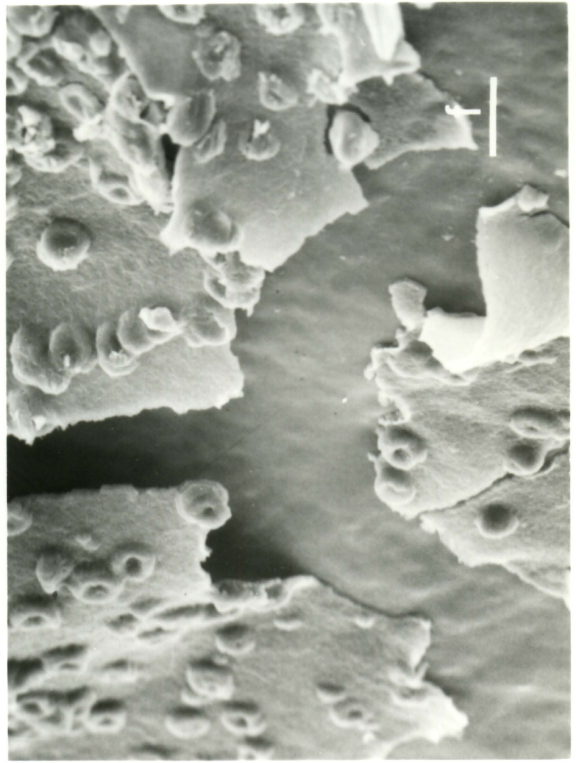
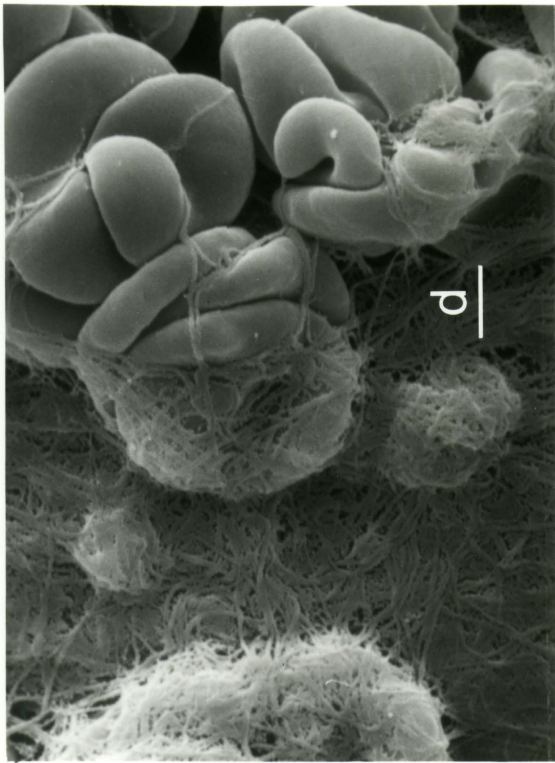
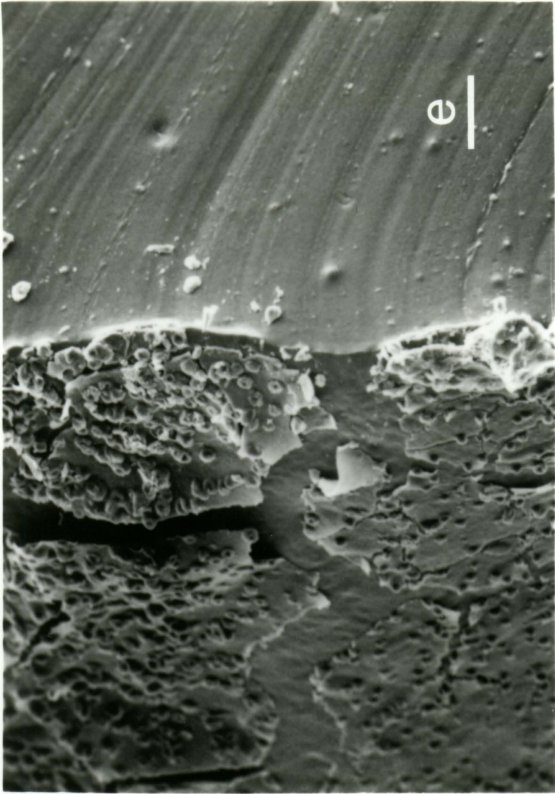


Figure 17d. Silastic<sup>®</sup> catheter, section 7, at 60 minutes  
(scale bar = 2  $\mu\text{m}$ ). 15 keV. dog 2146.

Figure 17e. Silastic<sup>®</sup> catheter, section 8, at 60 minutes  
(scale bar = 33.3  $\mu\text{m}$ ). 15 keV. 30° tilt.  
dog 2146.

Figure 17f. Higher magnification of Figure 17e (scale  
bar = 100  $\mu\text{m}$ ). 15 keV. 30° tilt. dog 2146.



Silastic<sup>®</sup>, dog 2130      Comparable results using Silastic<sup>®</sup> in dog 2130 are limited to those from one 15 minute trial because the adhering thrombi were stripped from the catheters during withdrawal in the 30 and 60 minute trials. The 15 minute trial results are shown in Figures 18a through 18c. Considerable fibrin deposition and platelet aggregation are evident. Figures 19a and 19b show the catheters from 30 minute and 60 minute trials. Although they appear to be clear of thrombus, a significant amount of material was deposited on the surfaces. The thrombi which were stripped from the catheter during withdrawal were retrieved from the vessel and are shown in Figure 19c.

20% HEMA/0% NVP

20% HEMA/0% NVP, dog 2146      The response of blood to the 20% HEMA/0% NVP formulation for dog 2146 is documented in Figures 20 through 22. The 15 minute time interval micrographs (Figures 20a through 20d) show a deposition of platelets and RBCs with a fibrin network developing. The deposition thickness was approximately 10  $\mu\text{m}$ . The 30 minute interval results (Figures 21a through 21e) show RBC deposition along with areas of leukocyte activity. The cellular deposition thickness for 30 minutes varied from 3-50  $\mu\text{m}$ . The 60 minute trial response is shown in Figures 22a and 22b to the heavy thrombus build up seen in Figure 22c. The cellular deposition thickness for this 60 minute trial was from 0 - 200  $\mu\text{m}$ .

In general, this formulation caused an increasing blood response with time as indicated by the increasing cellular deposition thickness.

Figure 18a. Scanning electron micrograph of Silastic<sup>®</sup> catheter, section 1, at 15 minutes (scale bar = 100  $\mu\text{m}$ ). 15 keV. dog 2130.

Figure 18b. Higher magnification of Figure 18a (scale bar = 10  $\mu\text{m}$ ). 15 keV. dog 2130.

Figure 18c. Silastic<sup>®</sup> catheter, section 7, at 15 minutes (scale bar = 10  $\mu\text{m}$ ). 15 keV. dog 2130.

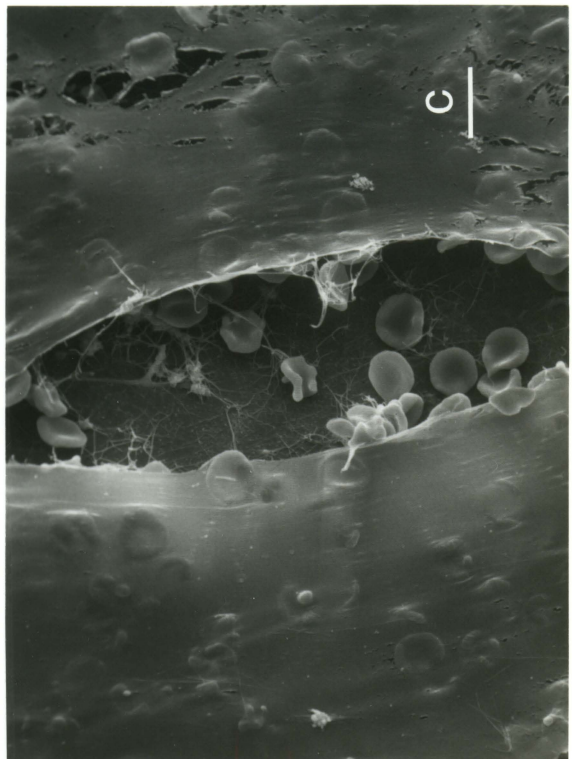
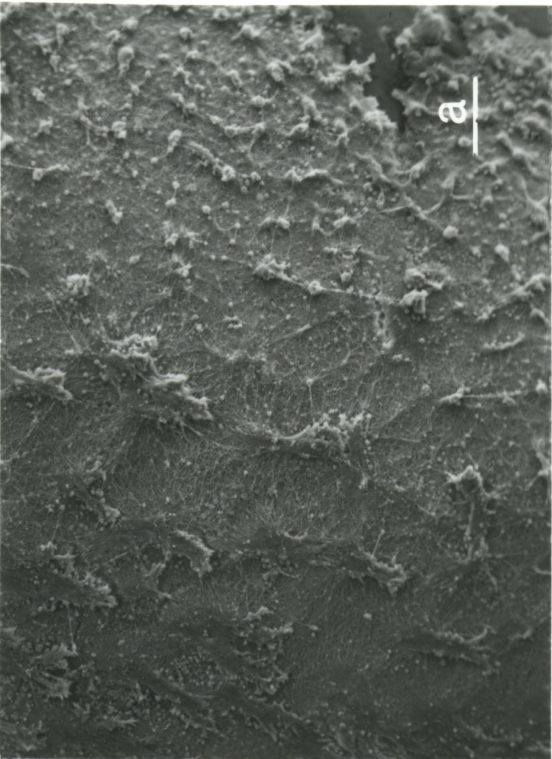
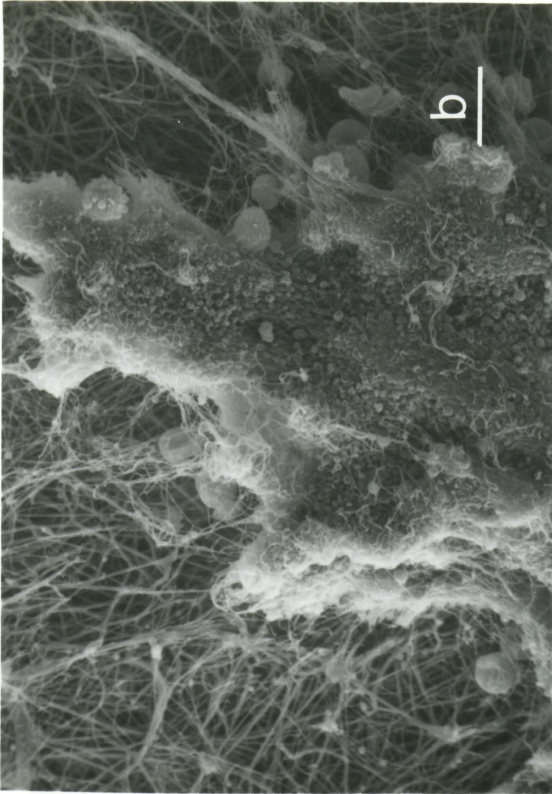
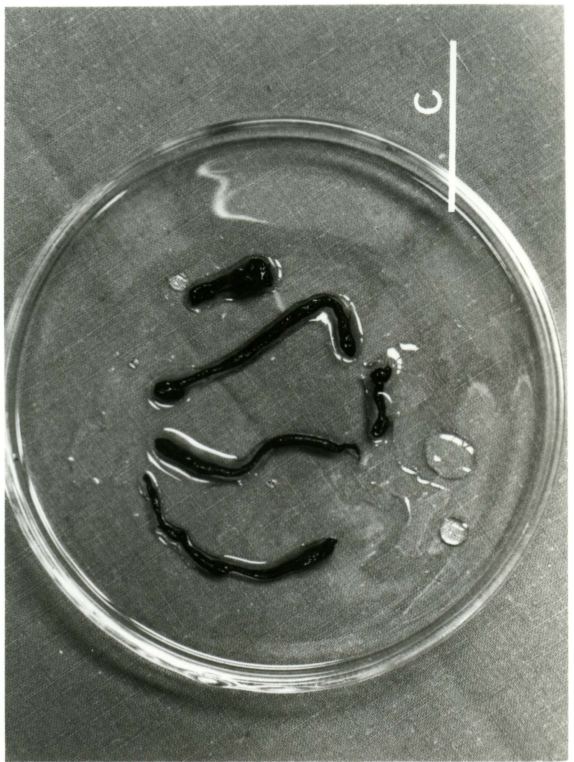
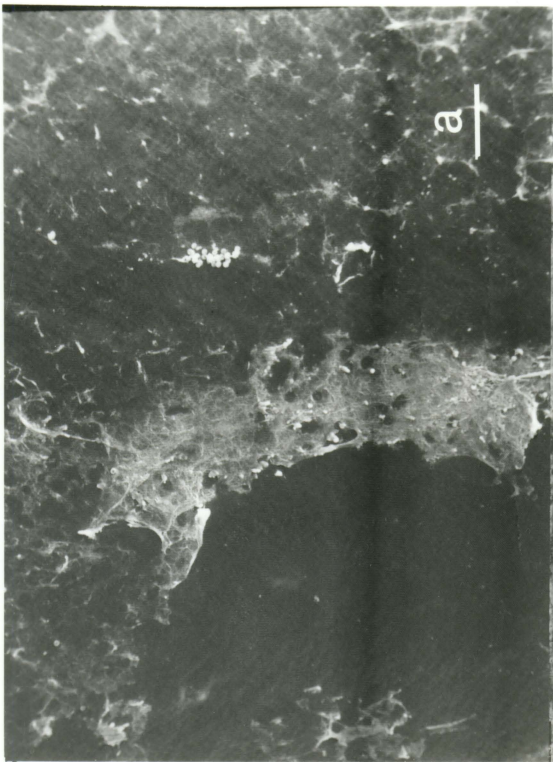
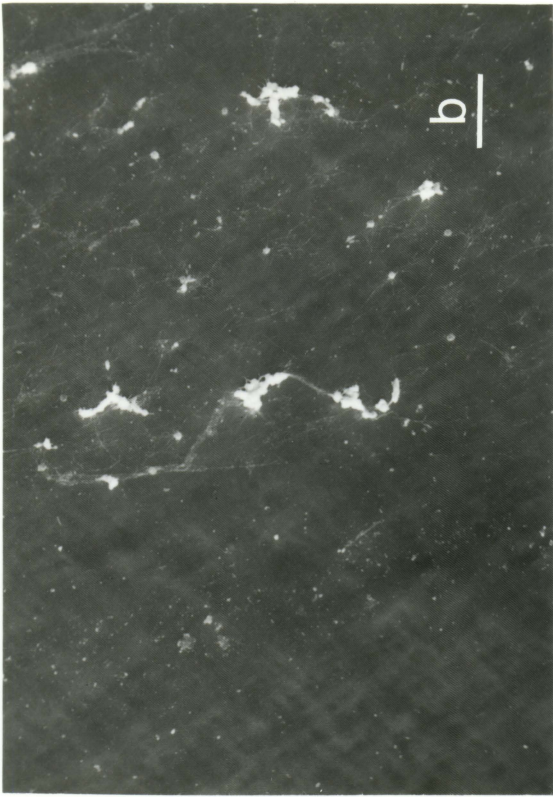


Figure 19a. Scanning electron micrographs of Silastic<sup>®</sup> catheter, section 1, at 30 minutes (scale bar = 100  $\mu$ m). 15 keV. dog 2130.

Figure 19b. Scanning electron micrograph of Silastic<sup>®</sup> catheter, section 1, at 60 minutes (scale bar = 100  $\mu$ m). 15 keV. dog 2130.

Figure 19c. Photograph of the recovered thrombi stripped during withdrawal (scale bar = 1 inch).



- Figure 20a. Scanning electron micrograph of the 20% HEMA/  
0% NVP grafted catheter, section 1, at 15  
minutes (scale bar = 100  $\mu\text{m}$ ). 15 keV. dog 2146.
- Figure 20b. Higher magnification of Figure 20a (scale bar =  
10  $\mu\text{m}$ ). 15 keV. dog 2146.
- Figure 20c. 20% HEMA/0% NVP, Section 2 at 15 minutes (scale  
bar = 20  $\mu\text{m}$ ). 15 keV. dog 2146.
- Figure 20d. 20% HEMA/0% NVP, Section 4, at 15 minutes  
(scale bar = 33.3  $\mu\text{m}$ ). 15 keV. dog 2146.

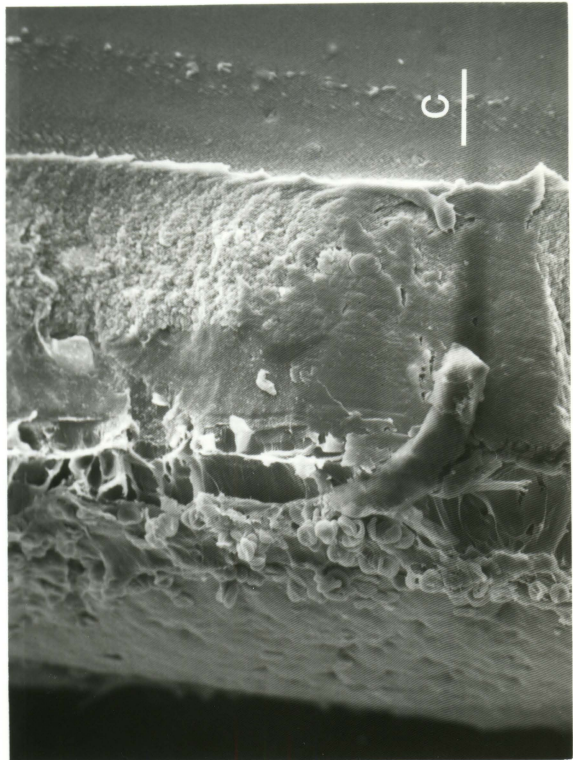
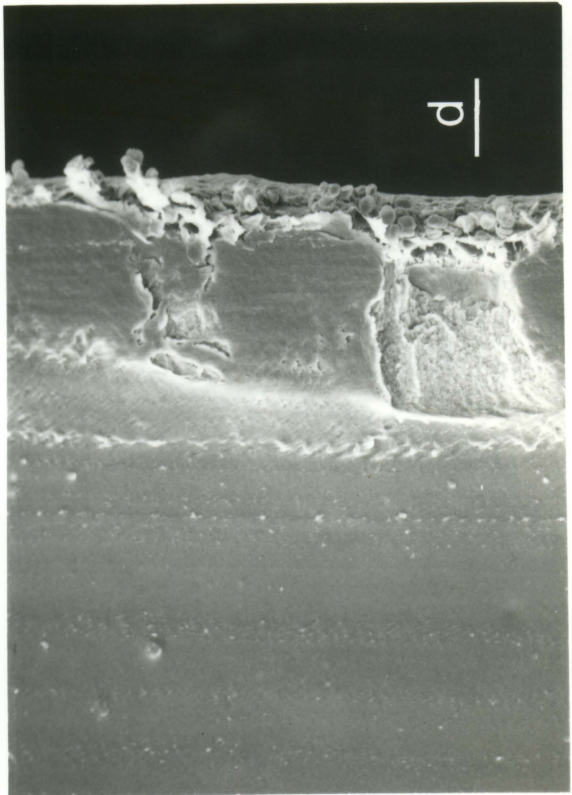
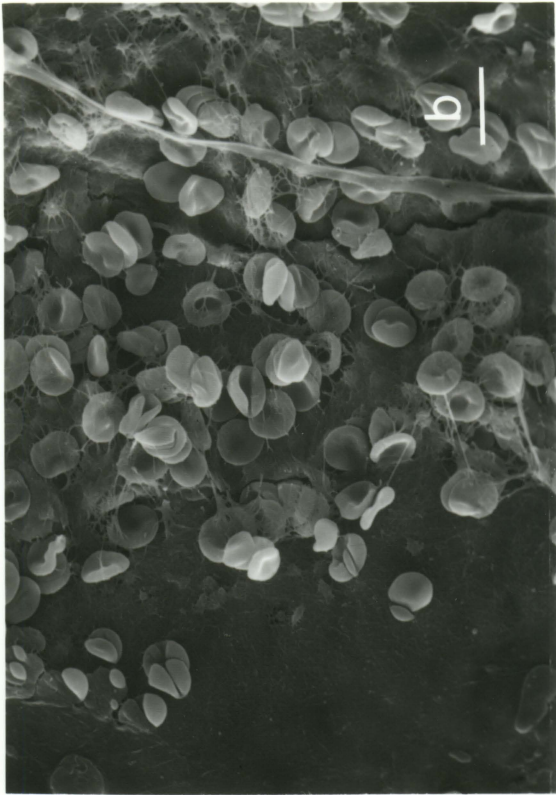


Figure 21a. Scanning electron micrograph of the 20% HEMA/  
0% NVP grafted catheter, section 1, at 30  
minutes (scale bar = 100  $\mu\text{m}$ ). 15 keV. dog 2146.

Figure 21b. Higher magnification of Figure 21a (scale bar =  
10  $\mu\text{m}$ ). 15 keV. dog 2146.

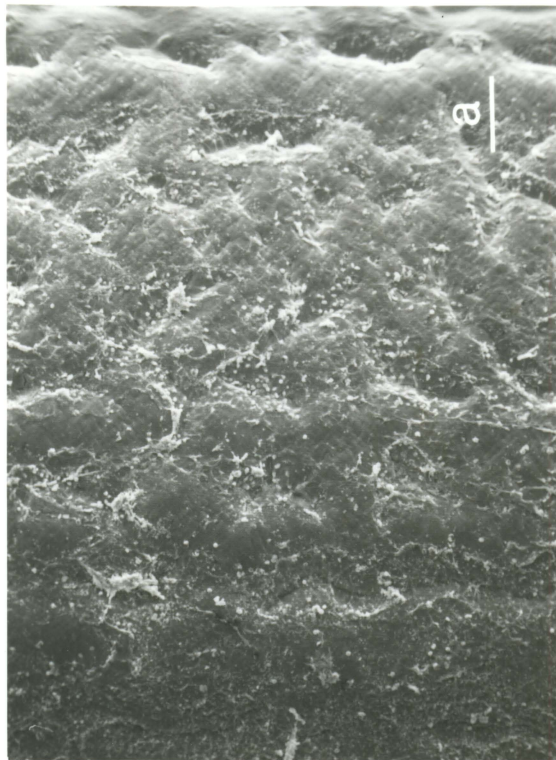
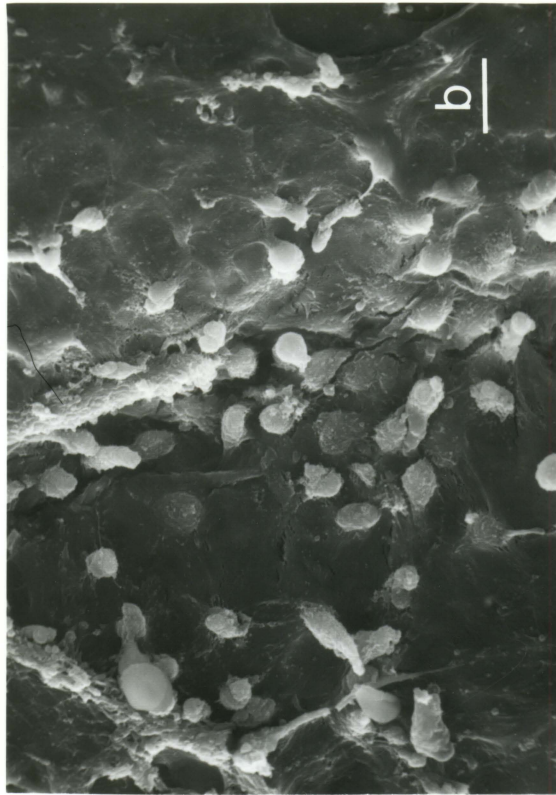


Figure 21c. 20% HEMA/0% NVP grafted catheter, section 2,  
at 30 minutes (scale bar = 33.3  $\mu\text{m}$ ). 15 keV.  
dog 2146.

Figure 21d. 20% HEMA/0% NVP grafted catheter, section 4,  
at 30 minutes (scale bar = 33.3  $\mu\text{m}$ ). 15 keV.  
dog 2146.

Figure 21e. 20% HEMA/0% NVP grafted catheter, section 7,  
at 30 minutes (scale bar = 10  $\mu\text{m}$ ). 15 keV.  
dog 2146.

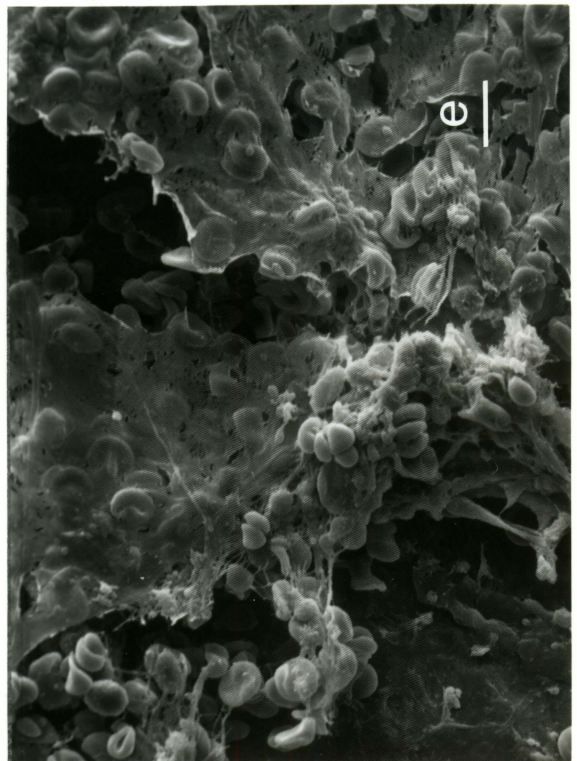
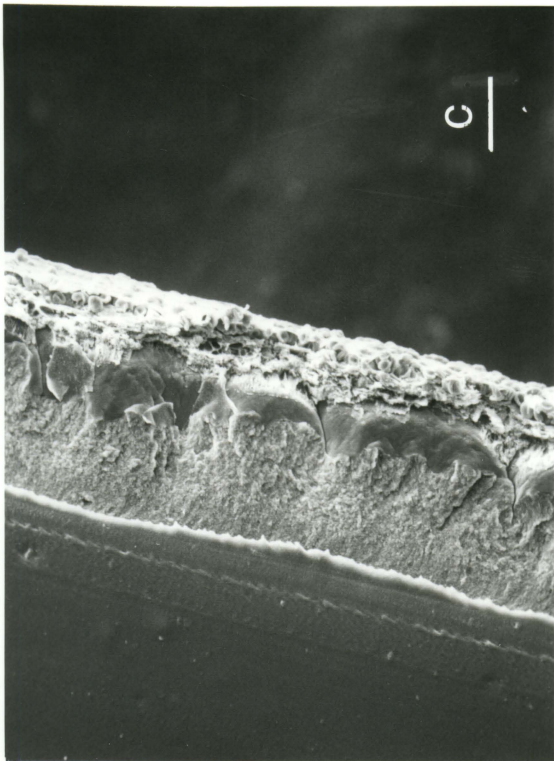
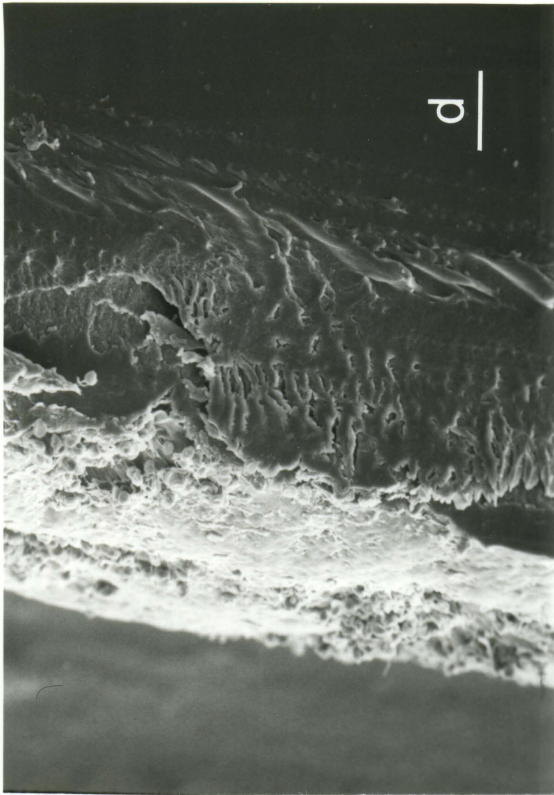
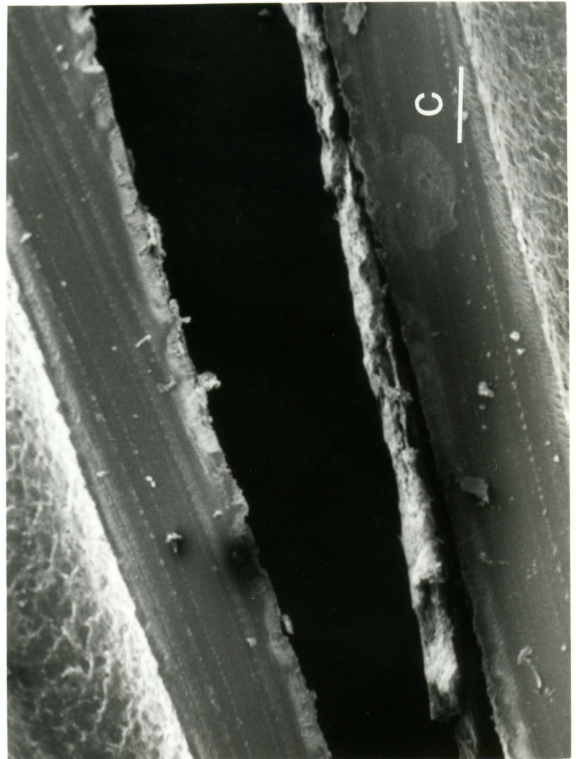


Figure 22a. Scanning electron micrograph of the 20% HEMA/  
0% NVP grafted catheter, section 1, at 60  
minutes (scale bar = 100  $\mu\text{m}$ ). 15 keV. dog  
2146.

Figure 22b. Higher magnification of Figure 22a (scale bar =  
10  $\mu\text{m}$ ). 15 keV. dog 2146.

Figure 22c. 20% HEMA/0% NVP grafted catheter, section 2, at  
60 minutes (scale bar = 0.4 mm). 15 keV.  
dog 2146.



Some catheters of this formulation had grooved surfaces (see Figure 20a). These depressions served as channels which collected RBCs and possibly acted as sites for the thrombus development. The grooves produced were probably a product of mechanical abrasion produced in the catheter preparation procedure, see the Materials and Methods section. This formulation also had the thickest graft deposition, 0.09 mm.

20% HEMA/0% NVP, dog 2130 In the 15 minute trial for dog 2130, a well-developed fibrin network was seen over all sections of the catheters. The adherent thrombus on the 30 minute trial, was lost due to stripping during withdrawal. In the 60 minute trial the catheter surface is covered with a fibrin sheath along its entire length. Note the abundance of leukocytes in Figures 23a through 23c. Figure 23c is near the end of section 1 where the fibrin sheath was pulled away. The leukocytes can be seen adhering to the surface. Cell spreading is also evident.

15% HEMA/5% NVP

15% HEMA/5% NVP, dog 2146 The blood response for the 15% HEMA/5% NVP formulation in dog 2146 is shown in Figures 4 through 6. Again the prevalent response is RBC deposition in a fibrin film. The 15 minute trial is shown in Figures 24a through 24h. RBC deposition appears uniform over the surface with a deposition thickness of approximately 10  $\mu\text{m}$ . The 30 minute trial response is shown in Figures 25a through 25j. A substantial amount of thrombus formed on the

Figure 23a. Scanning electron micrograph of the 20% HEMA/  
0% NVP grafted catheter, section 1, at 60  
minutes (scale bar = 100  $\mu\text{m}$ ). 15 keV.  
dog 2130.

Figure 23b. Higher magnification of Figure 23a (scale bar =  
10  $\mu\text{m}$ ). 15 keV. dog 2130.

Figure 23c. 20% HEMA/0% NVP grafted catheter, section 1,  
at 60 minutes (scale bar = 10  $\mu\text{m}$ ). Thrombus  
partially stripped. 15 keV. dog 2130.

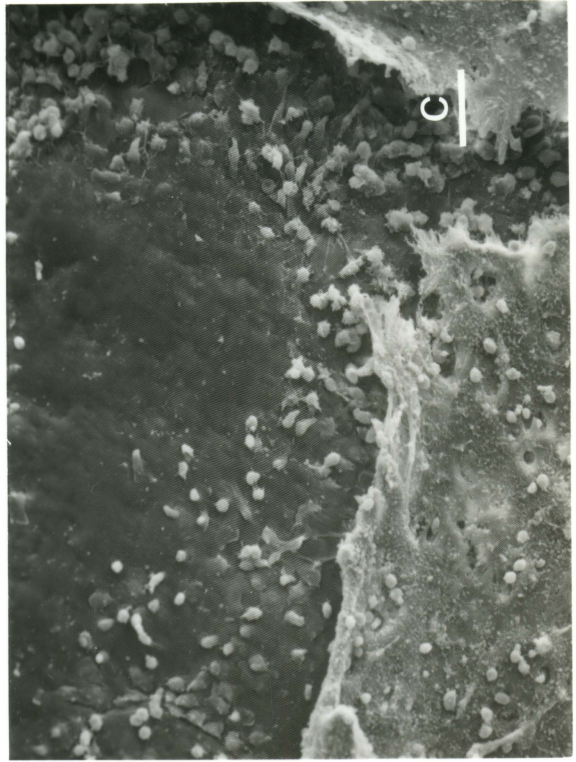
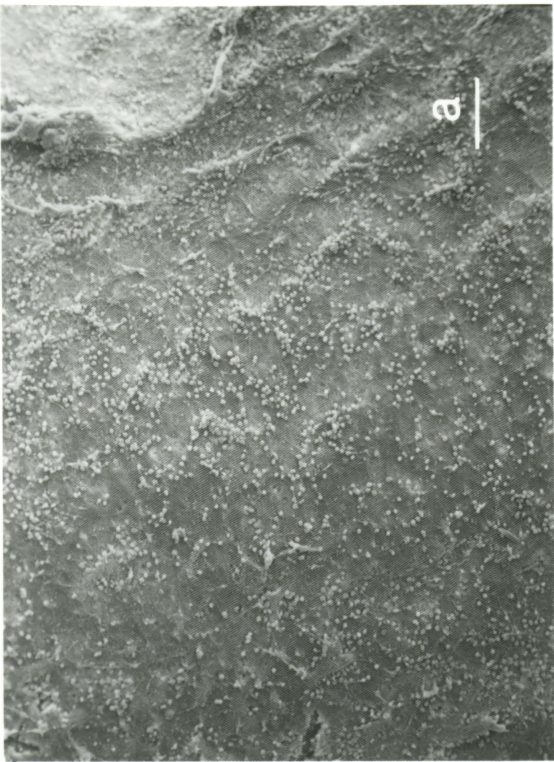


Figure 24a. Scanning electron micrograph of the 15% HEMA/  
5% NVP grafted catheter, section 1, at 15  
minutes (scale bar = 100  $\mu\text{m}$ ). 15 keV. dog  
2146.

Figure 24b. Higher magnification of Figure 24a (scale bar =  
10  $\mu\text{m}$ ). 15 keV. dog 2146.

Figure 24c. 15% HEMA/5% NVP, grafted catheter, section 2,  
at 15 minutes (scale bar = 10  $\mu\text{m}$ ). 15 keV.  
10 tilt. dog 2146.

Figure 24d. 15% HEMA/5% NVP, grafted catheter, section 3,  
at 15 minutes (scale bar = 10  $\mu\text{m}$ ). 15 keV.  
dog 2146.

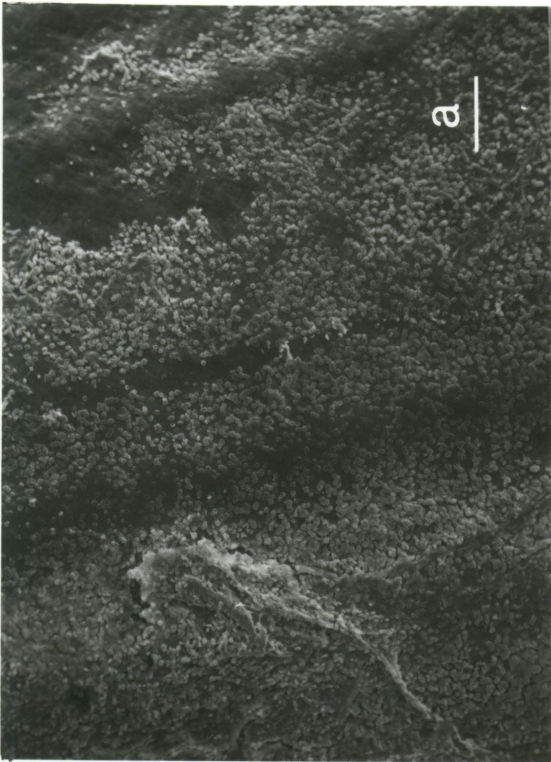
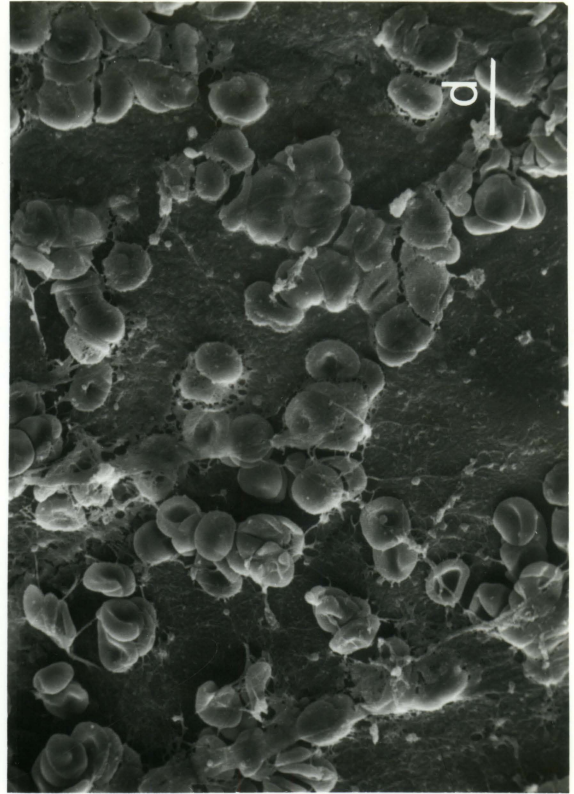
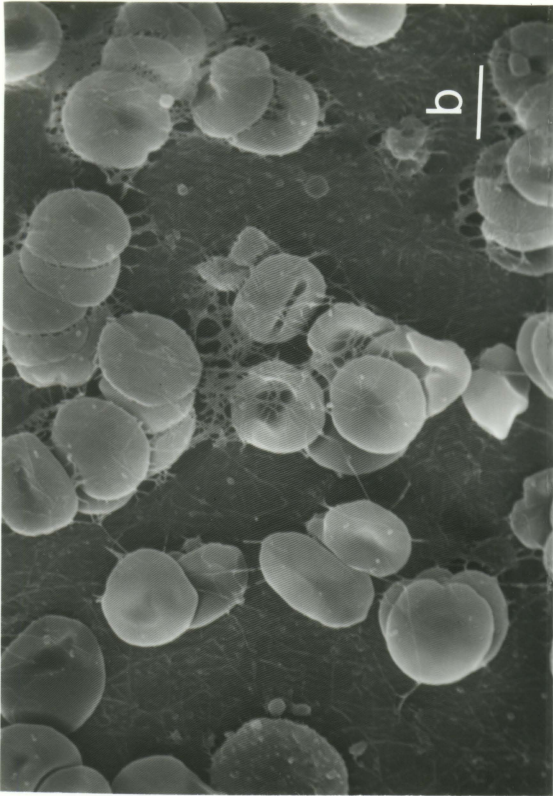


Figure 24e. The 15 % HEMA/5% NVP grafted catheter, section 4, at 15 minutes (scale bar = 10  $\mu$ m). 15 keV, 10° tilt. dog 2146.

Figure 24f. Lower magnification of Figure 24e (scale bar = 33.3  $\mu$ m). 15 keV. dog 2146.

Figure 24g. 15% HEMA/5% NVP grafted catheter, section 6, at 15 minutes (scale bar = 33.3  $\mu$ m). 15 keV. dog 2146.

Figure 24h. 15% HEMA/5% NVP grafted catheter, section 8, at 15 minutes (scale bar = 33.3  $\mu$ m). 15 keV. 10° tilt. dog 2146.

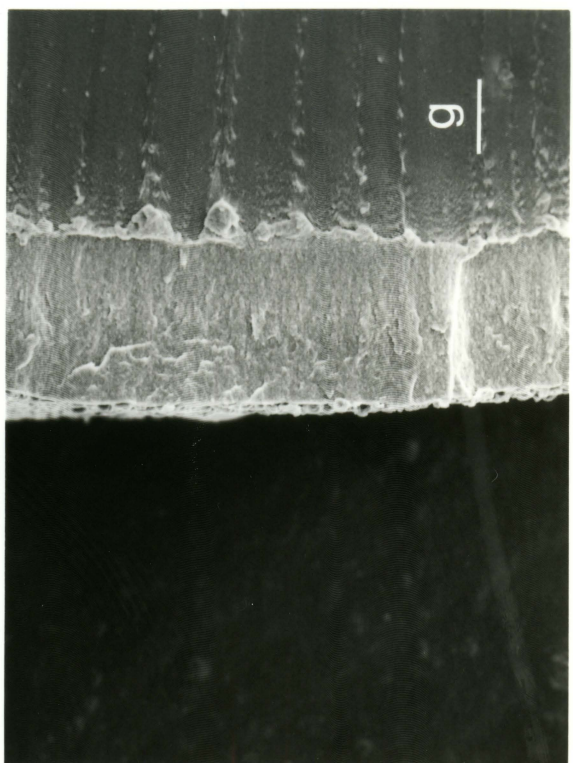
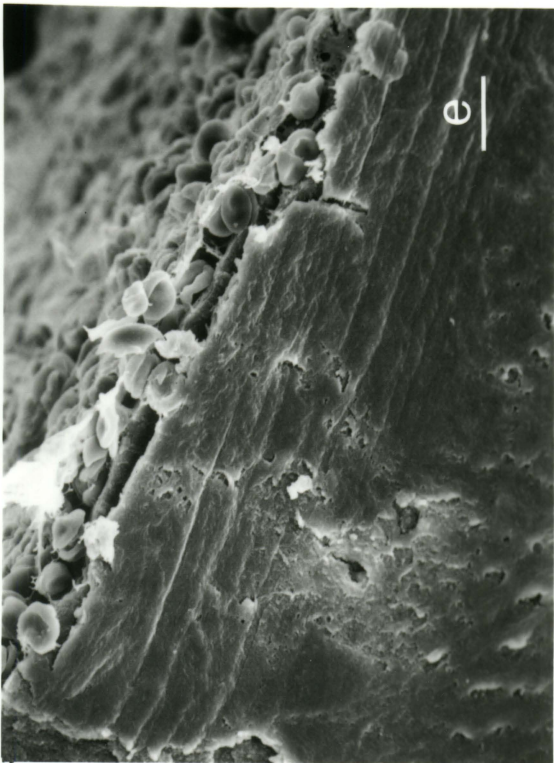
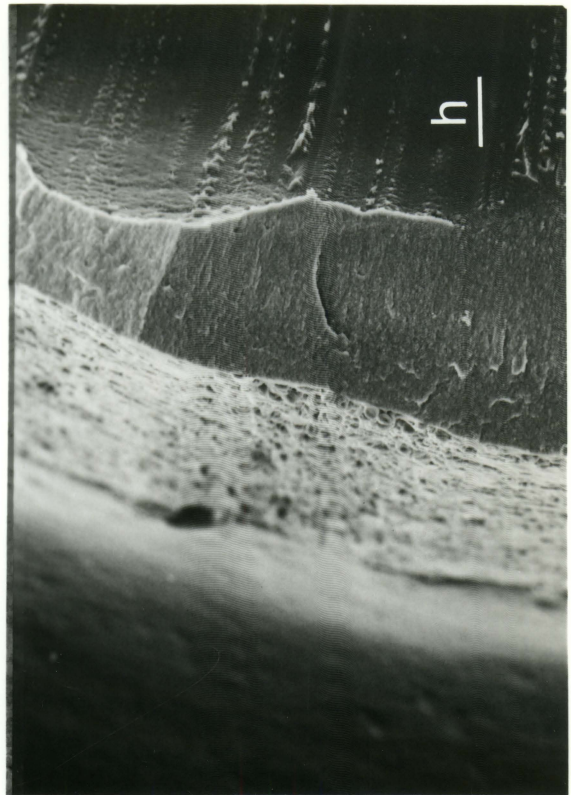


Figure 25a. Scanning electron micrograph of the 15% HEMA/  
5% NVP grafted catheter, section 1, at 30  
minutes (scale bar = 100  $\mu\text{m}$ ). 15 keV.  
dog 2146.

Figure 25b. Higher magnification of Figure 25a (scale bar =  
10  $\mu\text{m}$ ). 15 keV. dog 2146.

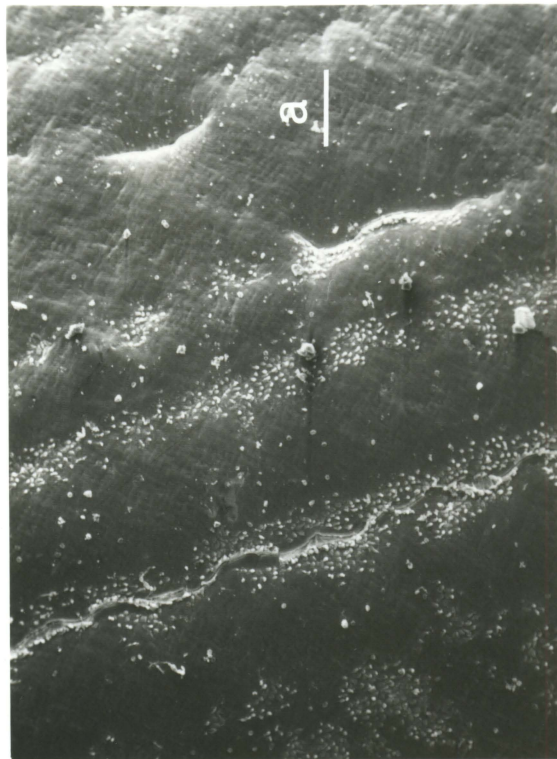


Figure 25c. The 15% HEMA/5% NVP grafted catheter, section 3, at 30 minutes (scale bar = 100  $\mu$ m). 15 keV. dog 2146.

Figure 25d. Higher magnification of Figure 25c. (scale bar = 10  $\mu$ m). 15 keV. dog 2146.

Figure 25e. 15% HEMA/5% NVP grafted catheter, section 2, at 30 minutes (scale bar = 0.25mm). 15 keV. dog 2146.

Figure 25f. 15% HEMA/5% NVP grafted catheter, section 4, at 30 minutes (scale bar = 0.25mm). 15 keV. dog 2146.

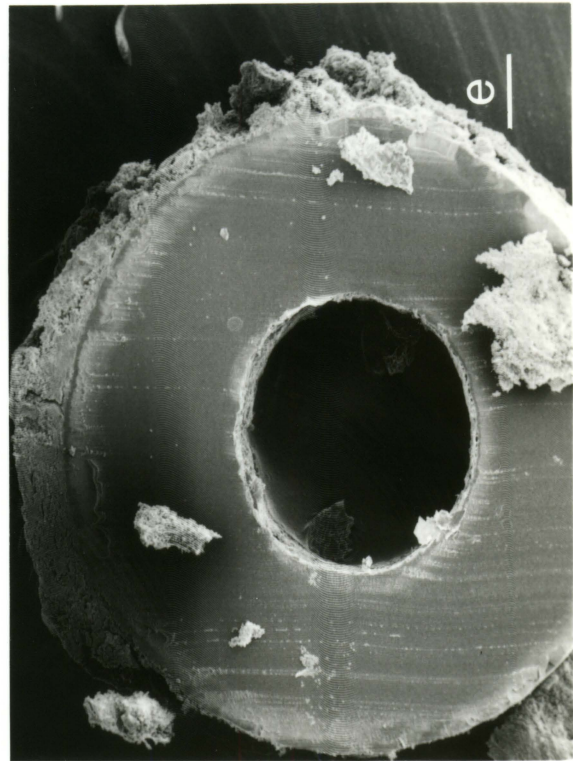
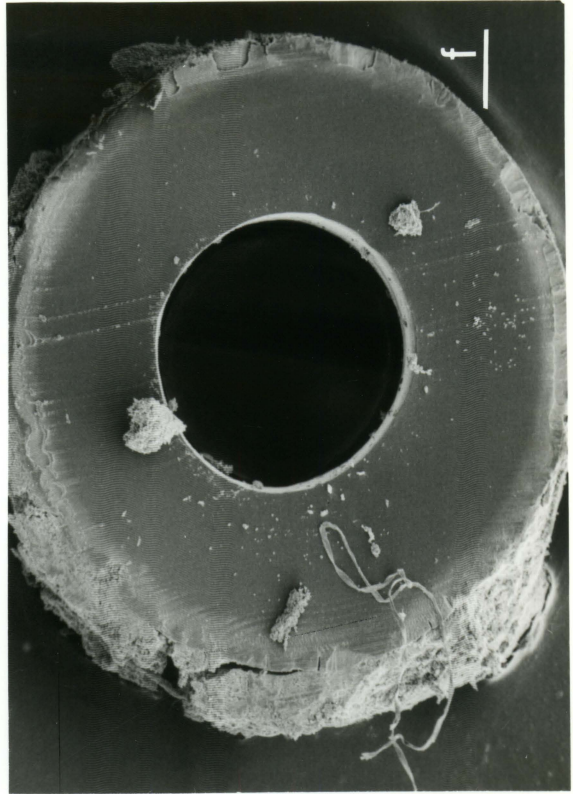
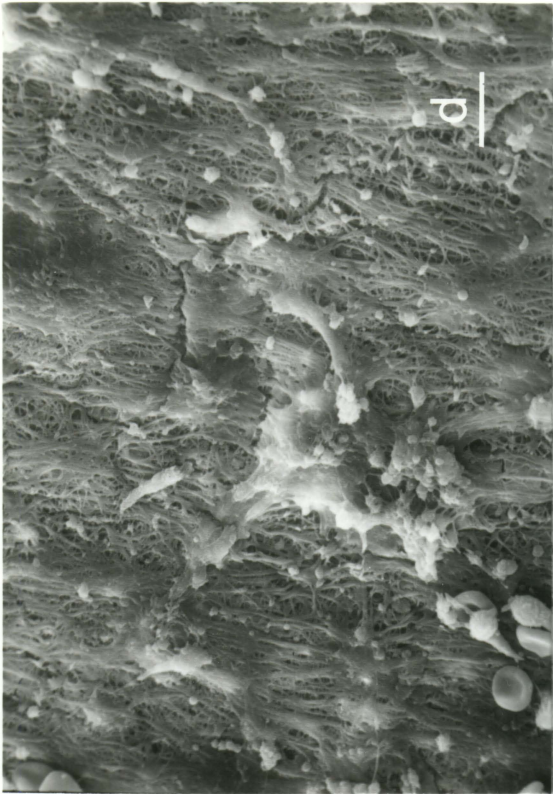
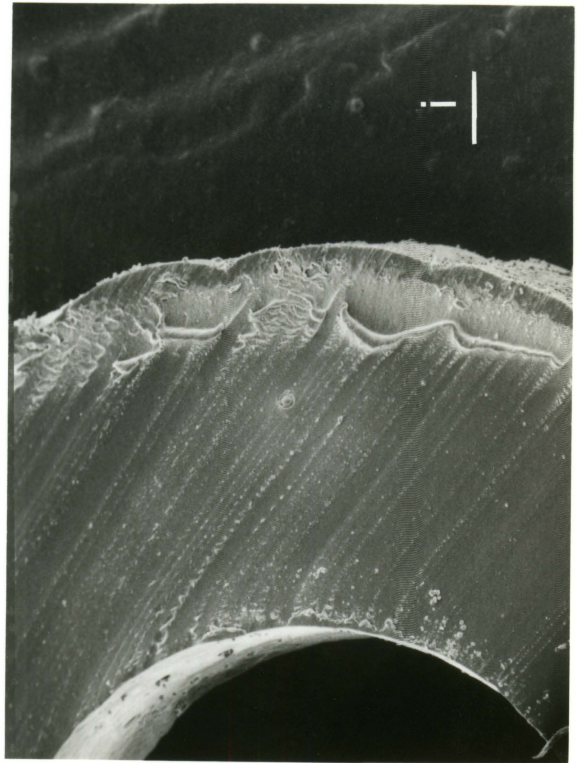
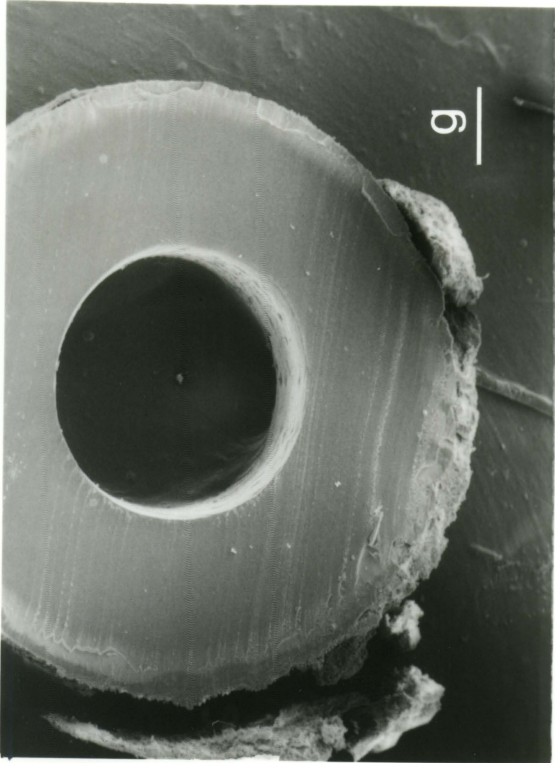
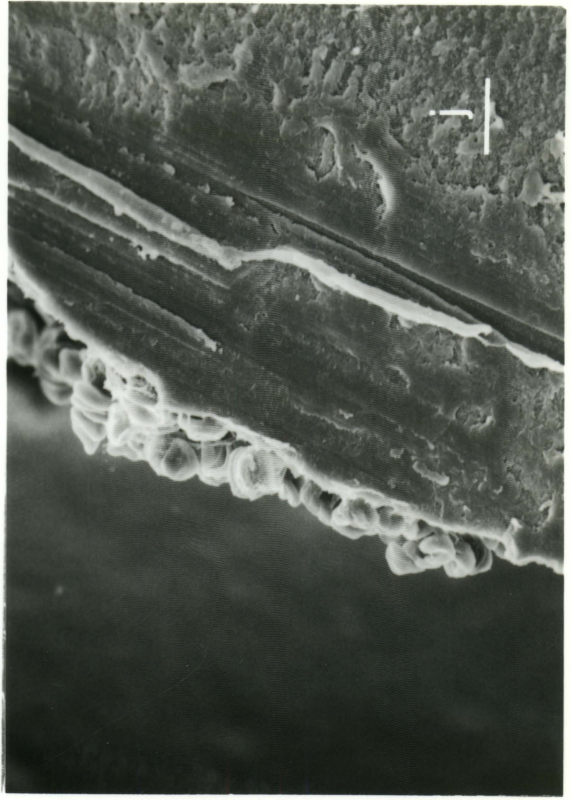
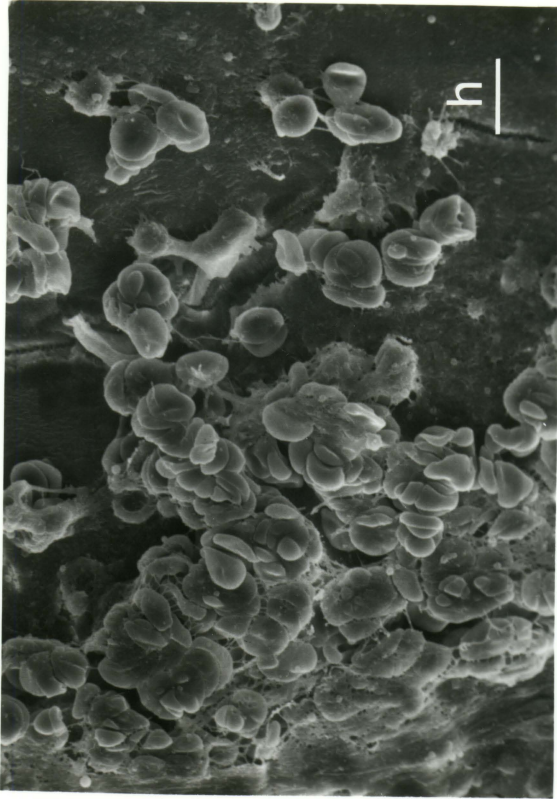


Figure 25g. The 15% HEMA/5% NVP grafted catheter, section 6, at 30 minutes (scale bar = 0.25 mm). 15 keV. dog 2146.

Figure 25h. 15% HEMA/5% NVP grafted catheter, section 7, at 30 minutes (scale bar = 10  $\mu$ m). 15 keV. dog 2146.

Figure 25i. 15% HEMA/5% NVP grafted catheter, section 8, at 30 minutes (scale bar = 100  $\mu$ m). 15 keV. dog 2146.

Figure 25j. Higher magnification of Figure 25i (scale bar = 10  $\mu$ m). 15 keV. dog 2146.



catheter in sections 2 through 6, Figures 25c through 25g. The deposition thickness ranges from 10 - 250  $\mu\text{m}$ . The 60 minute response is shown in Figures 26a through 26g. Deposition is relatively light with RBCs incorporated in a fine fibrin network; reaction is uniform along the length. The cellular deposition thickness is approximately 10  $\mu\text{m}$ .

This 15% HEMA/5% NVP formulation has a varied response which maximizes at 30 minutes. The return to the initial level of deposition indicates embolization may have occurred prior to the 60 minute measurement.

15% HEMA/5% NVP, dog 2130 The 15 minute trial results are shown in Figures 27a through 27d. Platelet adhesion with areas of aggregation can be seen. Also, a light fibrin network is developing in section 7, Figure 27d. The results of the 30 minute trial are comparable to the 15 minute results. Platelet deposition on an adherent film was seen. The results from the 60 minute trial show leukocyte deposition to be the prevalent response.

10% HEMA/10% NVP

10% HEMA/10% NVP, dog 2146 The 10% HEMA/10% NVP blood response sequence for dog 2146 is shown in Figures 28 through 30. The response after 15 minutes is shown in Figures 28a through 28d. In Figures 28a and 28b, fibrin formation, with platelet and leukocyte deposition, can be seen to be the primary event. Along the length of the catheter, a decreasing response is noted. The deposition thickness is approximately 5  $\mu\text{m}$ . The response after 30 minutes is shown in Figures

Figure 26a. Scanning electron micrograph of the 15% HEMA/  
5% NVP grafted catheter, section 1, at 60  
minutes (scale bar = 50  $\mu\text{m}$ ). 15 keV. dog  
2146.

Figure 26b. Higher magnification of Figure 26a (scale bar =  
3.33  $\mu\text{m}$ ). 15 keV. dog 2146.

Figure 26c. 15% HEMA/5% NVP grafted catheter, section 2 at  
60 minutes (scale bar = 10  $\mu\text{m}$ ). 15 keV. dog  
2146.

Figure 26d. 15% HEMA/5% NVP grafted catheter, section 4, at  
60 minutes (scale bar = 10  $\mu\text{m}$ ). 15 keV.  
10° tilt. dog 2146.

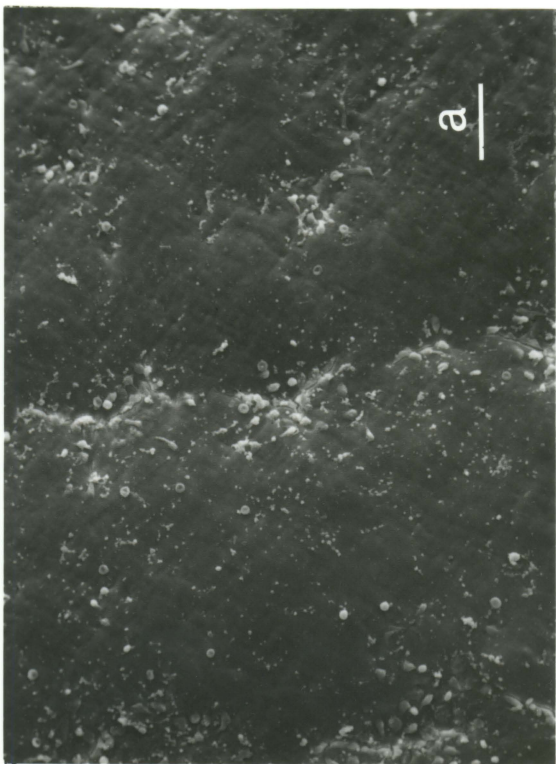
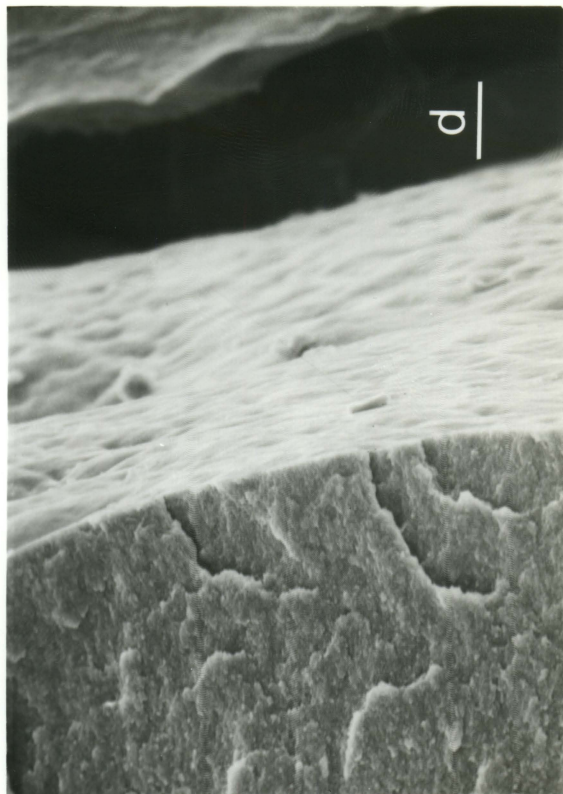
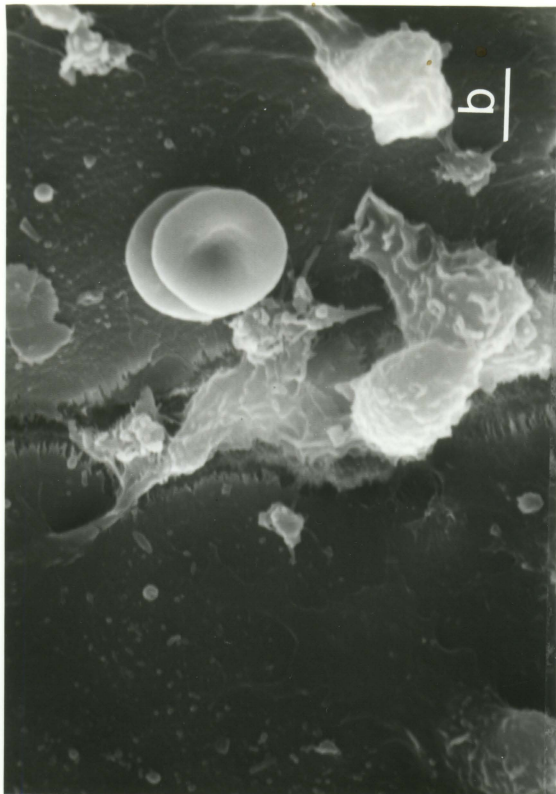


Figure 26e. The 15% HEMA/5% NVP grafted catheter, section 6,  
at 60 minutes (scale bar = 10  $\mu$ m). 15 keV.  
dog 2146.

Figure 26f. 15% HEMA/5% NVP grafted catheter, section 7,  
at 60 minutes (scale bar = 10  $\mu$ m). 15 keV.  
dog 2146.

Figure 26g. 15% HEMA/5% NVP grafted catheter, section 8,  
at 60 minutes (scale bar = 10  $\mu$ m). 15 keV.  
dog 2146.

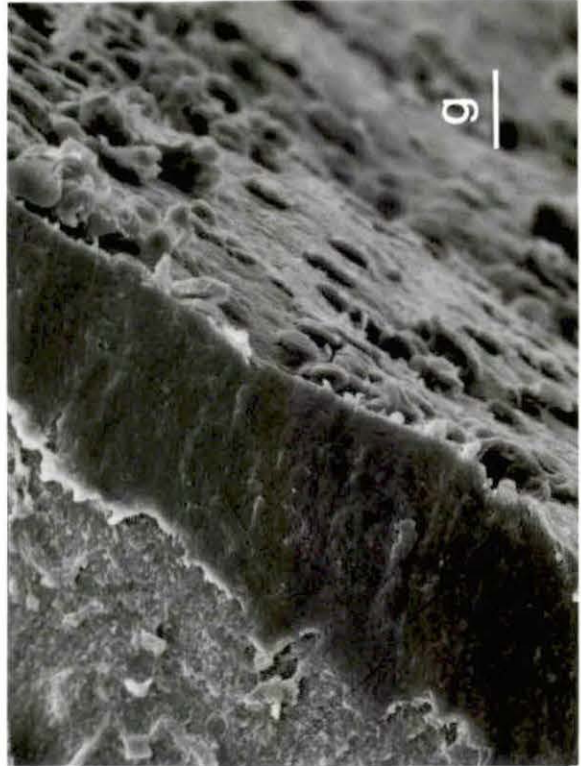
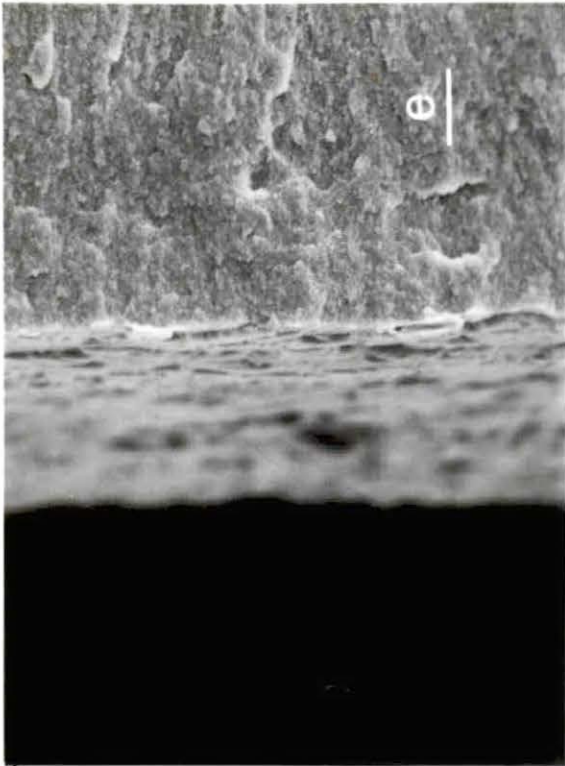


Figure 27a. Scanning electron micrograph of the 15% HEMA/  
5% NVP grafted catheter, section 1, at 15  
minutes (scale bar = 100  $\mu\text{m}$ ). 15 keV. dog  
2130.

Figure 27b. Higher magnification of Figure 27a (scale bar =  
10  $\mu\text{m}$ ). 15 keV. dog 2130.

Figure 27c. 15% HEMA/5% NVP, grafted catheter, section 1,  
at 15 minutes (scale bar = 10  $\mu\text{m}$ ). 15 keV.  
dog 2130.

Figure 27d. 15% HEMA/5% NVP grafted catheter, section 7,  
at 15 minutes (scale bar = 10  $\mu\text{m}$ ). 15 keV.  
dog 2130.

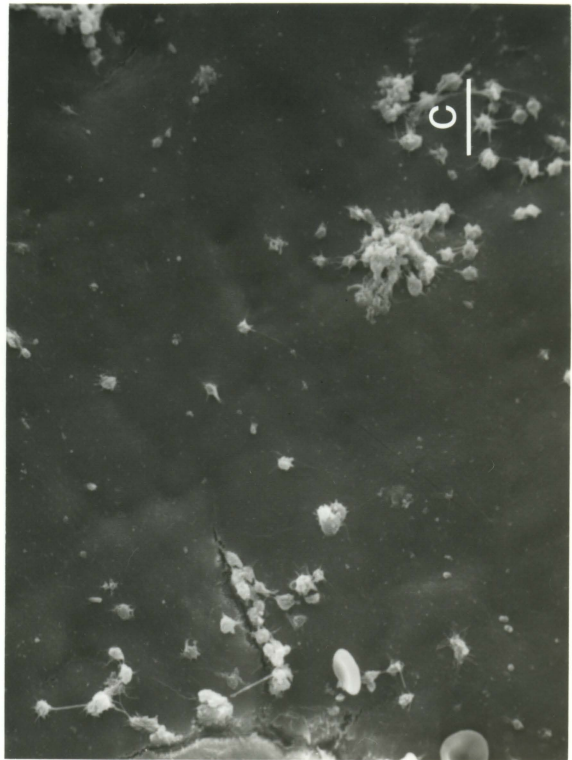
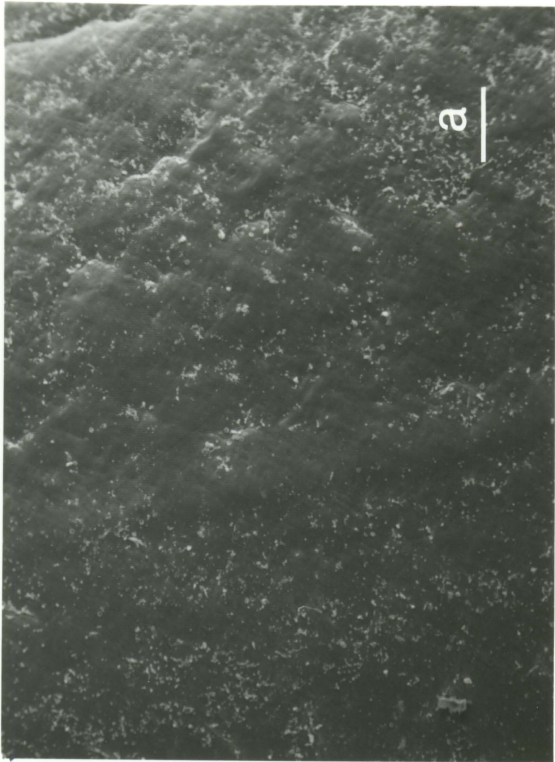
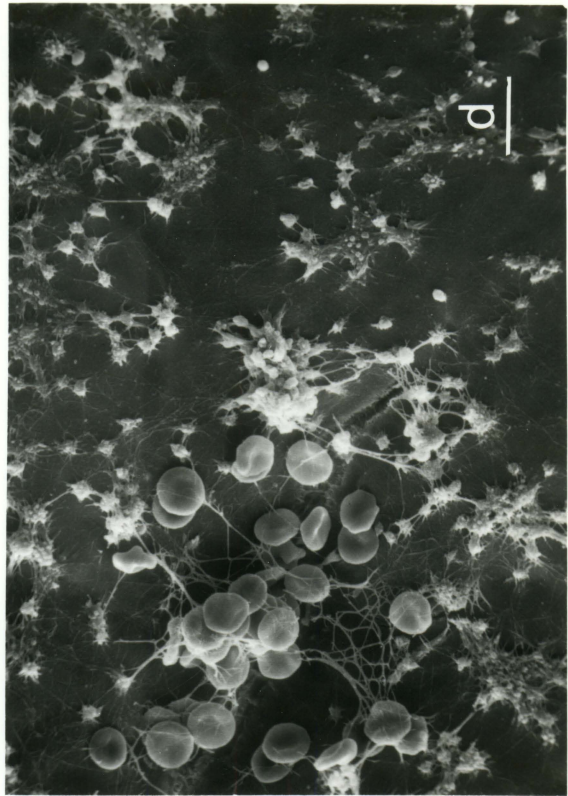
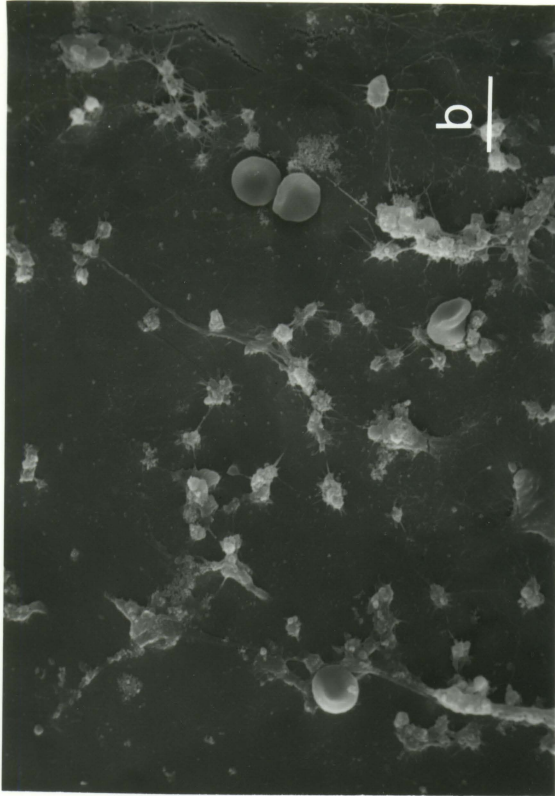


Figure 28a. Scanning electron micrograph of the 10% HEMA/  
10% NVP grafted catheter, section 1, at 15  
minutes (scale bar = 100  $\mu\text{m}$ ). 15 keV.  
dog 2146.

Figure 28b. Higher magnification of Figure 28a (scale bar =  
10  $\mu\text{m}$ ). 15 keV. dog 2146.

Figure 28c. 10% HEMA/10% NVP grafted catheter, section 2,  
at 15 minutes (scale bar = 10  $\mu\text{m}$ ). 15 keV.  
dog 2146.

Figure 28d. 10% HEMA/10% NVP grafted catheter, section 6,  
at 15 minutes (scale bar = 33.3  $\mu\text{m}$ ). 15 keV.  
30° tilt. dog 2146.

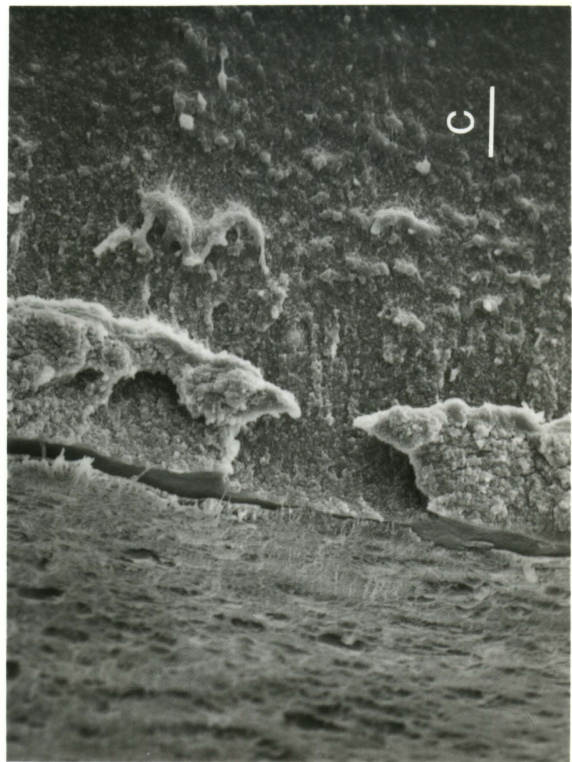
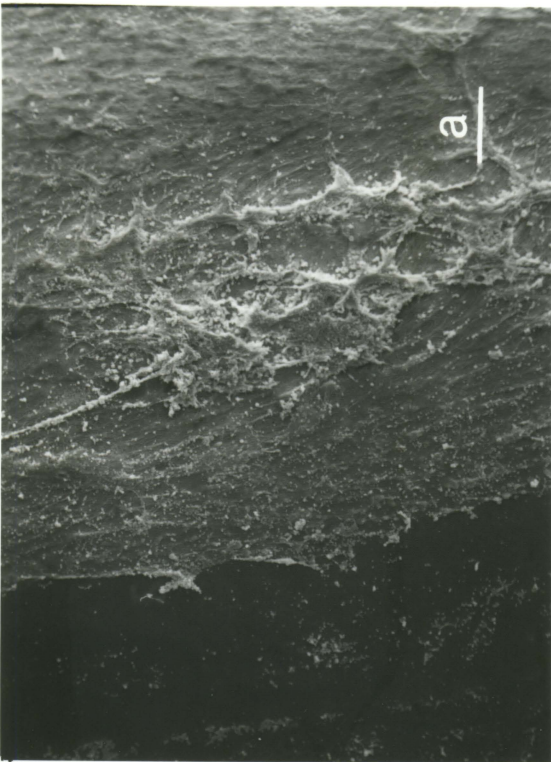
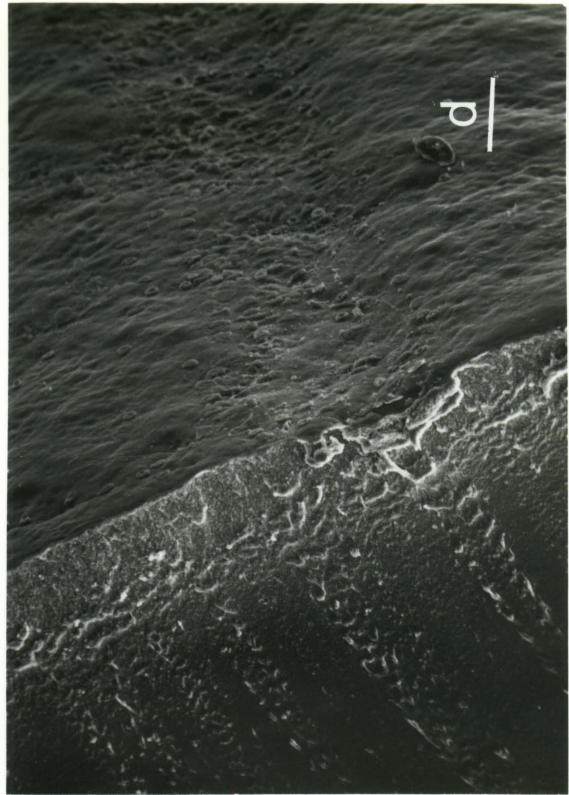
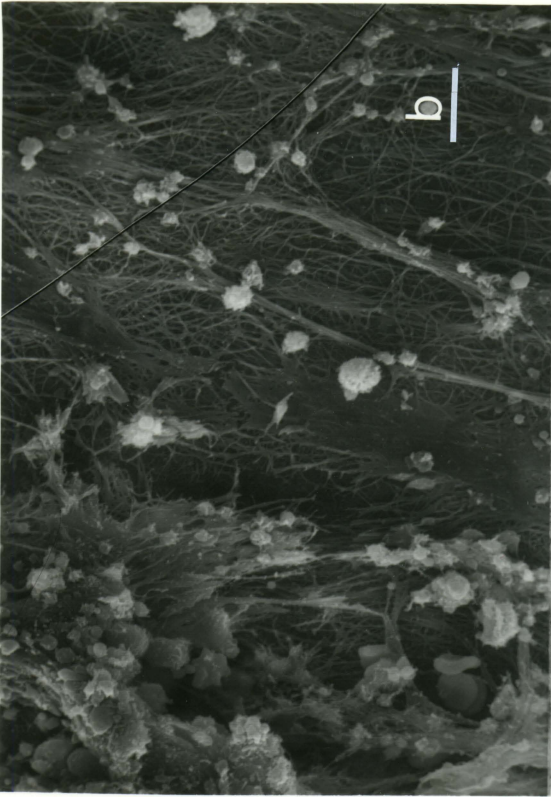


Figure 29a. Scanning electron micrograph of the 10% HEMA/  
10% NVP grafted catheter, section 1 at 30  
minutes (scale bar = 100  $\mu\text{m}$ ). 15 keV. dog  
2146.

Figure 29b. Higher magnification of Figure 29a (scale bar =  
10  $\mu\text{m}$ ). 15 keV. dog 2146.

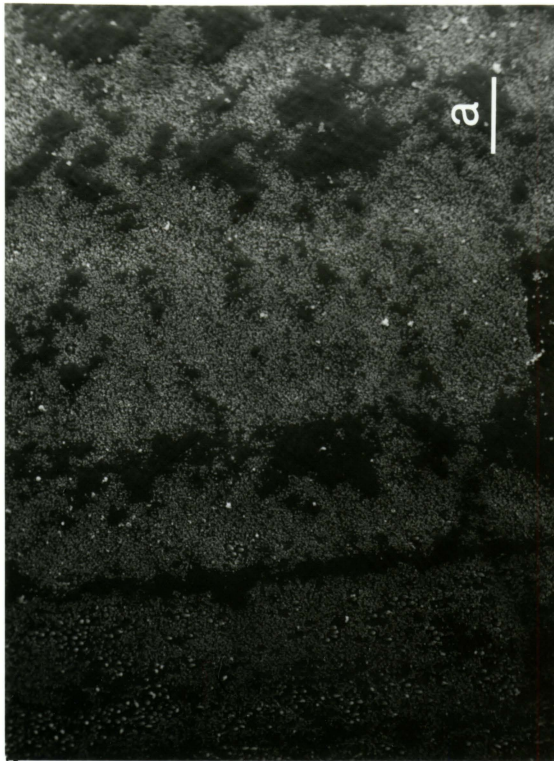
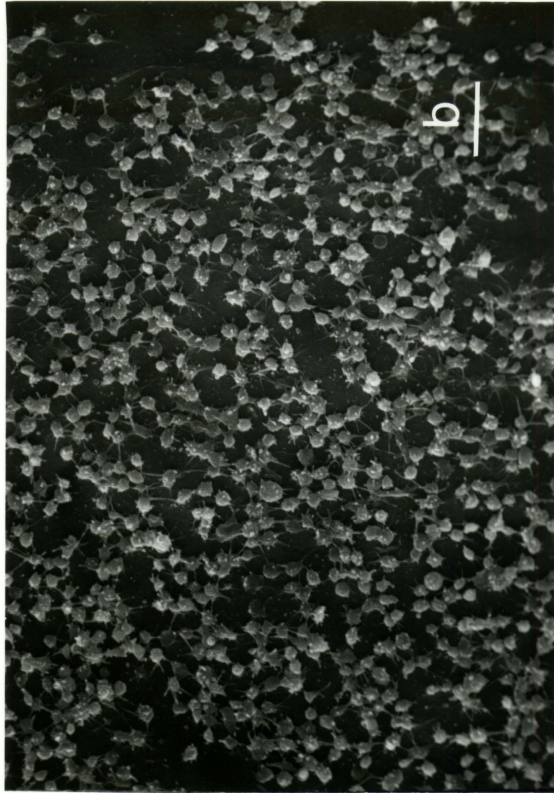
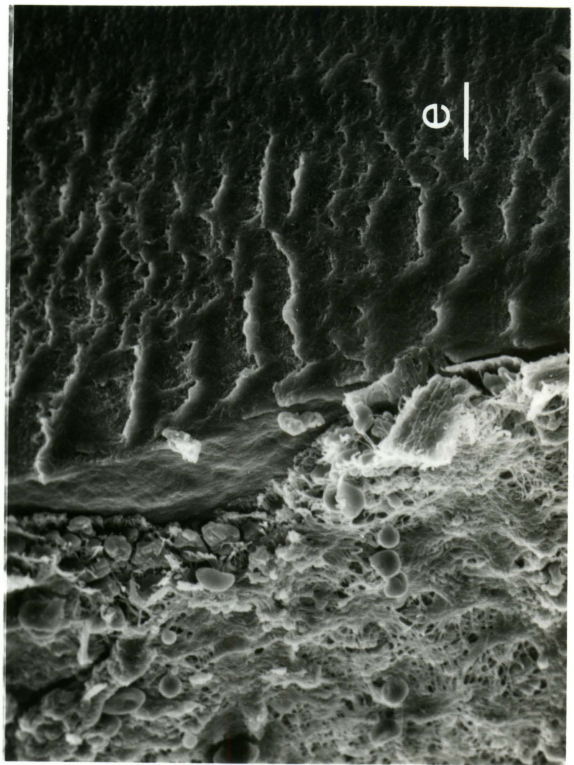
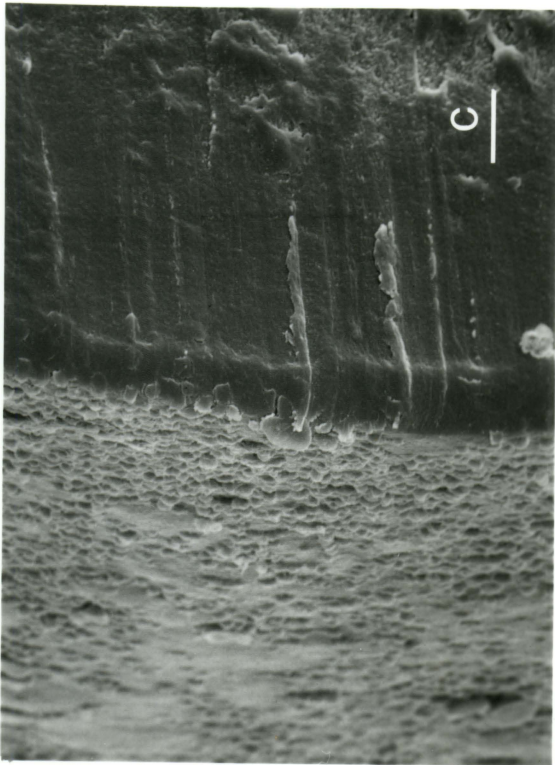
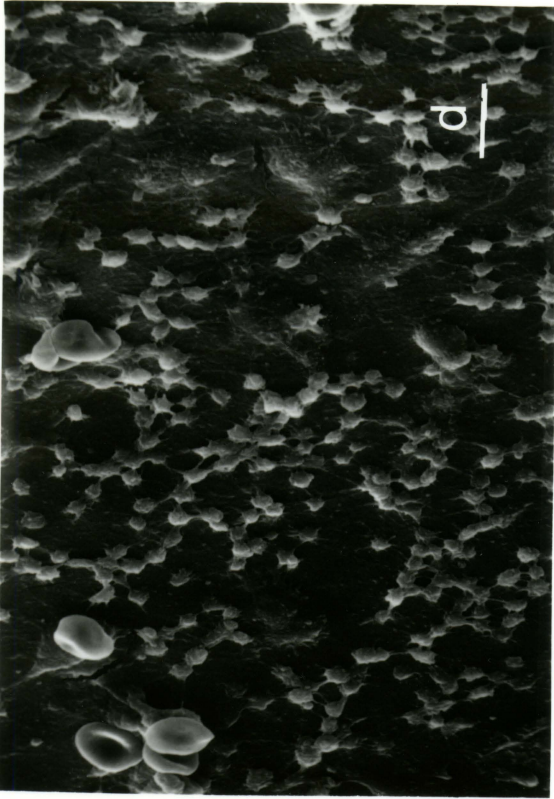


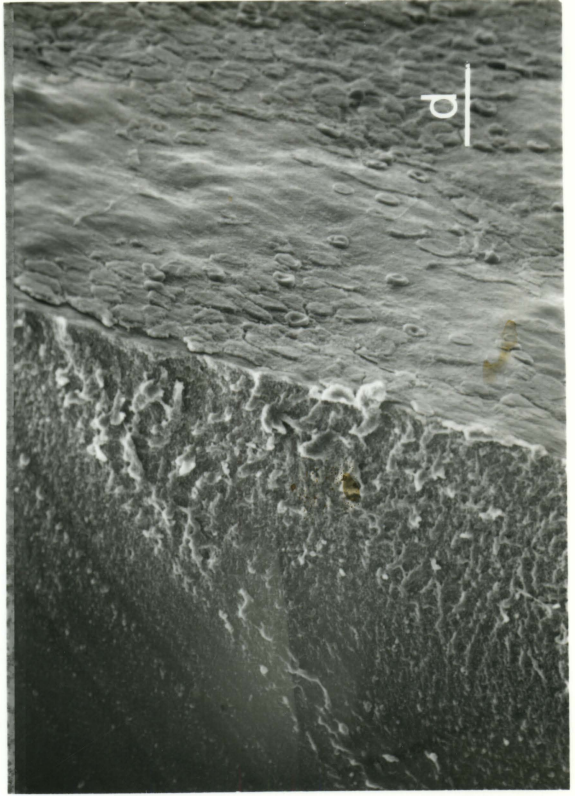
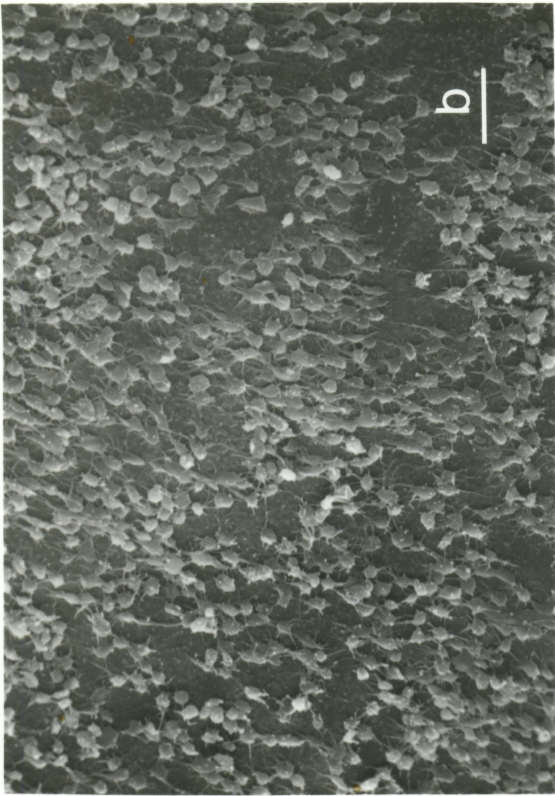
Figure 29c. 10% HEMA/10% NVP grafted catheter, section 2,  
at 30 minutes (scale bar = 10  $\mu$ m). 15 keV.  
20° tilt. dog 2146.

Figure 29d. 10 % HEMA/10% NVP grafted catheter, section 3,  
at 30 minutes (scale bar = 10  $\mu$ m). 15 keV.  
dog 2146.

Figure 29e. 10% HEMA/10% NVP grafted catheter, section 6,  
at 30 minutes (scale bar = 10  $\mu$ m). 15 keV.  
30° tilt. dog 2146.



- Figure 30a. Scanning electron micrograph of the 10% HEMA/  
10% NVP grafted catheter, section 1, at 60  
minutes (scale bar = 100  $\mu\text{m}$ ). 15 keV. dog  
2146.
- Figure 30b. Higher magnification of Figure 30a (scale bar =  
10  $\mu\text{m}$ ). 15 keV. dog 2146.
- Figure 30c. 10% HEMA/10% NVP grafted catheter, section 5,  
at 60 minutes (scale bar = 10  $\mu\text{m}$ ). 15 keV.  
dog 2146.
- Figure 30d. 10% HEMA/10% NVP grafted catheter, section 6,  
at 60 minutes (scale bar = 30  $\mu\text{m}$ ). 15 keV.  
20° tilt. dog 2146.



29a through 29c. The deposition ranges from adhering platelets with pseudopods, (Figures 29a and 29b) to a fibrin/red cell mat (Figures 29c through 29e). Note also in Figure 29d the adherence of platelets to an already developed layer. The deposition thickness for this 30 minute period is 5 - 10  $\mu\text{m}$ . The response after 60 minutes is shown in Figures 30a through 30d. The response ranges from platelet deposition, Figures 30a and 30b, to the RBC deposition with apparent incorporation in a fibrin mat, Figure 30d. The deposition thickness was less than 5  $\mu\text{m}$ .

This formulation remains fairly stable with a cellular deposition of less than 10  $\mu\text{m}$ .

10% HEMA/10% NVP, dog 2130 In the 15 minute trial, a well-developed fibrin network with leukocytes was seen. In the 30 minute trial, areas of platelet deposition and fibrin network development were seen. Platelet adhesion and fibrin deposition was also seen in section 5, but to a greater degree than on section 1. In the 60 minute trial, a highly reactive area with platelet masses and leukocyte deposition was seen. In section 7 a well-developed red thrombus was seen.

5% HEMA/10% NVP

5% HEMA/15% NVP, dog 2146 The response of blood to the 5% HEMA/15% NVP formulation for dog 2146 is shown in Figures 31 through 33. The 15 minute trial results are shown in Figures 31a through 31g. The cellular deposition is seen to progress from platelet adherence (Figures 31a through 31d), to fibrin formation (Figures 31e and 31f),

- Figure 31a. Scanning electron micrograph of the 5% HEMA/  
15% NVP grafted catheter, section 1, at 15  
minutes (scale bar = 100  $\mu\text{m}$ ). 15 keV. dog  
2146.
- Figure 31b. Higher magnification of Figure 31a (scale  
bar = 10  $\mu\text{m}$ ). 15 keV. dog 2146.
- Figure 31c. 5% HEMA/15% NVP grafted catheter, section 2,  
at 15 minutes (scale bar = 33.3  $\mu\text{m}$ ). 15 keV.  
20° tilt. dog 2146.
- Figure 31d. 5% HEMA/15% NVP grafted catheter, section 3,  
at 15 minutes (scale bar = 10  $\mu\text{m}$ ). 15 keV.  
dog 2146.

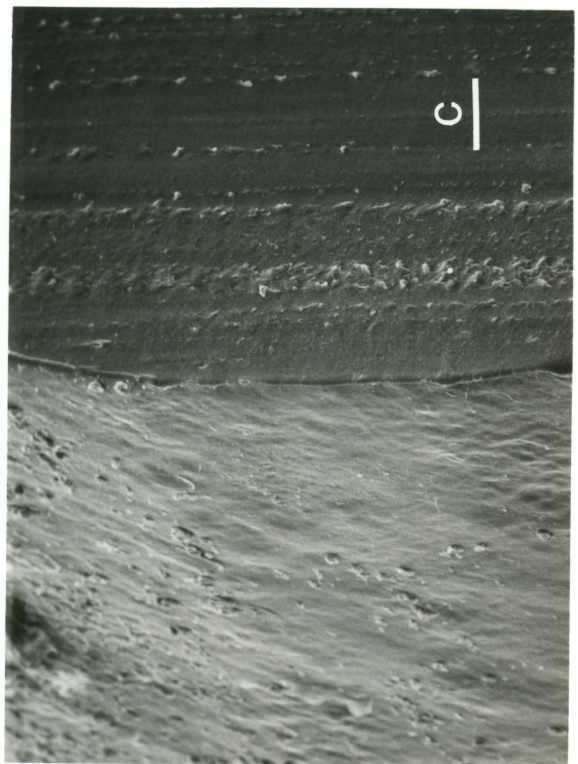
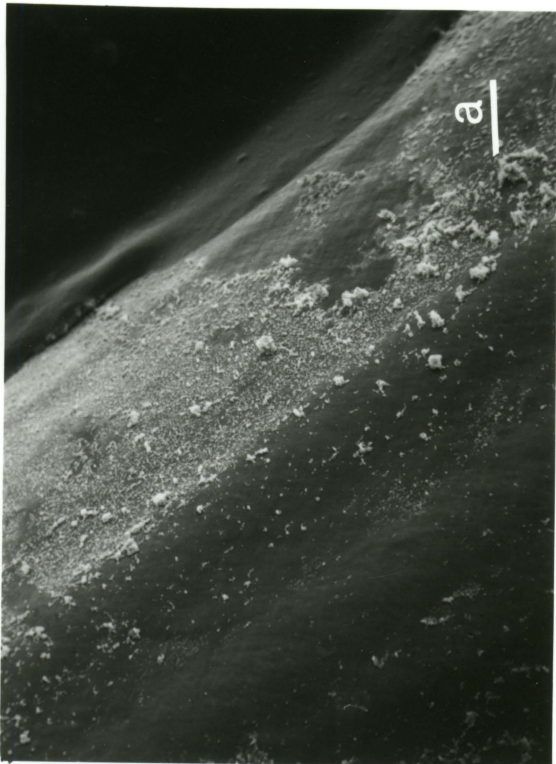
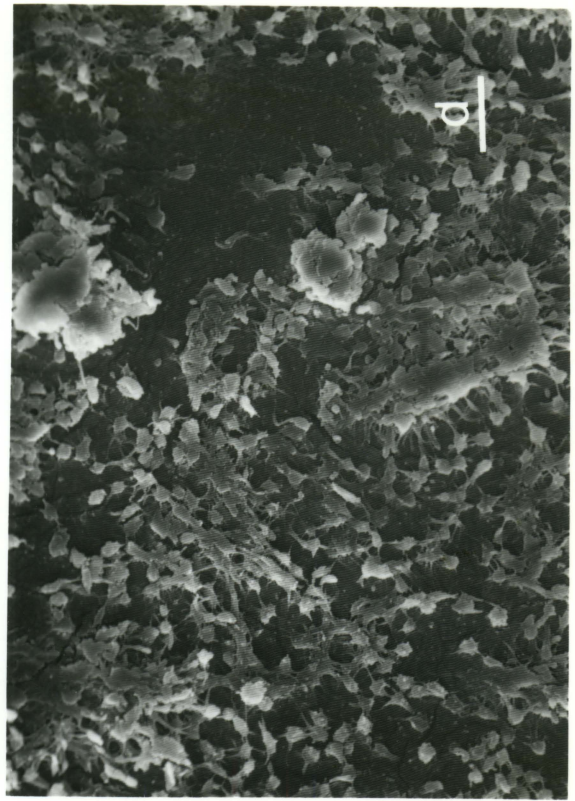
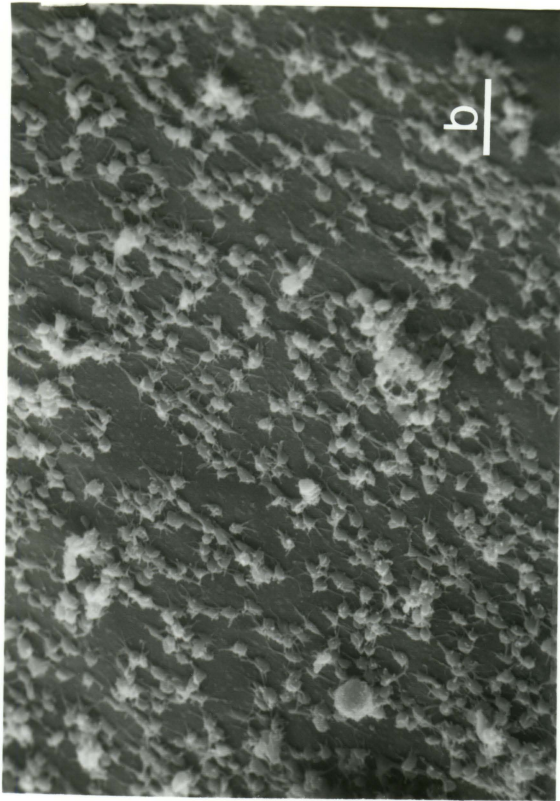


Figure 31e. 5% HEMA/15% NVP grafted catheter, section 5,  
at 15 minutes (scale bar = 10  $\mu\text{m}$ ). 15 keV.  
dog 2146.

Figure 31f. 5% HEMA/15% NVP grafted catheter, section 6,  
at 15 minutes (scale bar = 20  $\mu\text{m}$ ). 15 keV.  
20° tilt. dog 2146.

Figure 31g. 5% HMEA/15% NVP grafted catheter, section 7,  
at 15 minutes (scale bar = 10  $\mu\text{m}$ ). 15 keV.  
dog 2146.

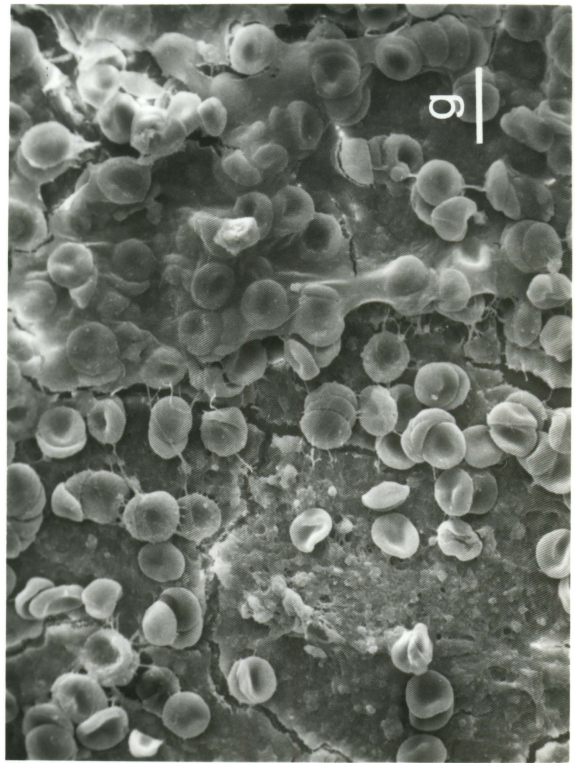
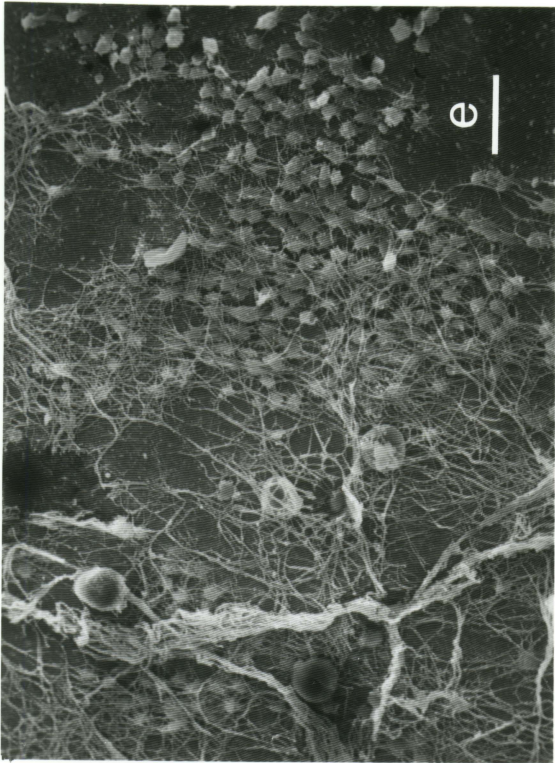
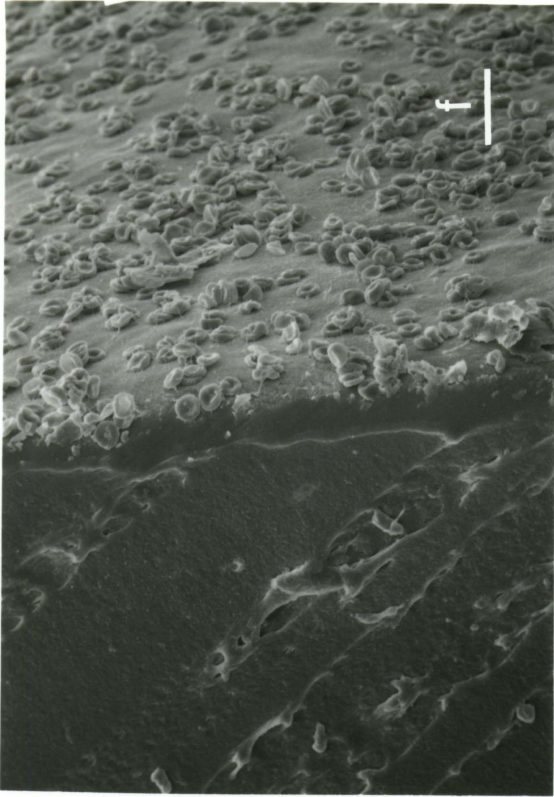


Figure 32a. Scanning electron micrograph of the 5% HEMA/  
15% NVP grafted catheter, section 1, at 30  
minutes (scale bar = 100  $\mu\text{m}$ ). 15 keV. dog  
2146.

Figure 32b. Higher magnification of Figure 32a (scale  
bar = 10  $\mu\text{m}$ ). 15 keV. dog 2146.

Figure 32c. 5% HEMA/15% NVP grafted catheter, section 2,  
15 30 minutes (scale bar = 33.3  $\mu\text{m}$ ). 15 keV.  
20° tilt. dog 2146.

Figure 32d. 5% HEMA/15% NVP grafted catheter, section 3,  
at 30 minutes (scale bar = 10  $\mu\text{m}$ ). 15 keV.  
dog 2146.

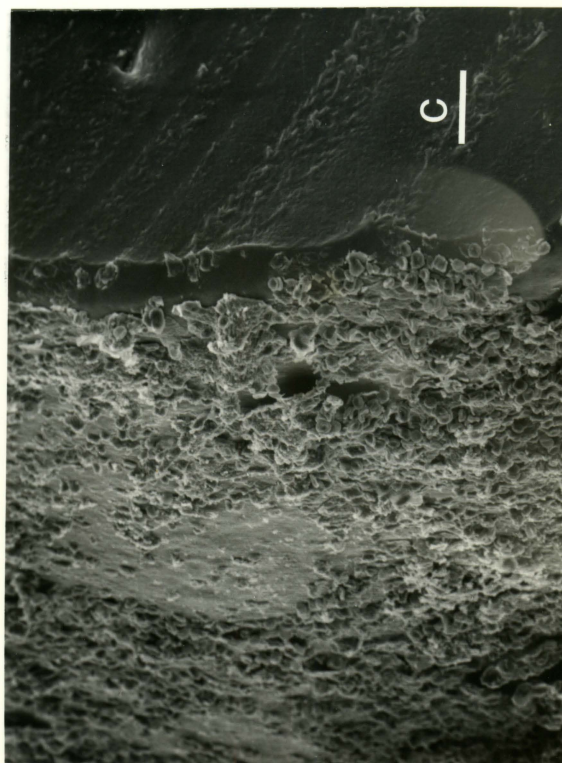
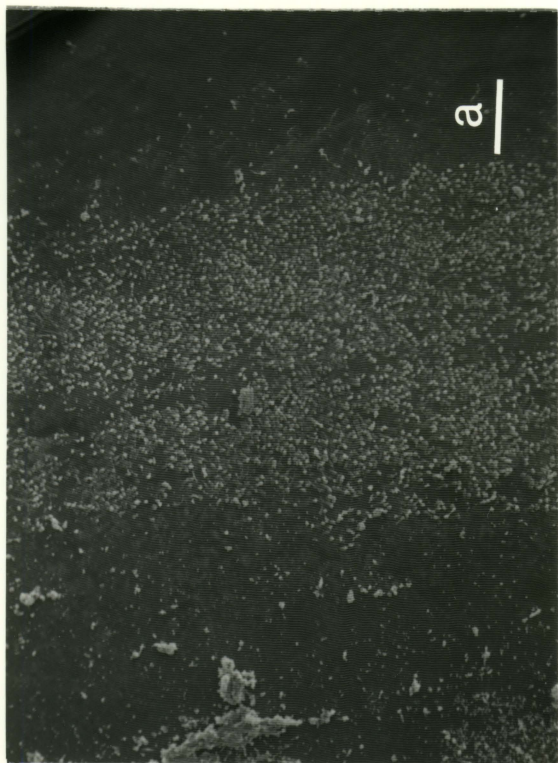
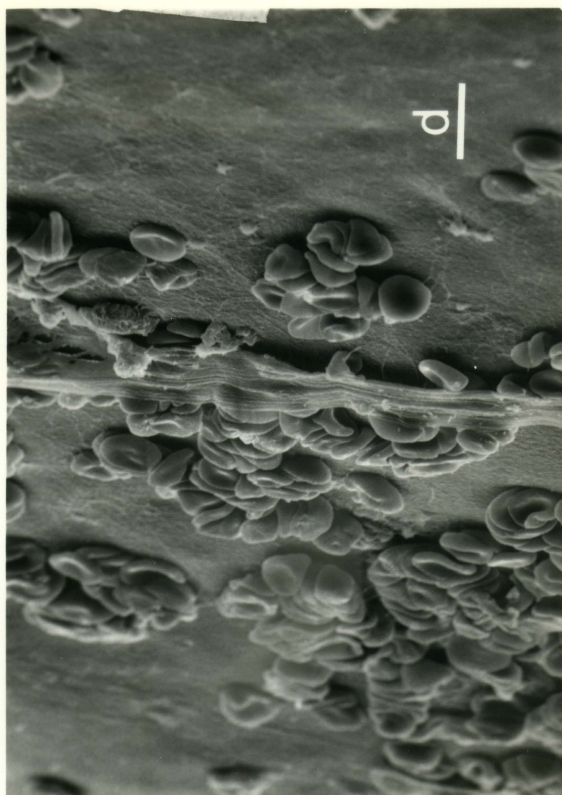
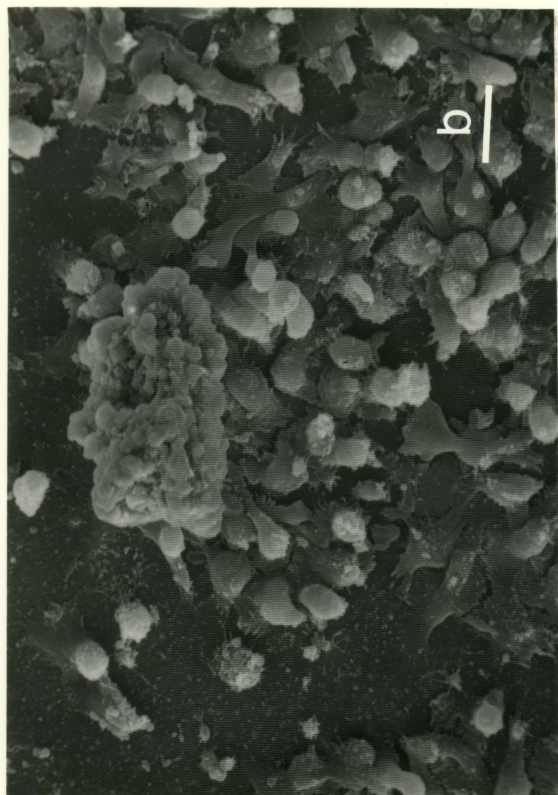


Figure 32e. 5% HEMA/15% NVP grafted catheter, section 4,  
at 30 minutes (scale bar = 33.3  $\mu\text{m}$ ). 15 keV.  
dog 2146.

Figure 32f. Figure 32e at 30° tilt (scale bar = 33.3  $\mu\text{m}$ ).  
15 keV. dog 2146.

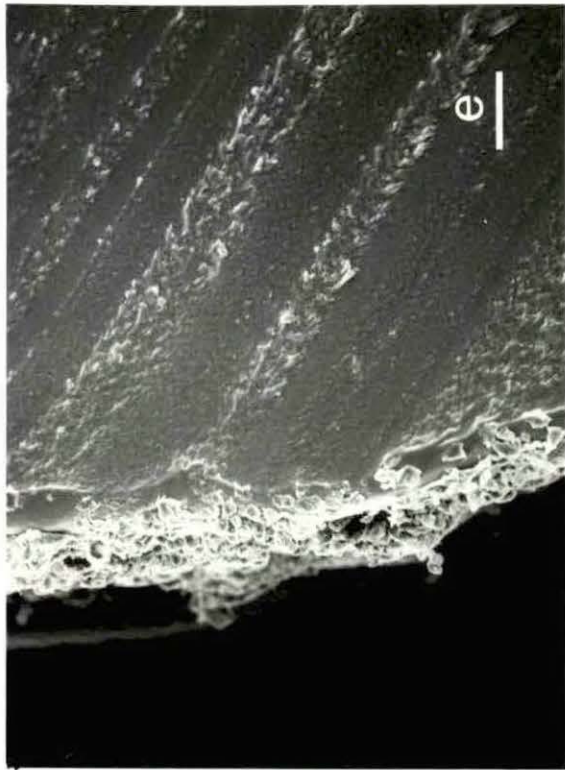
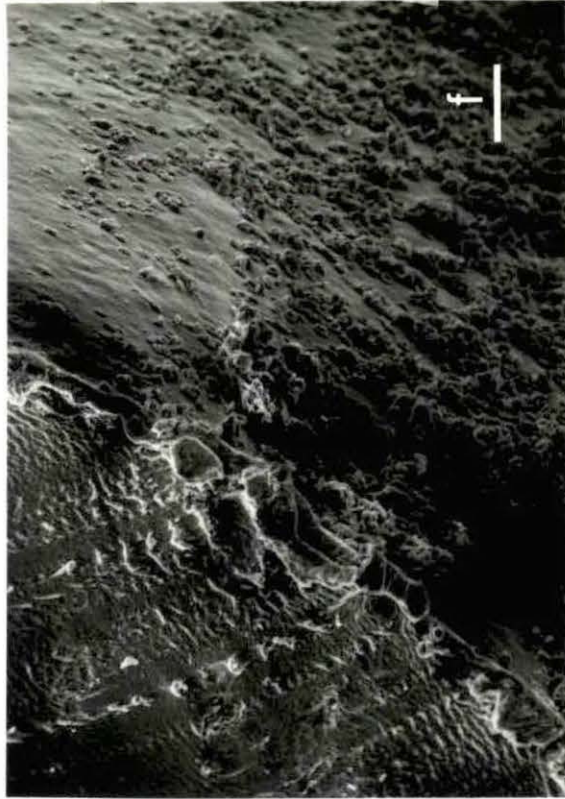
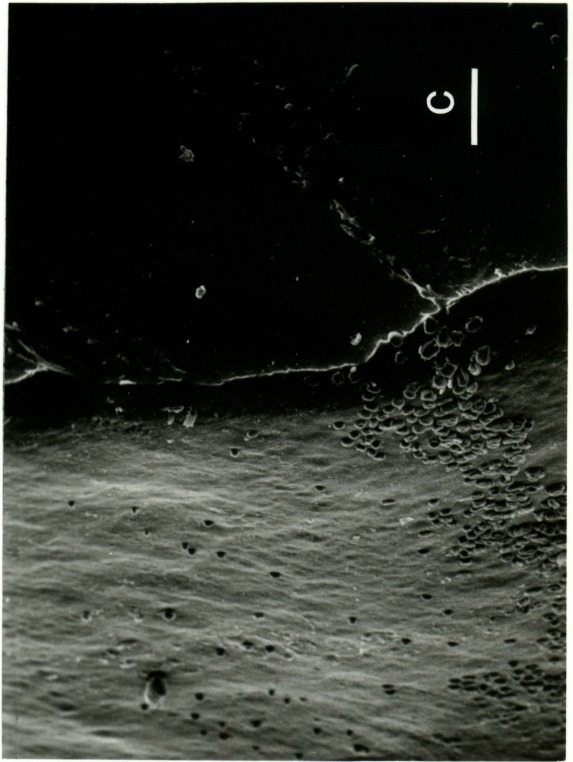
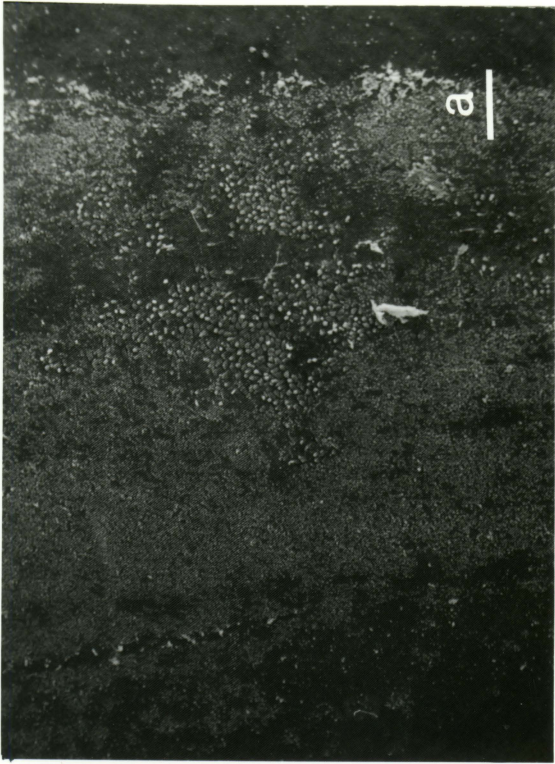
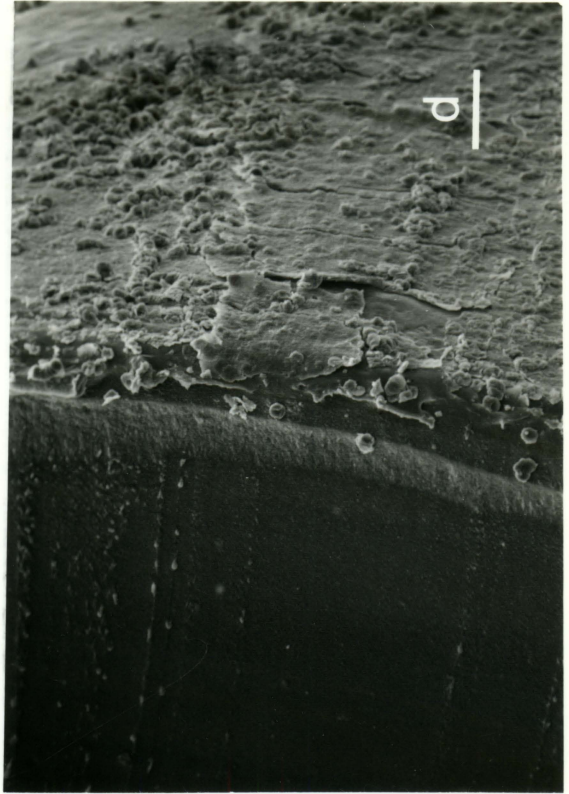
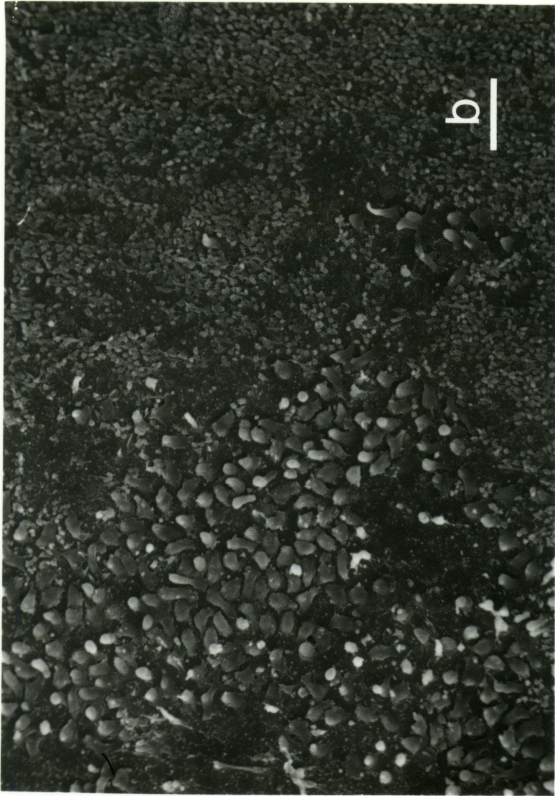


Figure 33a. Scanning electron micrograph of the 5% HEMA/  
15% NVP grafted catheter, section 1, at 60  
minutes (scale bar = 100  $\mu\text{m}$ ). 15 keV.  
dog 2146.

Figure 33b. Higher magnification of Figure 33a (scale bar =  
33.3  $\mu\text{m}$ ). 15 keV. dog 2146.

Figure 33c. 5% HEMA/15% NVP grafted catheter, section 2,  
at 60 minutes (scale bar = 33.3  $\mu\text{m}$ ). 15 keV.  
20° tilt. dog 2146.

Figure 33d. 5% HEMA/15% NVP grafted catheter, section 6,  
at 60 minutes (scale bar = 33.3  $\mu\text{m}$ ). 15 keV.  
20° tilt. dog 2146.



to RBCs incorporated in a fibrin film (Figure 31g). The deposition thickness is less than 5  $\mu\text{m}$ . The response after 30 minutes is shown in Figures 32a through 32f. Leukocyte deposition occurs on section 1, Figures 32a and 32b, with a covering of RBCs in the following sections (Figures 32c through 32f). The cellular deposition thickness ranges from 5-30  $\mu\text{m}$ . The 60 minute trial results are shown in Figures 33a through 33d. The response increases from adherent platelets and leukocytes in Figures 33a and 33b to RBCs incorporated in a fine fibrin layer, Figure 33d. The cellular deposition thickness is less than 5  $\mu\text{m}$ .

This formulation remains fairly stable with respect to cellular layer formation.

5% HEMA/15% NVP, dog 2130 In the 15 minute trial for dog 2130, fibrin covers the surface of section 1. In the 30 minute trial, aggregated platelets cover the surface of section 1. In the 60 minute trial, a well developed fibrin net covers both sections 1 and 5.

0% HEMA/20% NVP

0% HEMA/20% NVP, dog 2146 The response of blood to the 0% HEMA/20% NVP formulation in dog 2146 is shown in Figures 34 through 36. The response after 15 minutes is shown in Figure 34a through 34d. The response ranges from adherent platelets to the developed fibrin net on catheter sections 5 and 7. The cellular deposit thickness was approximately 5  $\mu\text{m}$ . The response after 30 minutes is shown in Figures 35a through 35f. This series of micrographs also shows a range from

Figure 34a. Scanning electron micrograph of the 0% HEMA/  
20% NVP grafted catheter, section 1, at 15  
minutes (scale bar = 100  $\mu\text{m}$ ). 15 keV. dog  
2146.

Figure 34b. 0% HEMA/10% NVP grafted catheter, section 2,  
at 15 minutes (scale bar = 10  $\mu\text{m}$ ). 15 keV.  
5° tilt. dog 2146.

Figure 34c. 0% HEMA/20% NVP grafted catheter, section 5,  
at 15 minutes (scale bar = 10  $\mu\text{m}$ ). 15 keV.  
dog 2146.

Figure 34d. 0% HEMA/20% NVP grafted catheter, section 6,  
at 15 minutes (scale bar = 10  $\mu\text{m}$ ). 15 keV.  
30° tilt. dog 2146.

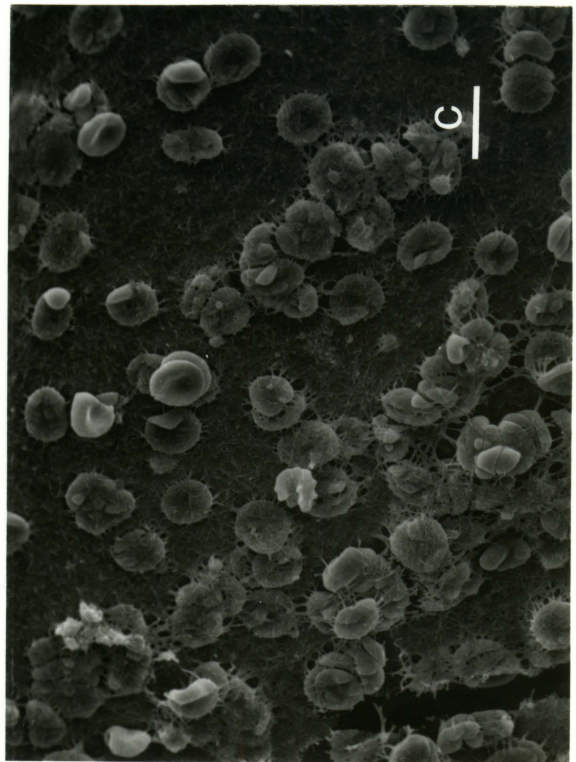
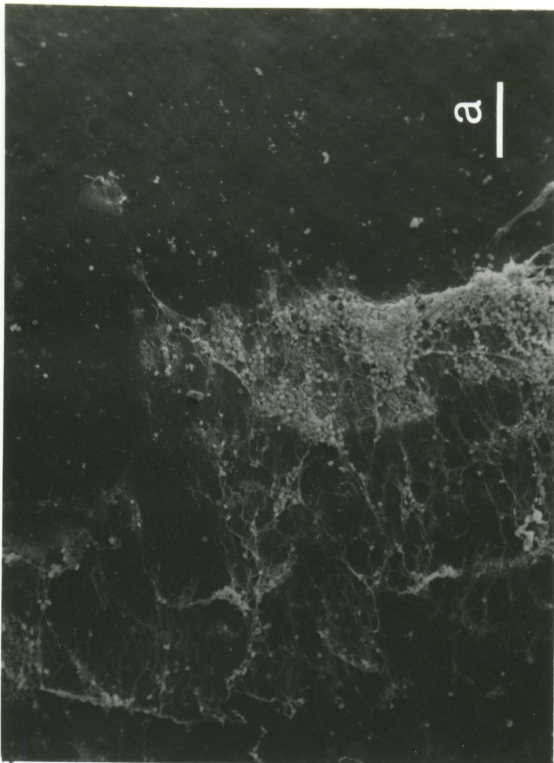
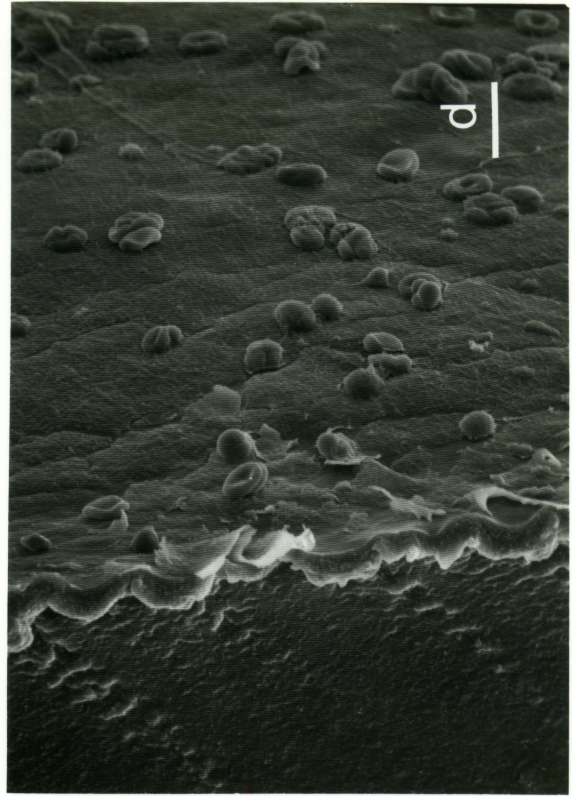
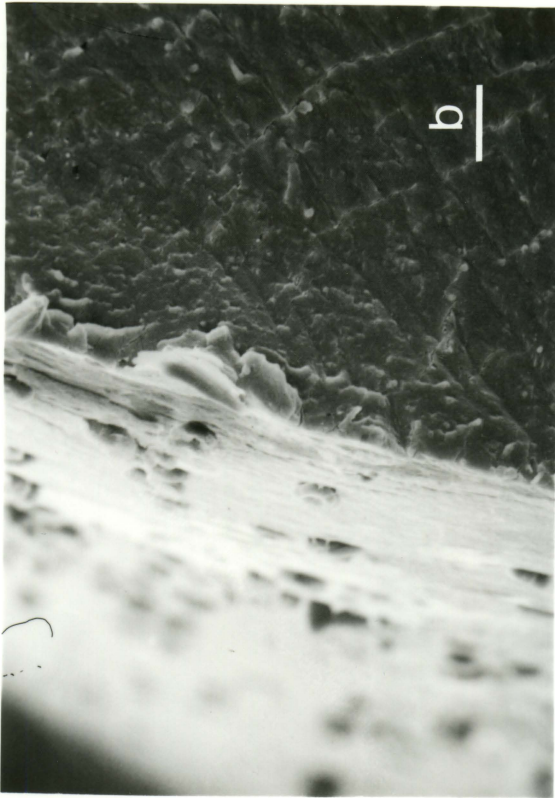


Figure 35a. Scanning electron micrograph of the 0% HEMA/  
20% NVP grafted catheter, section 1, at 30  
minutes (scale bar = 100  $\mu\text{m}$ ). 15 keV. dog  
2146.

Figure 35b. Higher magnification of Figure 35a (scale  
bar = 10  $\mu\text{m}$ ). 15 keV. dog 2146.

Figure 35c. 0% HEMA/20% NVP grafted catheter, section 2,  
at 30 minutes (scale bar = 33.3  $\mu\text{m}$ ). 15 keV.  
20° tilt. dog 2146.

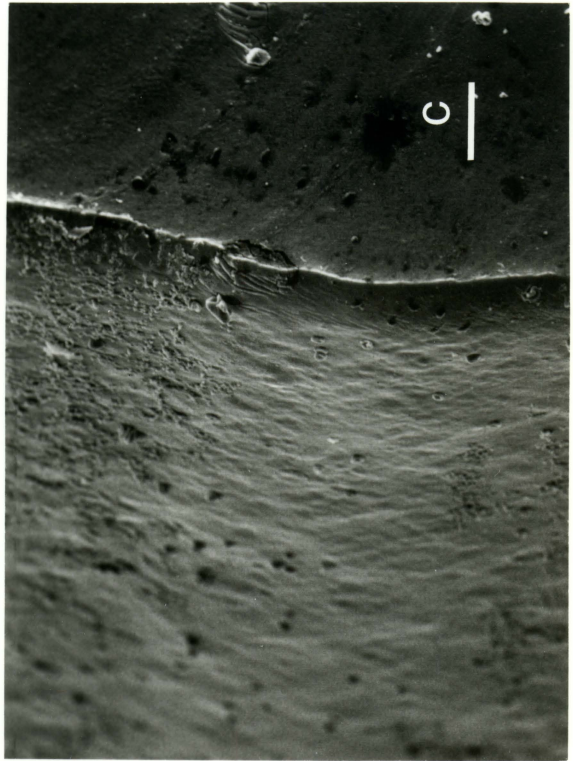
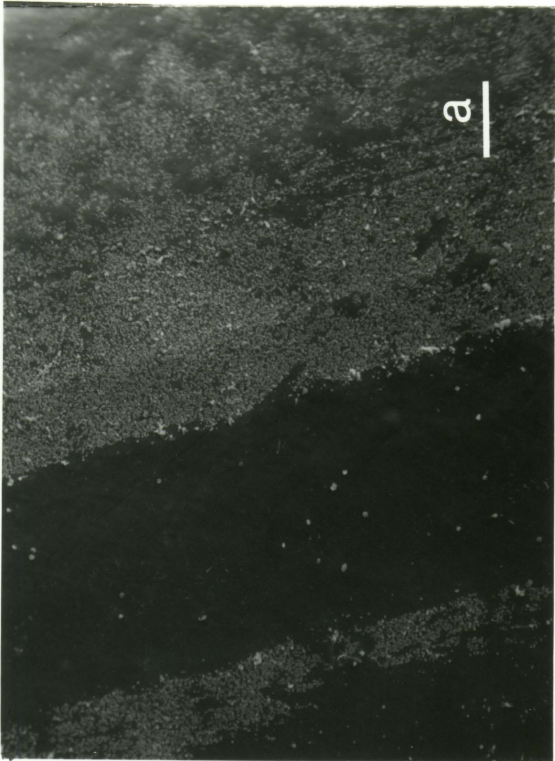
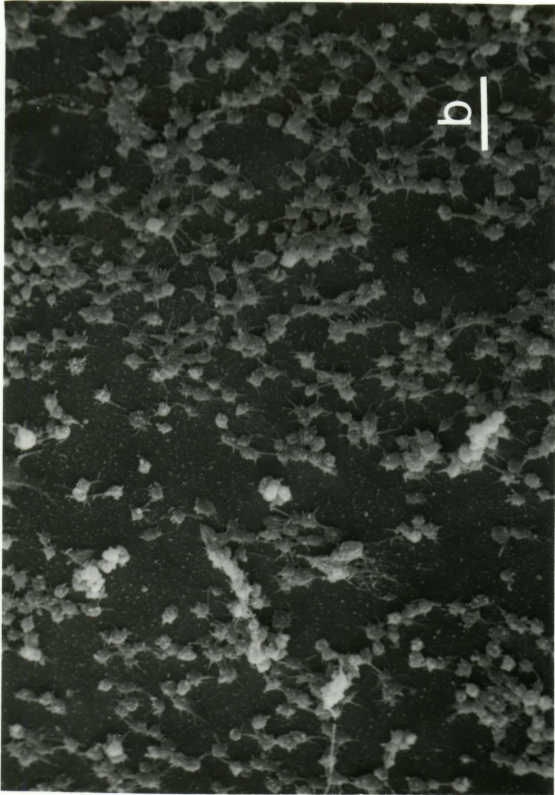


Figure 35d. 0% HEMA/20% NVP grafted catheter, section 6,  
at 30 minutes (scale bar = 33.3  $\mu\text{m}$ ). 15 keV.  
20° tilt. dog 2146.

Figure 35e. 0% HEMA/20% NVP grafted catheter, section 7,  
at 30 minutes (scale bar = 10  $\mu\text{m}$ ). 15 keV.  
dog 2146.

Figure 35f. 0% HEMA/20% NVP grafted catheter, section 7,  
at 30 minutes (scale bar = 10  $\mu\text{m}$ ). 15 keV.  
dog 2146.

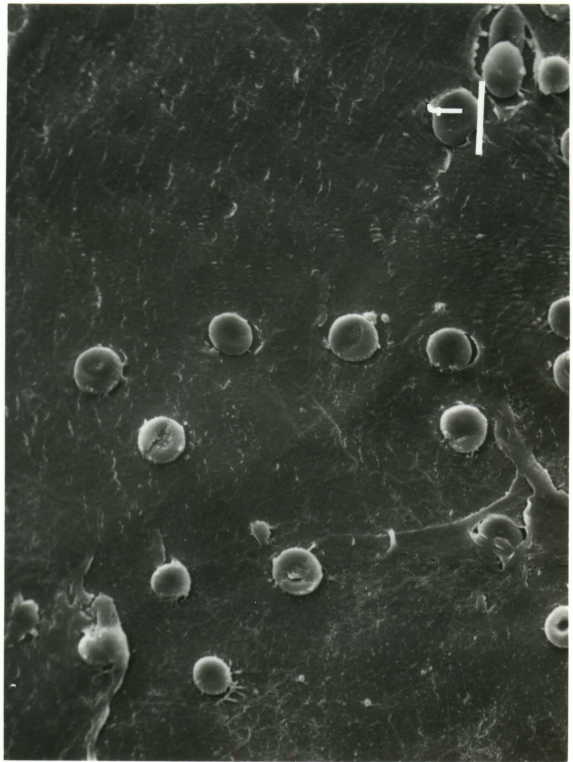
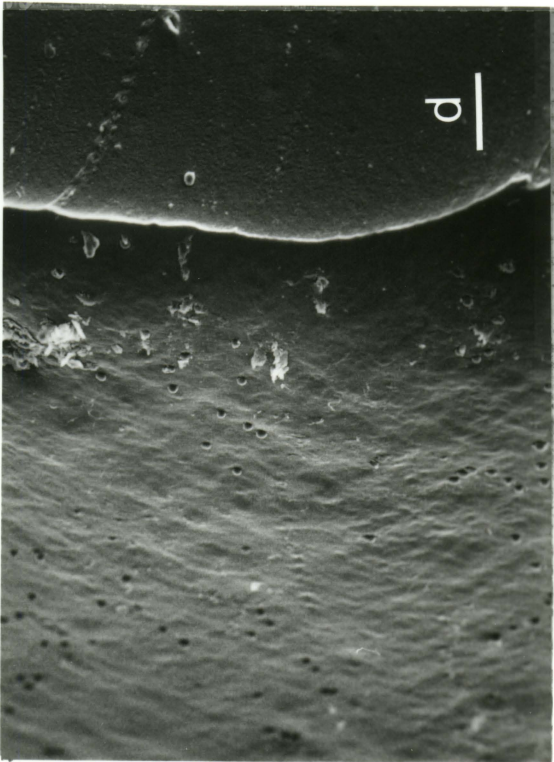
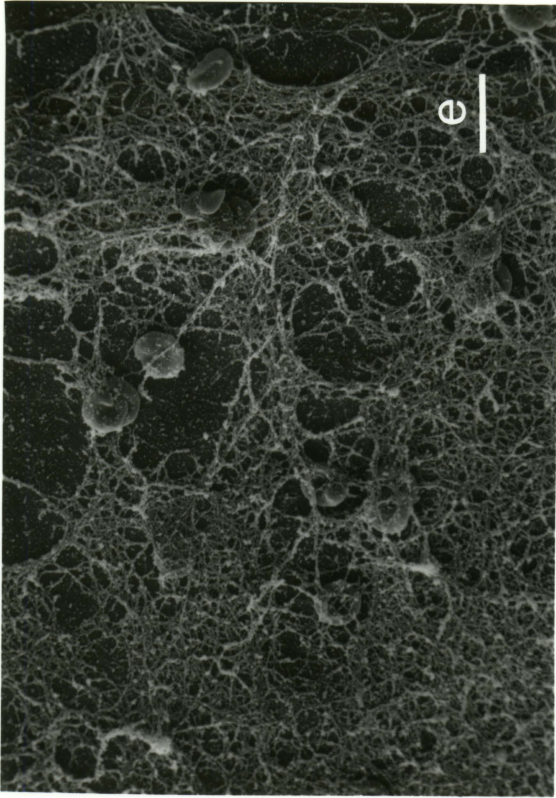


Figure 36a. Scanning electron micrograph of the 0% HEMA/  
20% NVP grafted catheter, section 1, at 60  
minutes (scale bar = 100  $\mu\text{m}$ ). 15 keV. dog  
2146.

Figure 36b. Higher magnification of Figure 36a (scale  
bar = 10  $\mu\text{m}$ ). 15 keV. dog 2146.

Figure 36c. 0% HEMA/20% NVP grafted catheter, section 2,  
at 60 minutes (scale bar = 33.3  $\mu\text{m}$ ). 15 keV.  
20° tilt. dog 2146.

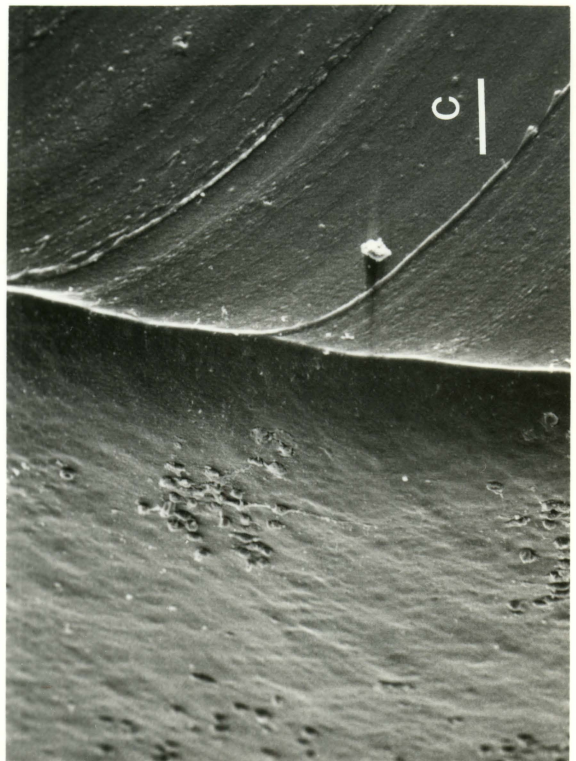
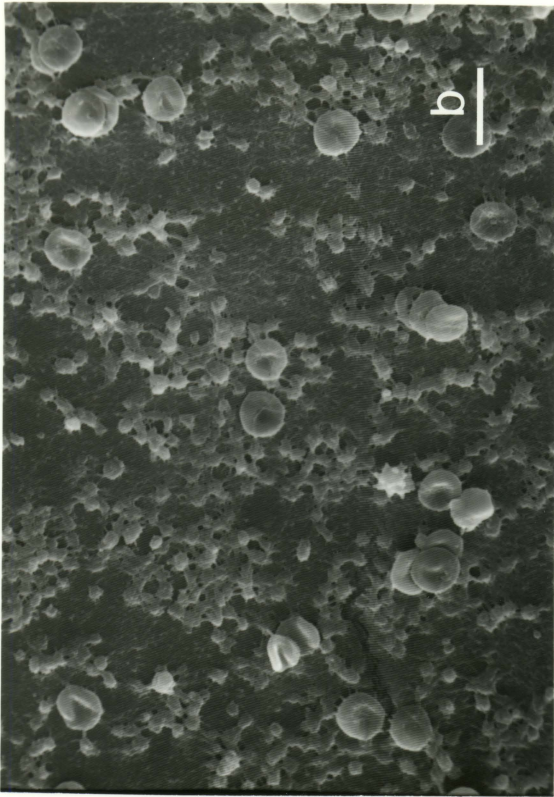
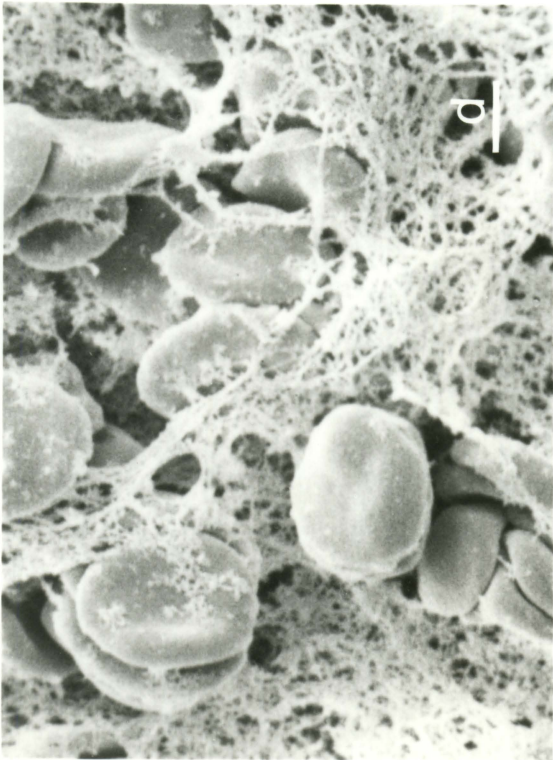
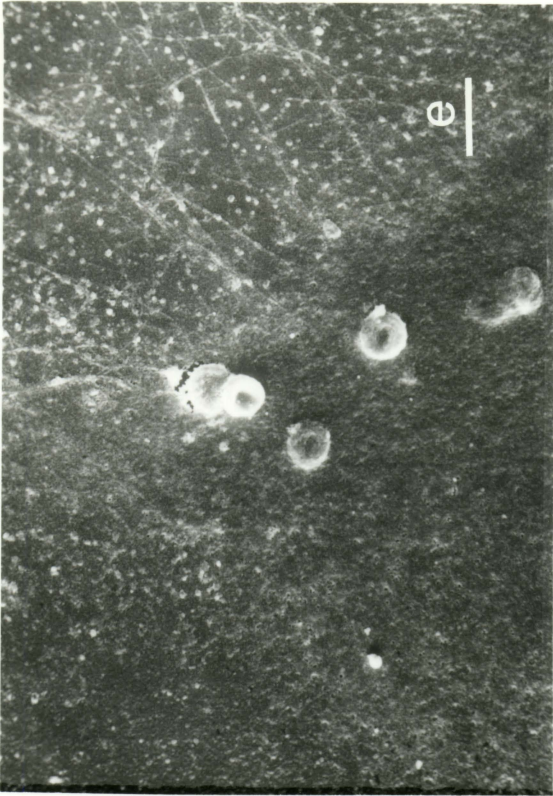


Figure 36d. 0% HEMA/20% NVP grafted catheter, section 5,  
at 60 minutes (scale bar = 3.33  $\mu\text{m}$ ). 15 keV.  
dog 2146.

Figure 36e. 0% HEMA/20% NVP grafted catheter, section 7,  
at 60 minutes (scale bar = 10  $\mu\text{m}$ ). 15 keV.  
dog 2146.

Figure 36f. 0% HEMA/20% NVP grafted catheter, section 8,  
at 60 minutes (scale bar = 33.3  $\mu\text{m}$ ). 15 keV.  
20° tilt. dog 2146.



platelet adhesion in section 1, Figures 35a and 35b, to a developing fibrin net in section 7, Figures 35e and 35f. The cellular deposition was approximately 5  $\mu\text{m}$ . The response is after 60 minutes is shown in Figures 36a through 36f. The cellular deposit thickness was, again, approximately 5  $\mu\text{m}$ .

0% HEMA/20% NVP, dog 2130 The results of the 0% HEMA/20% NVP formulation trials in dog 2130 are shown in Figures 37 and 38. The 15 minute trial results are shown in Figures 37a and 37b. Platelet aggregation can be seen over the surface of section 1. The 30 minute trial results are shown in Figure 38a and 38b. Thrombus formation is well-developed over sections 1 through 2. The deposits on the 60 minute trial catheters were lost due to stripping of the surface during withdrawal.

The cellular deposition thickness for the catheters tested in dog number 2146 are shown in Table 10. While the surface elements shown are useful in the determination of the relative type of deposition, this cross-sectional information is also important in the analysis of each catheter's performance.

From the information in Table 10, it appears that the more hydrophobic formulations, 5% HEMA/15% NVP and 0% HEMA/20% NVP, and the most hydrophilic formulation, 10% HEMA/10% NVP, have responses comparable to the silicone rubber. The midrange formulations, 20% HEMA/0% NVP and 15% HEMA/5% NVP, have considerable thrombus at 60 minutes and 30 minutes, respectively.

Figure 37a. Scanning electron micrograph of the 0% HEMA/  
20% NVP grafted catheter, section 1, at 15  
minutes (scale bar = 100  $\mu\text{m}$ ). 15 keV. dog 2130.

Figure 37b. Higher magnification of Figure 37a (scale bar =  
10  $\mu\text{m}$ ). 15 keV. dog 2130.

Figure 38a. Scanning electron micrograph of the 0% HEMA/  
20% NVP grafted catheter, sections 1-2, at 30  
minutes (scale bar = 100  $\mu\text{m}$ ). 15 keV. dog  
2130.

Figure 38b. Higher magnification of Figure 38a (scale bar =  
10  $\mu\text{m}$ ). 15 keV. dog 2130.

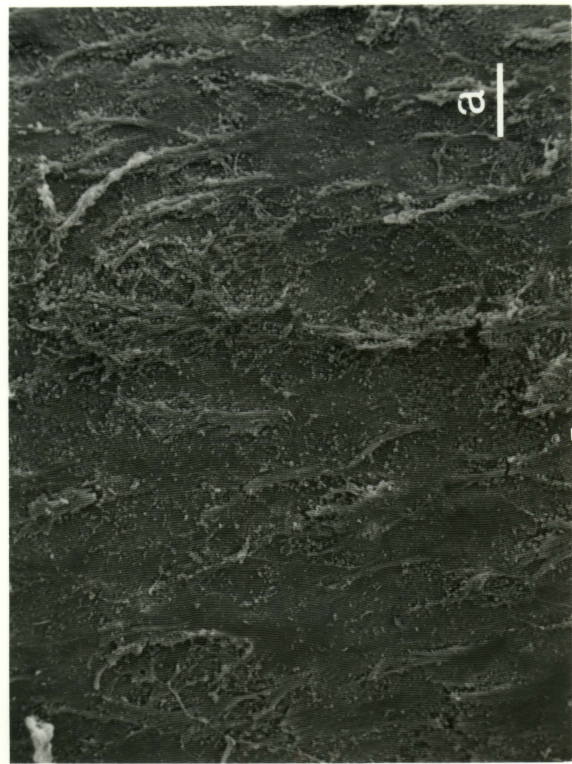
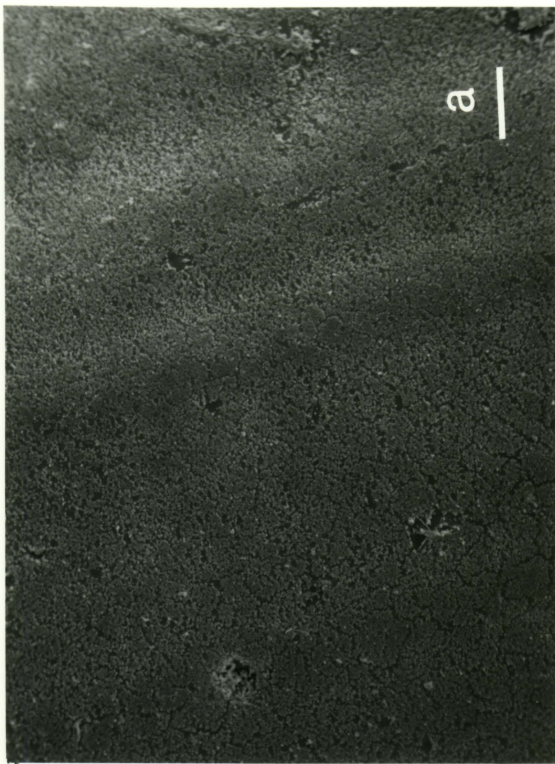
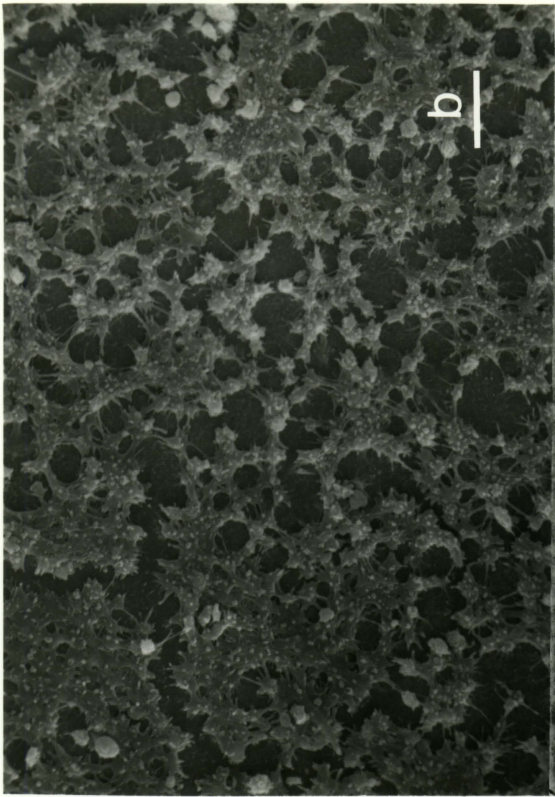


Table 10. Analysis of cellular deposition thickness on catheter surfaces for dog number 2146

Formulation	Contact Angle with H <sub>2</sub> O	Cellular Deposit Thickness (15 min) (μm)	Cellular Deposit Thickness (30 min) (μm)	Cellular Deposit Thickness (60 min) (μm)
Silastic	100 <sup>b</sup>	5	5	5
0% HEMA 20% NVP	91 <sup>b</sup>	5	5	5
5% HEMA 15% NVP	81 <sup>a</sup>	5	5-30	5
10% HEMA/ 10% NVP	70 <sup>b</sup>	5	5-10	5
20% HEMA 5% NVP	67 <sup>a</sup>	10	3-50	0-200
15% HEMA 5% NVP	58 <sup>b</sup>	10	8-250	10

<sup>a</sup>Values reported by Vale (1980).

<sup>b</sup>Values measured in experiments reported in this thesis.

Table 11 represents a qualitative indication of the responses, based on the SEM micrographs. The control, Silastic<sup>®</sup>, has been compared to the 5 trial formulations. A response greater than the control's response is indicated by a plus (+), and a lesser response is indicated by a (-). The silicone rubber is consistently less responsive than the 20% HEMA/0% NVP and 15% HEMA/5% NVP formulations. The 10% HEMA/10% NVP, 5% HEMA/15% NVP, and 0% HEMA/20% NVP formulations vary in response and equal or better the response of the silicone rubber.

Table 11. Formulations compared to the Silastic<sup>®</sup> control, method 2

	<u>Dog 2146</u>			<u>Dog 2130</u>		
	<u>15</u>	<u>30</u>	<u>60</u>	<u>15</u>	<u>30</u>	<u>60</u>
10% HEMA/10% NVP	+	0	-	0	NA <sup>a</sup>	NA
20% HEMA/0% NVP	+	+	+	0	NA	NA
15% HEMA/5% NVP	+	+	+	-	NA	NA
Silastic	0	0	0	0	NA	NA
5% HEMA/15% NVP	+	+	0	0	NA	NA
0% HEMA/20% NVP	+	-	+	-	NA	NA

<sup>a</sup> Not applicable due to loss of control thrombus.

### Method 3

The experimental data for Method 3 are presented in Table 12. In method 3, the catheters were introduced for a 5 minute trial, then

retrieved by slitting the vessel as described in Materials and Methods. This permitted implant retrieval without stripping of the thrombus but did not allow for multiple insertions.

Table 12. Experimental data for dogs 2442, 2504, 2232, and 2297, Method 3

Dog Number	2441	2504	2232	2297
Activated Clotting Time (seconds)	85	90	90	75
Implantation time (min)	5	5	5	5
Formulation and Implantation site for all four dogs				
Silastic	Right Jugular Vein			
10% HEMA/10% NVP	Left Jugular vein			
15% HEMA/5% NVP	Rt. Femoral vein			
0% HEMA/20% NVP	Left Femoral vein			

The results shown in Table 13, of the 5 minute implantations of the four catheter groups indicate that the silicone rubber had the lowest thrombogenicity index ( $0.04 \text{ mg/mm}^2$ ). The 15% HEMA/5% NVP and 0% HEMA/20% NVP formulations had indexes of  $0.07 \text{ mg/mm}^2$ , while the index for the 10% HEMA/10% NVP formulation was  $0.09 \text{ mg/mm}^2$ .

The difference between the thrombogenicity index for the silicone rubber and that for the 10% HEMA/10% NVP formulation is significant ( $p. \leq 0.005$ ), but the differences between the indexes for the silicone

Table 13. Results of the 5 minute implantation of catheters, Method 3

Formulation Position	Thrombogenicity Index (mg/mm <sup>2</sup> )			
	Dog 2442	Dog 2504	Dog 2232	Dog 2297
<u>Silastic<sup>®</sup></u> Rt. Jugular Vein	0.03	0.04	0.08	0.04
<u>10% HEMA/10% NVP</u> Lt. Jugular Vein	0.08	0.10	0.03	0.10
<u>15% HEMA/5% NVP</u> Rt. Femoral Vein	0.07	0.07	0.02	0.05
<u>0% HEMA/20% NVP</u> Lt. Femoral Vein	0.07	0.05	----	0.09

and the 15% HEMA/5% NVP formulation and the silicone rubber and the 0% HEMA/20% formulation, are not significant ( $p = 0.12$  and  $p = 0.08$  respectively). While statistically these differences are not significant (at the 95% confidence level), there appears to be a trend toward three populations: (1) silicone rubber, (2) 15% HEMA/5% NVP and 0% HEMA/20% NVP and (3) 10% HEMA/10% NVP. Further tests using greater numbers of implants may indicate that there is a significant difference.

Based on critical surface tension values, the silicone rubber and the 0% HEMA/20% NVP formulation should have caused similar responses, whereas the 15% HEMA/5% NVP and 10% HEMA/10% NVP formulations should show increasingly adverse responses. This trend is not clearly evident, but increasing critical surface tension does appear to cause an increase in response, see Figure 39. It should be noted that dog 2232 was not included in this analysis. The thrombogenicity index was considerably different from that of the other three trials and were considered in error.

The decrease in hydrophobicity of silicone rubber did not appear to enhance the hemocompatibility. There was no correlation between hydrophilicity and decreased thrombogenicity. Figure 40 shows the opposite trend; the more hydrophobic materials had the lowest thrombogenicity index.

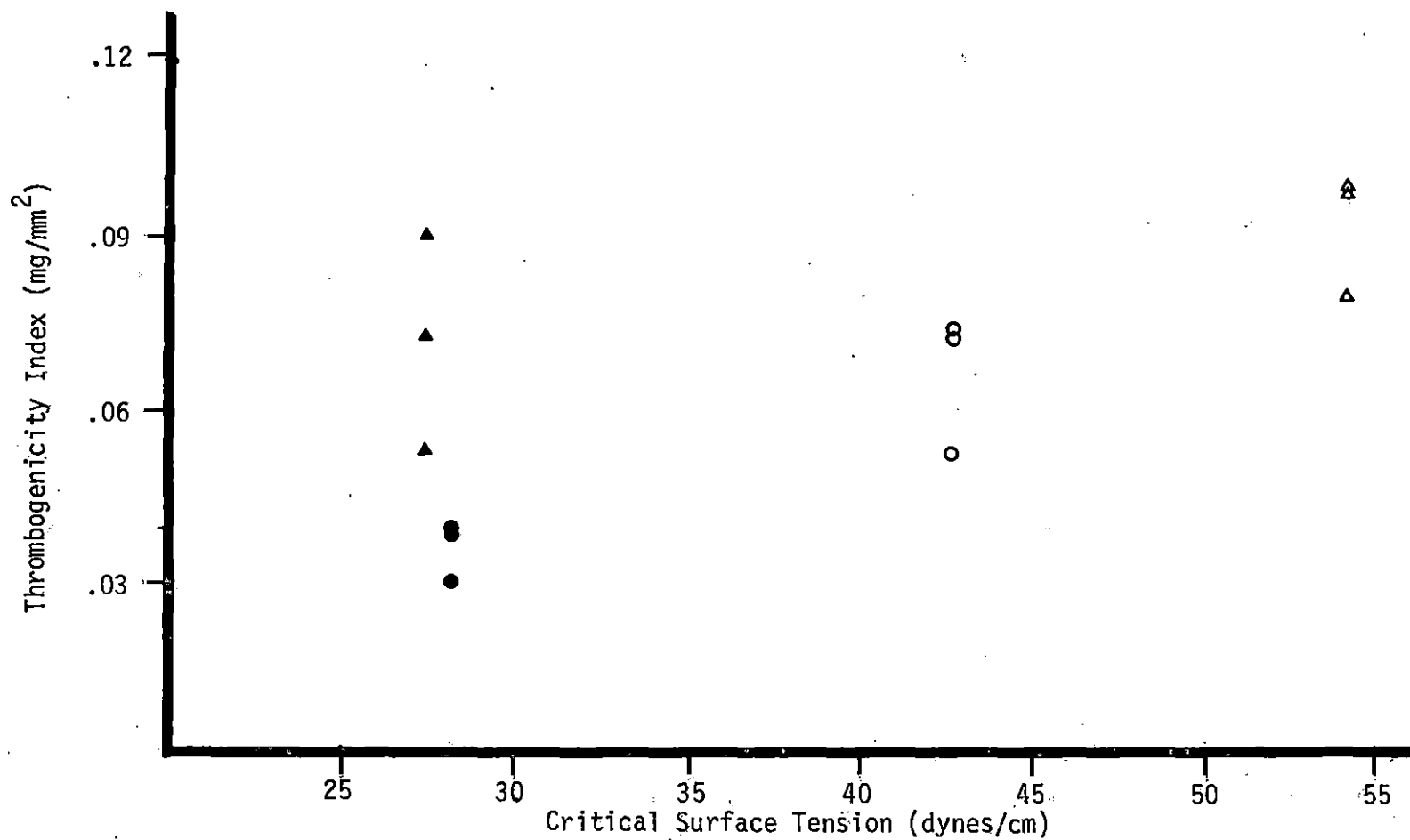


Figure 39. Thrombogenicity index vs. critical surface tension for experimental animals 2442, 2504, and 2297. (●) is silicone rubber, (○) is 15% HEMA/5% NVP, (▲) is 10% HEMA/10% NVP, (△) is 0% HEMA/20% NVP.

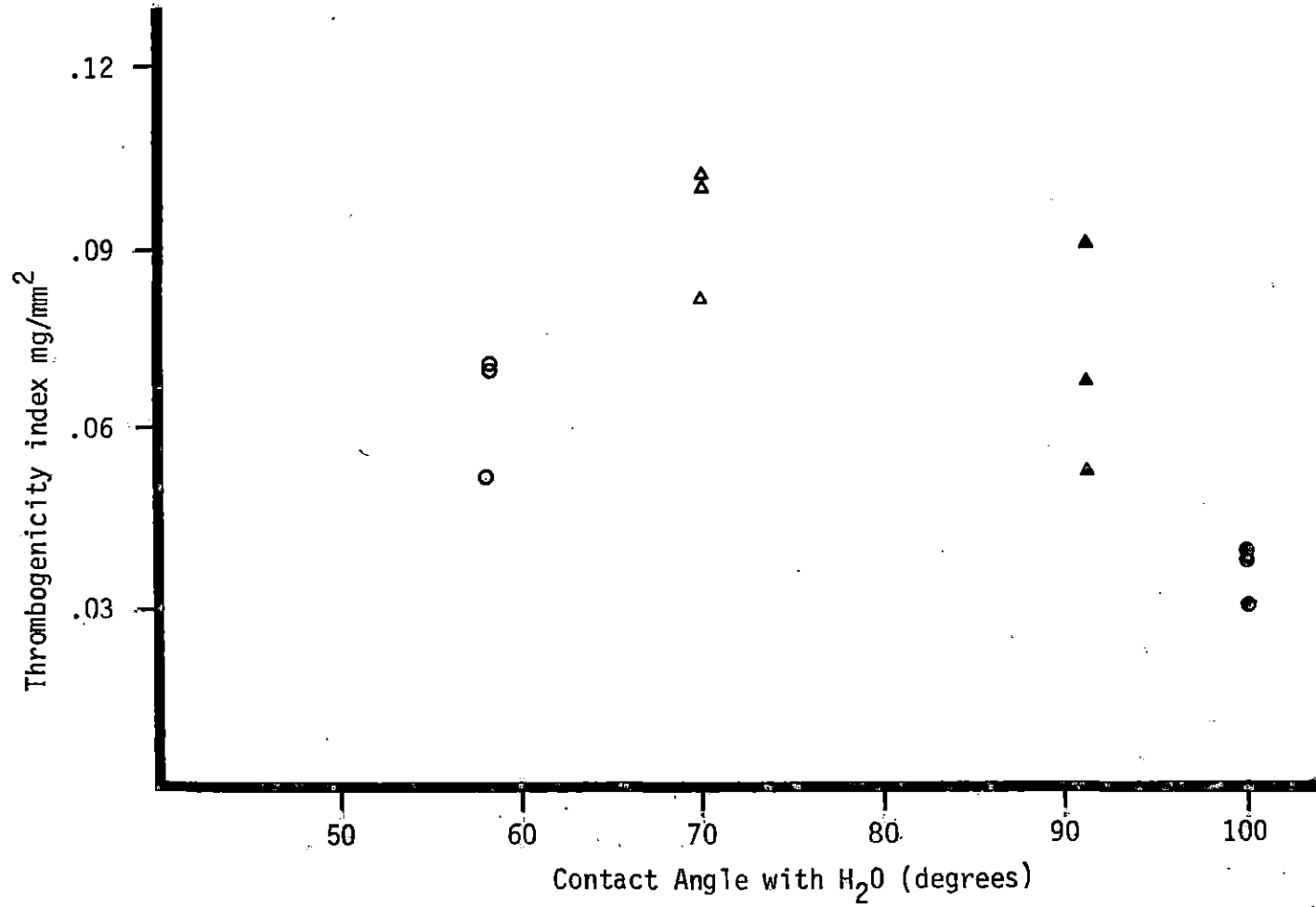


Figure 40. Thrombogenicity index vs. contact angle for experimental animals 2442, 2504, and 2297. (●) is silicone rubber, (○) is 15% HEMA/5% NVP, (△) is 10% HEMA/10% NVP, (▲) is 0% HEMA/20% NVP.

## DISCUSSION

## SEM Analysis

From the SEM analysis, the Silastic<sup>®</sup> control appears to be the least reactive while the more hydrophilic surfaces (10% HEMA/10% NVP and 15% HEMA/5% NVP) produce an increased reaction. Table 11 shows this comparison well. The silicone rubber is rated at zero and pluses and minuses indicate whether the responses were greater (+) or less (-) than the control. In most cases the results indicate that the silicone rubber was less reactive than the 5 trial formulations. This result appears to indicate that hydrophobic materials may offer sites that are less adhesive than hydrophilic surfaces. The exception is the 10% HEMA/10% NVP formulation which is the most hydrophilic, and also has a high water content. With time, the response lessens and at 60 minutes it is less reactive than the silicone rubber. This may indicate a passivating surface is being developed; the 10% HEMA/10% NVP formulation may be a good candidate for long-term testing.

The 20% HEMA/0% NVP and 15% HEMA/5% NVP formulations have a greater structural conformity, approaching a weak 3-dimensional gel, which may be roughened. This would implicate surface roughness and preparation as possible preclotting factors.

SEM analysis is quite good for examining the type and morphology of the cellular elements adhering to the surface, but does not provide a quantitative description of the deposition. The thrombus weight

along with the SEM data offers a more complete analysis.

### Contact Angle

Surface energy is thought to be an effector of thrombosis as discussed by Andrade (1973). Baier (1972) has stated that a critical surface tension in the range of 20 to 30 dynes/cm should be biocompatible. If this is true, the Silastic<sup>®</sup> and the 0% HEMA/20% NVP formulation should perform better than the other formulations.

### Thrombogenicity Index

Method 3 trials used a shorter time interval in an attempt to evaluate the catheters with less thrombus present. Yet after only 5 minutes a number of the surfaces were covered by a dense fibrin sheath. In this case, the amount of thrombus per unit surface area was determined. The Silastic<sup>®</sup> control was found to produce the least reaction.

The results of these trials tend to corroborate the findings of Welch, et al. (1974), Boros, et al. (1975), Hoar, et al. (1978) and Hecker (1979) whom reported thrombus formation on all surfaces. Also there is an indication that surface roughness may be an effector of thrombosis, or at least offer a site for adhesion of the thrombus.

Baier's (Baier, 1972) concept of a 20-30 dyne/cm compatible zone and Wilner's (Wilner, et al., 1978) suggestion of mid range critical surface tensions would indicate that Silastic<sup>®</sup> and the 0% HEMA/20% NVP

formulation should have the most favorable responses. However, they were found to exhibit different responses. The results do suggest that a low energy hydrophobic surface is desirable as indicated by Lyman (1972).

## CONCLUSION

The results of this investigation can be summarized in the following manner: experimental design, materials characteristics, analysis techniques, and resulting experimental information.

The experimental design was modeled after the techniques of Anderson (1974) and was found to be inadequate due to thrombus formation within the introducing tube. This subsequently led to the stripping of the thrombus from the catheter surface. Therefore, this method is not recommended. Method 2 allowed for repeated entry into the venous system with less susceptibility to thrombus loss, although this method was also prone to thrombus loss on occasion. Method 3 did not allow for repeated access, but did allow for catheter removal with no thrombus loss. This method is well-suited for long term implantation studies.

The materials used in this investigation allowed for testing different composite materials with similar texture, but different characteristics. The ability to control these surface characteristics is useful for studying the effects of such parameters as surface energy, hydrophilicity, and % water imbibed.

The two analysis techniques, SEM and gravimetric, used in conjunction can adequately characterize the materials and results. The utilization of scanning electron microscopy for morphological investigations of the surfaces, both before and after implantation, yields information on surface texture, cellular elements adhering, and

cross-sectional information, while gravimetric techniques indicate the average nature of the response.

The trends observed in this investigation indicate a smooth, low energy, hydrophobic material should offer an optimum surface. The response of blood to the materials lessened with decreasing surface energy and increasing hydrophobicity.

## RECOMMENDATIONS FOR FUTURE RESEARCH

Further studies concerning thrombus formation on a catheter should consider the following:

- (1) A more complete materials analysis is needed to characterize the composites with respect to variations in hydrophilicity due to components used and to reproducibility of surface energy measurements.
- (2) Long-term tests of these composite materials using both SEM and gravimetric analysis techniques would indicate transient and steady state variations.
- (3) Experimental procedures are needed to study embolization occurring on the materials tested.

## LITERATURE CITED

- Abrahams, R. A. and S. H. Ronel. 1976. Blood compatible coatings of hydron hydrophilic polymers. *Polymer News* 3:11-19.
- Anderson, J. H., C. J. Gianturco, and G. D. Dodd. 1974. A Scanning Electron Microscopic Study of Angiographic Catheters and Guide Wires. *Radiology* 111:567-571.
- Andrade, J. D. 1973. Interfacial phenomena and biomaterials. *Medical Instrumentation* 7:110-120.
- Baier, R. E. 1972. The role of surface energy in thrombogenesis. *Bull. N.Y. Academy Medicine* 48:257-272.
- Baier, R. E. and C. K. Akers. 1978. Blood-surface interactions: recognized factors and unsettled questions. *Transaction of the American Society of Artificial Internal Organs* 24:770-773.
- Baier, R. E. and R. C. Dutton. 1969. Initial events in interactions of blood with a foreign surface. *J. Biomedical Materials Research* 3:191-206.
- Barber, T. A., T. Mathis, J. V. Ihlenfeld, S. L. Cooper, and D. F. Mosher. 1978. Short-term interactions of blood with polymeric vascular graft materials: protein adsorption, thrombus formation, and leukocyte deposition. Pages 431-440, in O. Johari, ed. *Scanning electron microscopy/1978/II*. SEM Inc., AMF O'Hare, Illinois.
- Barber, T. A., L. K. Lambrecht, D. L. Mosher, and S. L. Cooper. 1979. Influence of serum proteins on thrombosis and leukocyte adherence on polymer surfaces. Pages 881-892 in O. Johari, ed. *Scanning electron microscopy/1979/III*. SEM Inc., AMF O'Hare, Illinois.
- Beugeling, T. 1979. Interaction of polymer surfaces with blood. *Journal of Polymer Science, Polymer Symposium* 66:419-428.
- Boros, S. J., T. R. Thompson, J. W. Reynolds, W. Jarvis, and J. W. Williams. 1975. Reduced thrombus formation with silicone elastomer: Silastic umbilical artery catheters. *Pediatrics* 56(6): 981-986.
- Bottino, J., K. B. McCredie, D. H. M. Groschel, and M. Lawson. 1979. Longterm intravenous therapy with peripherally inserted silicone elastomer central venous catheters in patients with malignant diseases. *Cancer* 43(5):1937-1943.

- Bourassa, M. G., M. Cantin, E. B. Sandborn, and E. Pederson. 1976. Scanning electron microscopy of surface irregularities and thrombogenesis of polyurethane and polyethylene coronary catheters. *Circulation* 53(6):992-996.
- Clawson, C. C. and S. J. Boros. 1978. Surface morphology of PVC and silicone elastomer umbilical artery catheters. *Pediatrics* 62(5):702-705.
- Durst, S., J. Leslie, R. Moore, and K. Amplatz. 1974a. A comparison of the thrombogenicity of commercially available catheters. *Radiology* 113:599-600.
- Durst, S., B. Johnson, and K. Amplatz. 1974b. The effect of silicone coatings on thrombogenicity. *Am. J. Roentgenol. Radium Ther. Nucl. Med.* 120:904-906.
- Dutton, R. C., A. J. Webber, S. A. Johnson, and R. E. Baier. 1969. Microstructure of initial thrombus formation of foreign materials. *J. Biomedical Materials Research* 3:13-23.
- Fromageot, H. P. M., J. N. Groves, A. R. Sears, and J. F. Brown, Jr. 1976. The interaction of macromolecular solutions with macromolecular monolayers adsorbed on a hydrophobic surface. *J. Biomedical Materials Research* 10:455-469.
- Greer, R. T. and R. L. Knoll. 1980. Controlled microstructure of two stage poly-hydroxyethyl methacrylate coatings on polyethylene terephthalate substrates for potential prosthetic applications. Pages 227-290 in O. Johari, ed. *Scanning electron microscopy/1980/II*. SEM Inc., AMF O'Hare, Illinois.
- Hayat, M. A. 1970. Principles and techniques of electron microscopy: Biological applications volume 1. Van Nostrand Reinhold Company, New York. 412 pp.
- Hecker, J. F. 1979. Thrombus formation and renal infarction induced by aortic catheters in sheep. *Trans. Am. Soc. Artif. Intern. Organs* 25:294-498.
- Hecker, J. F. and R. O. Edwards. 1981. Effects of roughness on the thrombogenicity of a plastic. *Journal of Biomedical Materials Research* 15:1-7.
- Hoar, P. F., J. G. Stone, A. W. Wicks, R. N. Edic and J. V. Scholes. 1978. Thrombogenesis associated with Swan-Ganz catheters. *Anesthesiology* 48(6):445-447.

- Hoffman, A. S. and C. Harris. 1972. Radiation-grafted hydrogels on silicone rubber surfaces -- new biomaterial. A.C.S. Polymer Preprints 13:740.
- Hoffman, A. S., T. A. Horbett, and B. D. Ratner. 1977. Interactions of blood and blood components at hydrogel interfaces. Annals of the New York Academy of Sciences 283:372-382.
- Jhon, M. S. and J. D. Andrade. 1973. Water and hydrogels. Journal of Biomedical Materials Research 7:509-522.
- Kaganov, A. L., J. Stamberg, and P. Synek. 1979. Hydrophilized polyethylene catheters. J. Biomedical Materials Research 10:1-7.
- Knoll, R. L. 1980. Analysis of polyhydroxyethyl methacrylate coatings on polyethylene terephthalate fabric for cardiovascular prosthetic applications. PhD. Dissertation. Iowa State University. 230 pp.
- Kronick, P. L. and A. Rembaum, 1977. Reactions of human platelets with microspheres of polyhydroxyethyl methacrylate and polyacrylamide. Journal of Biomedical Materials Research, Symposium 8:39-50.
- Lisback, C. V. and K. R. Kollmeyer. 1979. Role of catheter surface morphology on intravascular thrombosis of plastic catheters. J. Biomedical Materials Research 13:459-466.
- Lymen, O. J. 1972. Biomedical polymers, their problems and promise. Pp. 12-34 in A. C. Bennet, Jr., ed. Biomaterials. University of Washington Press, Seattle.
- Mortensen, J. D. and R. N. Schaap. 1980. Further experience with an acute intra-arterial implantation screening test for thrombogenicity of intravascular catheters. Transactions of the American Society for Artificial and Internal Organs 26:284-288.
- Nakashima, T., K. Takakura, and Y. Komoto. 1977. Thromboresistance of graft-type copolymers with hydrophilic-hydrophobic microphase-separated structure. Journal of Biomedical Materials Research 11:787-798.
- Predecki, P. 1974. A method for Hydron impregnation of silicone rubber. J. Biomedical Materials Research 8:487-489.
- Ratner, B. D. and A. S. Hoffman. 1974. The effect of cupric ion on the radiation grafting of N-vinyl-2-Pyrrolidone and other hydrophilic monomers onto silicone rubber. Journal of Applied Polymer Science 18:3183-3204.

- Ratner, B. D. and A. S. Hoffman. 1975. Radiation grafted hydrogels on silicone rubber as new biomaterials. Pages 159-171 in H. P. Gregor, ed. Biomedical applications of polymers. Plenum Publication Corp., New York.
- Singh, M. P. and D. G. Melrose. 1971. Hydron coated terylene sutures; a pilot study. Bio-medical Engineering April:157-159.
- Vale, B. H. 1980. Hydrogel/silicone rubber composite materials: Fabrication, compatibility, and ex vivo blood responses. PhD. Dissertation. Iowa State University, Ames, Iowa. 154 pp.
- Welch, G. W., D. W. McKeel, Jr., P. Silverstein, and H. L. Walker. 1974. The role of catheter composition in the development of thrombophlebitis. Surgery, Gynecology, and Obstetrics 138:421-424.
- Wilner, G. D., W. J. Casarella, R. Baier, and C. M. Fenoglio. 1978. Thrombogenicity of angiographic catheters. Circulation Research 43(3):424-428.
- Witcherle, O. and D. Lim. 1960. Hydrophilic gels in biological use. Nature (London) 185:117-118.
- Yonaha, T. 1978. SEM observations of the thrombus on inner surfaces of in-dwelling catheters. Journal of Electron Microscopy 27(4):366.

## ACKNOWLEDGEMENTS

I would like to express sincere appreciation to my major professor, Dr. Raymond T. Greer, for the support and advice he has offered throughout my graduate work. I would also like to thank Drs. N. Cholvin, F. Hembrough, and M. H. Greer for their suggestions and encouragement. Special thanks to Mrs. Joyce Feavel for her surgical assistance, to Debi Stambaugh and her associates in the BMC for their assistance with the photographic reproductions, and to Dave Padget, Brad Vale and Randy Knoll for their helpful discussions.

Many thanks must also go to my wife, Marcia, for her support and encouragement throughout my work and for typing this thesis.

Michael D. Baudino